2022-12-01

Determination Of Oxidation-Reduction Potential And Iron Chemistry For Solutions Generated During The Hydrometallurgical Extraction Of Copper

Jiahao Xu
University of Texas at El Paso

DETERMINATION OF OXIDATION-REDUCTION POTENTIAL AND IRON CHEMISTRY FOR SOLUTIONS GENERATED DURING THE HYDROMETALLURGICAL EXTRACTION OF COPPER

JIAHAO XU

Doctoral Program in Materials Science and Engineering

APPROVED:

Guikuan Yue, Ph.D., Chair

Antonio Arribas, Ph.D.

Devesh Misra, Ph.D.

Stephen Crites, Ph.D.
Dean of the Graduate School

DETERMINATION OF OXIDATION-REDUCTION POTENTIAL AND IRON CHEMISTRY FOR SOLUTIONS GENERATED DURING THE HYDROMETALLURGICAL EXTRACTION OF COPPER

by

JIAHAO XU, B.S.

DISSERTATION

Presented to the Faculty of the Graduate School of

The University of Texas at El Paso

in Partial Fulfillment

of the Requirements

for the Degree of

DOCTOR OF PHILOSOPHY

Department of Metallurgical, Materials & Biomedical Engineering

THE UNIVERSITY OF TEXAS AT EL PASO

December 2022

ACKNOWLEDGEMENT

First of all, I would like to express my sincere gratitude to my supervisor, Dr. Guikuan Yue, for his encouragement, excellent guidance and continuous support during the last 5 years. His guidance, critical discussions and advice on my experiment and research every day helped and accelerated my study a lot. Without his great guidance this work would not have been possible and completed smoothly.

I would also like to thank my dissertation committee members, Dr. Devesh Misra and Dr. Antonio Arribas, for their great help and suggestions. I also express my thanks to Dr. Yongteng Dong who helped me for the modeling and speciation study.

I gratefully acknowledge the financial support from The University of Texas at El Paso, Engineering STARs Program Funding from The University of Texas System, SKU-UTEP Grant, and Freeport-McMoRan, Inc.

ABSTRACT

Oxidation-reduction potential (ORP) based on iron chemistry is one of the key operating parameters during the hydrometallurgical extraction of copper. A novel ORP equation was developed previously only based on the variables of temperature and nominal ferric/ferrous ratio to predict the redox potential of the quaternary H_2SO_4-$Fe_2(SO_4)_3$-$FeSO_4$-H_2O system. However, its applicability in more complex acidic iron sulfate solutions during the hydrometallurgical extraction of copper with different temperatures, acidic concentration, cupric concentration, nominal ferric/ferrous ratio, and total and l iron concentration has not been extended and validated. This work evaluates the applicability of novel oxidation-reduction potential equation in the H_2SO_4-$Fe_2(SO_4)_3$-$FeSO_4$-H_2O and H_2SO_4-$CuSO_4$-$Fe_2(SO_4)_3$-$FeSO_4$-H_2O systems with various solution compositions in the temperature range of 5-60℃ typically employed in the industry, and also investigate the species distribution based on a developed thermodynamic model to better understand the iron chemistry.

The broader range of applicability of this equation to other complicated acidic iron solutions containing cupric ions has been extended and validated. Synthetic iron-containing solutions with cupric ion based on the industrial processes of heap leaching (for pregnant leaching solution, PLS), solvent extraction (SX), traditional copper electrowinning (Cu EW), and novel copper electrowinning have been employed to measure the ORP at different temperature (5-60 ℃). This equation was validated by reliable and accurate prediction of measured redox potential and thus is highly useful to understand the iron chemistry of industrial leaching, solvent extraction, and copper electrowinning processes.

According to the species distribution study, most Fe (III) is distributed as complexes and the free ferric ion accounts for only a minor percentage, with the existence of a large

amount of Fe(II) in the form of a free ferrous ion. The change of redox potential with temperature for various nominal ferric/ferrous ratios could be explained well by the speciation model results for all the solutions mentioned above generated in industrial processes.

The findings from this work contribute to the research on ORPs and speciation of acid iron sulfate solutions under various conditions and the understanding of iron chemistry of industrial processes for the hydrometallurgical extraction of copper.

TABLE OF CONTENTS

LIST OF TABLES

LIST OF FIGURES

1. INTRODUCTION

1.1 General Information on Extraction of Copper Ores

Copper has various applications in all kinds of fields due to its high electrical/thermal conductivity, excellent corrosion resistance, and outstanding workability. Nowadays, high-purity copper essential for electrical applications (its most important and common application) is in high demand worldwide. According to published literature, total copper production in 2010 was around 20 million tons produced from mining industry and from end-of-us copper scrap [1]. According to the recent United States Geological Survey (USGS) report, total copper production in 2021 was around 21 million tons produced from mining industry and Chile is the largest copper producer accounting for 27% of the global production. Copper-iron-sulfide/copper sulfide minerals, oxidized minerals (carbonates, oxides, hydroxy-silicates, sulfates), and scrap copper/alloy are three significant sources of copper production. Chalcopyrite ($CuFeS_2$) and chalcocite (CuS_2) are the most widely existing source in the earth's crust for pyrometallurgical/hydrometallurgical production of pure metallic copper. As mentioned, pyrometallurgical method of copper production accounts for around 80% of global copper production of the difficulty of dissolving the Cu-Fe-S minerals in aqueous solutions and includes the three main processes of concentration, smelting, and refining. Although the traditional pyrometallurgical method still plays an important and dominant role in the copper production industry, high capital costs caused by the smelting process, the limited capacity of smelters to deal with growing concentrations of impurities (such as As, Sb), increasing much lower grade copper ores, and the air pollution (the emission of SO_2), make the pyrometallurgical production need improvement or the alternative method. Nowadays, the concentration of copper ores is as low as 0.5% Cu, and there are more low-grade copper ores

to be treated in the future, which makes the hydrometallurgical production method to extract pure copper from copper ore more and more attractive, profitable and practical. The hydrometallurgical production method with leaching, solvent extraction, and copper electrowinning processes has many advantages of lower-grade copper ores, and 20% of global copper production is obtained through the hydrometallurgical production method [1, 2].

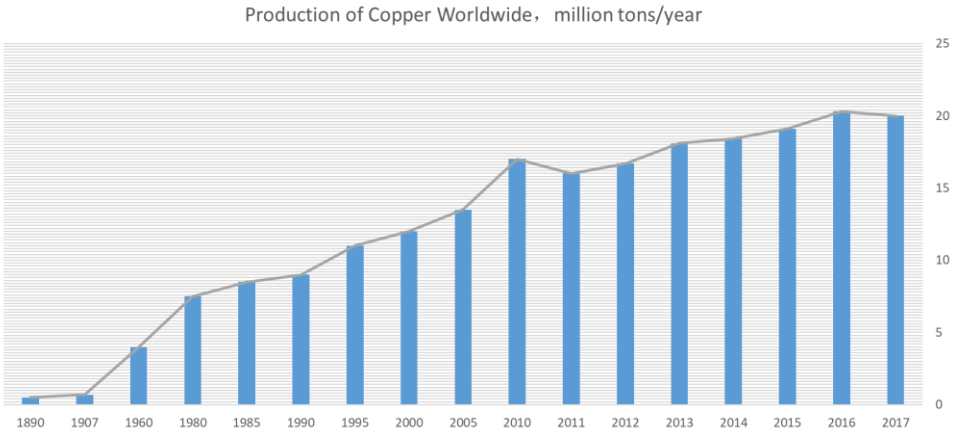

Figure 1-1 Global copper production from 1890 to 2017 in a million tons per ye

1.2 Hydrometallurgical Production of Copper

As mentioned above, pyrometallurgical processes that convert copper sulfide ores into high-purity electro-refined copper account for about 80% of primary copper production worldwide. Hydrometallurgical methods (leaching, solvent extraction SX, and copper electrowinning Cu EW) treating mainly copper oxide and chalcocite ores account for 20% of primary copper production worldwide. The high-purity electrowon cathode copper is the final product of the copper electrowinning (Cu EW) process a. It is equal to or often greater in purity than electro-refined copper in the final pyrometallurgical process (copper electrorefining) [1, 3].

Although pyrometallurgical production of metallic copper is still the dominated

production method globally, hydrometallurgical production of high-purity copper is steadily increasing due to the ability of the treatment of lower grade copper ore [1, 4]. The profitable extraction of copper from low-grade ores requires low-cost processing methods, such as in situ or heap leaching [1, 36].

Pyrometallurgy （80%, 15.8 million tons）	Hydrometallurgy （20%, 3.8 million tons）
Concentration, Smelting, Fire- or Electro-refining	Leaching, Solvent Extraction, Copper Electrowinning
Downstream slag cleaning, High capital and operating costs SO_2 emission, Dust	Environment friendly, low energy consumption, high purity 99.999%
1200°C	1.8-2.5 kWh/kg, 50-65 °C

Figure 1-2 The comparison between pyrometallurgical and hydrometallurgical extraction of copper

Heap leaching started its application in the 1950s when heap leaching technology was developed by the former Bureau of Mines of the United States in order to recover precious metals from low-grade heaps of ore with the use of toxic cyanide solutions, adsorption onto activated carbon, and recovery by electrowinning [5, 35]. In 1968 Bluebird copper oxide mine developed the first modern copper heap leach operation, according to the literature [1, 5, 22], then followed in the early 1970s by a few other small operations in the Western United States. In 1980 three major copper projects were commissioned in Chile and large-scale heap leaching operation was employed there [1, 5-8, 31-35].

Since the early 1970s mentioned above, continuously developed, modified modern technologies have made the application of heap leaching to various types of minerals, climates,

and different sizes of operations [5-10, 35]. Today heap leaching technology was applied to various industrial mineral processing besides copper ores, including gold-bearing pyritic ores, uranium, and nonmetallic minerals as well as soil remediation [1, 9-15, 18, 20].

Although heap leaching obtained considerable success in mineral processing, there are both technical and commercial challenges that hinder heap leaching technology from achieving its full potentials [1, 6-8, 34-36].

While heap leaching technology looks very easy to be applied, heap reactors are more difficult to aerate efficiently, resulting in a somewhat careless attitude in the early days of the gold heap as well as the undesirable formation of gradients of pH and leaching in the 1970s and 1980s. These mentioned challenges make heap leaching technology difficult to be launched by small companies with limited technical support and understanding of the heap leaching process, ultimately resulting in lots of failed projects [1, 5, 6, 16-21, 35]. Besides, the real ferric concentration in the leaching solution is needed to be obtained in order to do research on the reduction behavior of ferric ions and further understand its effect on the leaching rate [65, 77, 92]. According to the published literature [65, 66, 77, 83], copper extraction was mainly controlled by the redox potential of the solution or a function of the ferric/ferrous ratio. In order to understand the leaching process better and develop a more efficient leaching process, a complete understanding of the factors affecting the redox potentials in leaching solution is necessary. Therefore, the deeper understanding of species distribution, composition of leaching solution, iron chemistry, pH, ionic strength, and further investigation of the reliable determination of ORP values in the PLS are very important to develop heap leaching technology [1, 6, 92, 102].

During the heap leaching process, crushed ore is piled on an impermeable pad, and then leaching reagents are imported by irrigation from the top. According to the various types of copper ores to be further processed, the chemical compositions of leaching solution are totally different. After the extraction of the desired copper minerals, the produced solution becomes increasingly loaded as it percolates via the pile. According to the literature, micro-organisms resident within the ore bed, especially in the presence of sulfide minerals, could facilitate the leaching process. The drainage system at the base of the pile is employed to effectively collect the PLS and then the collected PLS will be channeled to the PLS pond. After the collecting and the channeling, the PLS will be pumped to the processing facility where the value metal is recovered. Different from the treatment of the PLS, the barren leach solution (BLS) is transported to the barren solution pond from, where, after solution make-up, it is reapplied to the surface of the heap [23-30, 36].

The impure PLS is fed to the SX circuit and is treated by SX process in order to purify and upgrade the PLS to produce an electrolyte that contains the high concentration of cupric ion and is also applicable for the process of Cu EW. The specific organic solvent (an extractant) reacts and loads with cupric ion selectively. Then, copper is stripped from the loaded organic solvent into the advanced electrolyte prepared for the Cu EW process [1, 2].

Cupric ion is dissolved in an electrolyte and reduced on the cathode surface to produce metallic sheets with a high purity in the industrial process of Cu EW. Industrial Cu EW process takes place in each Cu EW cell with the assistance of DC current independent circuits in the installed large tank houses. Different from lab-scale research, the top considerations for industrial production of metallic copper are product quality, yield rate, and energy consumption.

But energy consumption, current efficiency, product quality, and cell voltage are lab-scale considered in lab scale research [1, 4-6].

The capacity of producing high purity copper at low cost has been greatly increased by the process of copper electrowinning in the last 30 years [1]. Industrial electrowinning (EW) requires pure copper rich electrolytes (45-55 g/l Cu) with high conductivity. This high concentration of copper ion ensures that Cu ions are always available for plating at the cathode surface at current densities that allow economical rates of plating, being readily renewed by mass transfer and gives smooth, dense, high purity, readily marketable cathode copper. The high conductivity of the electrolyte is provided by a high acid concentration, typically 175-190 g/l H_2SO_4. The combined technology of SX-EW continues to grow in importance as more copper is produced by leaching and lower grade materials are treated for recovery of copper [1-3].

Copper electrowinning (Cu EW) process includes 3 parts: 1. Immersing metal cathodes and conductive anodes into a purified electrolyte containing $CuSO_4$ and H_2SO_4; 2. Applying a direct electrical current from an external source, such as a rectifier, which causes current to flow through the electrolyte between the cathodes and anodes; 3. Plating pure metallic copper from the electrolyte onto the cathodes using the energy provided by the electrical current to drive the reduction of the Cu^{2+} ions to Cu^0 metal [1, 2].

The cathodes are usually stainless-steel blanks. The anodes are usually rolled Pb-alloy sheets. Copper is electroplated onto the cathodes for 6-7 days, after which the plated copper is machine-stripped from the stainless-steel cathode blanks, washed, and sold [1, 2].

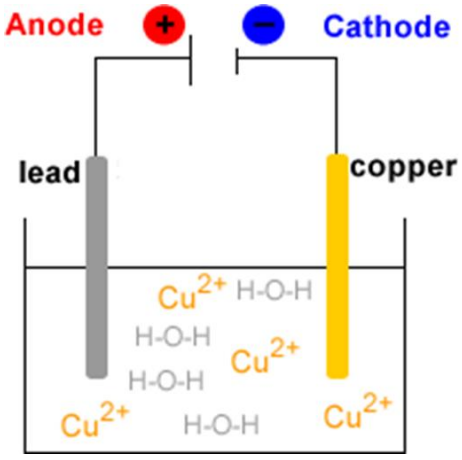

Figure 1-3 Schematic diagram of the copper electrowinning cell of the house tank

1.3 Electrowinning of Copper

Copper Electrowinning (EW) process account for 25% of global copper production, estimated at 17.0 million tons according to the USG Survey report of 2013 with the method of leach/SX/EW technology [1]. About 4.5 million tons of copper are electrowon per year [1, 4]. Production of copper using this technology continues to increase due to the growth of leaching process as a process technology for copper [2].

For hydrometallurgical process, copper electrowinning process is the most important process used to produce high quality, high purity copper. Besides the Cu EW, electrowinning process could be performed to produce nickel, aluminum, gold, silver, lead, Zn, etc. This technology has developed well in last 25 years [1].

However, in traditional Cu EW process, there are several disadvantages needed to be improved. These disadvantages include a low mass transfer rate, low specific cathode surface, harmful acid mist, high energy consumption [1, 4].

Conventional copper electrowinning consumes lots of electricity energy mainly because 70% of the total voltage is due to the anode potential [5].

In Cu EW process, commonly used flat plate limits current densities to values up to 450 A/m^2 [2]. The space time yield of large electrowinning tank house is low. Besides, there are other drawbacks, such as unstable short life PbO_2 anodes, the addition of chemical additives, contamination of the electrodeposited copper [3].

In order to improve and upgrade the Cu EW process, current efficiency (CE) and energy consumption (EC) affecting operational and capital costs need to be maximized. The values of current efficiency (CE), energy consumption (EC), and space time yield(Y) need to be calculated and evaluated to lower the energy cost and increase production rate [1].

Beside the above-mentioned lowering energy cost, and increasing production rate, one of the goals in studying copper electrowinning is to obtain better understanding of copper electrodeposition process, with emphasis on the role of additives and transport on electro crystallization [4]. With the increasing demand of high purity copper, an electric current is utilized to remove the copper from solution and deposit it onto flat sheets of metal in the copper electrowinning tank house [5]. In each copper electrowinning electrolytic cell, electrical current pass via electrolyte from the anode to the cathode. In the copper electrowinning process, the electrolyte is an aqueous solution containing copper sulfate ($CuSO_4$) and sulfuric acid (H_2SO_4) at the temperature ranging from 25°C to 45°C [4].

Conventional copper electrowinning cells have many limitations of limited mass transfer rates, limited cathode specific surface area, high specific energy consumption, environmental problems [1], which have leaded to the development of several alternative designs [2], such as the fluidized bed cell [3-6, 38], the spouted bed cell [39-41] and the squirrel cage cell [42]. Alternative cell designs include the use of membranes to separate catholyte from anolyte, alternative cathode geometries in order to increase the specific surface area of the cathode and

using alternative reactions so as to replace water oxidation to gaseous oxygen [43, 44].

	Novel	Traditional
Anode	$2Fe^{2+} = 2Fe^{3+} + 2e^-$	$2H_2O = 4H^+ + O_2 + 4e^-$
Cathode	$CuSO_4 + 2e^- = Cu + SO_4^{2-}$	$CuSO_4 + 2e^- = Cu + SO_4^{2-}$
Overall	$CuSO_4 + 2Fe^{2+} = Cu + SO_4^{2-} + 2Fe^{3+}$	$2CuSO_4 + 2H_2O = 2Cu + 4H^+ + 2SO_4^{2-} + O_2$
Advantage	1.no acid mist 2. electropotential 1.23V to 0.77V 3.lower energy consumption	

Figure 1-4 The comparison between Traditional Cu EW and Novel EW processes

In order to protect the environment and the workers' health, in the 1990s the advanced research was finished by the USA Bureau of Mines (USBM) in the hydrometallurgical extraction processes for metallic copper to evaluate the choices for electrowinning copper without acid mist generation, which utilized the replacement of the decomposition of water to form oxygen gas with an alternative anode reaction that was free from any gas emission. The SX-EW integrated pilot plant with 4 electrowinning cells in 1995 designed and operated by USBM successfully made copper electrowinning carry out with the ferrous/ferric oxidation anodic reaction in conjunction with reduction reaction of ferric ion external to the cell using sulfur dioxide and an activated carbon catalyst. The sulfuric acid generated by this reaction was extracted from the circuit for using solvent extraction process. In 2003 Freeport-McMoRan Copper & Gold Inc. Technology Center runs its SX-EW Test Facility continuously electrowinning copper using the ferrous/ferric oxidation as the anodic reaction [1].

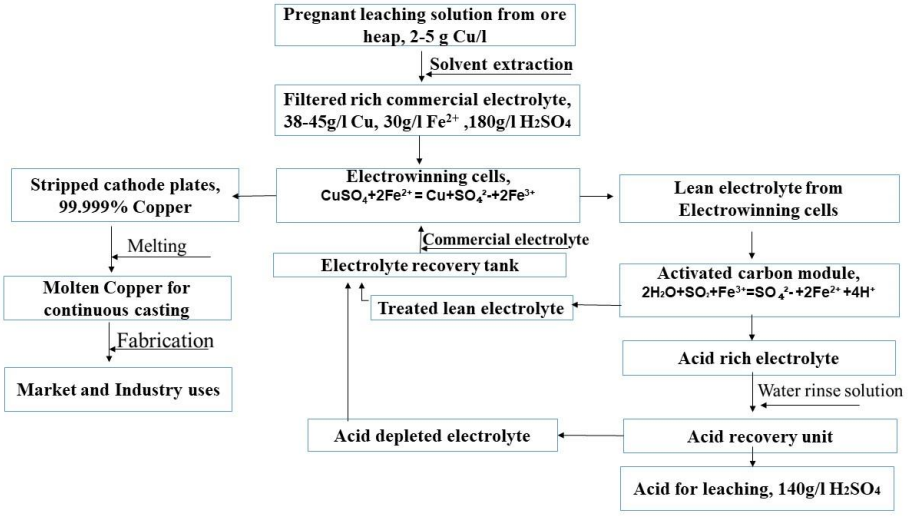

Figure 1-5 The hydrometallurgical extraction of copper with the alternative anode reaction technology (AART) applied to novel Cu EW process according to the information of Freeport-McMoRan test facility

The new development in the area of copper electrowinning has resulted in many progress and achievement including modifying anodic reactions and avoiding oxygen evolution anodic reaction proposed to reduce electricity energy consumption. In actual research experiment and industrial production, the influence of different anode materials, concentration of sulfuric acid, copper ion, ferric ion, ferrous ion, current density i, electrolyte flow rate, temperature and anode potential will be investigated completely [4]. Laboratory analysis equipment and methods for chemical copper quality measurement are electrochemical impedance spectroscopy (EIS), X-ray photo-electron spectroscopy (XPS) and scanning electron microscopy (SEM).

1.4 Scope of the Present Study and Thesis Organization

This work is first to validate and extend the application of previously developed equation that predict and determine the redox potential of the quaternary H_2SO_4-$Fe_2(SO_4)_3$-$FeSO_4$-H_2O system only based on the variables of temperature and nominal ferric/ferrous ratio to the

solutions generated during industrial hydrometallurgical extraction of copper during 5 to 60℃. This equation was validated by reliable accurate prediction of measured redox potential, comparison of the ORP test results. The accurate prediction and measurement of redox potential is highly useful to understand the iron chemistry of industrial leaching, solvent extraction and copper electrowinning processes.

In chapter 2, various important topics and conclusions found in the literature highly related to the present project will be summarized and discussed in details. Chapter 3 will present the objective of this thesis. Chapter 4 provides the content and detail of the methodology utilized and involved, including experimental procedures for the electrochemical and analytical methods. Chapter 5 provides the results and discussion of the validation of the applicability of the equation to other complicated acidic iron solutions containing cupric ion. In Chapter 5 Synthetic iron-containing solutions with cupric ion based on the industrial processes of heap leaching, solvent extraction (SX), traditional copper electrowinning (Cu EW), and novel copper electrowinning are employed to measure the ORP in different temperature (5-60 ℃).

Besides the validation of the applicability in more complex acidic iron sulfate solutions, typically employed in the industry with different temperature (5-60℃), with a broader range of various acidic concentration, cupric concentration, nominal ferric/ferrous ratio, and total iron concentration in both the H_2SO_4-$Fe_2(SO_4)_3$-$FeSO_4$-H_2O and H_2SO_4-$CuSO_4$-$Fe_2(SO_4)_3$-$FeSO_4$-H_2O systems in Chapter 5, this thesis evaluates and investigates the species distribution based on a thermodynamic model to make a contribution to the understanding of iron chemistry for hydrometallurgical extraction of copper.

In the speciation study in Chapter 6, 7, 8, the previous conclusion obtained in Chapter 5 that the ORP of acidic iron sulfate solutions containing with cupric ion with a high total iron

and cupric ion concentration can still by only determined by the nominal ferric/ferrous ratio and experiment temperature was strongly supported by the analysis of the speciation results.

Chapter 6, 7, 8 utilize a previously developed thermodynamic model of H_2SO_4-$CuSO_4$-$Fe_2(SO_4)_3$-$FeSO_4$-H_2O system to reliably simulate the species distribution in PLS, SX solution, and Traditional Cu EW solution, respectively. The change of redox potential with temperature for various nominal ferric/ferrous ratios are explained well by the speciation model results. Besides the species study, the pH and effective ionic strength are also discussed. These findings make a great contribution to further investigating the speciation of other solutions generated during hydrometallurgical extraction of copper.

Finally, Chapter 9 presents the conclusions, industrial applications and recommendations for future work in this research area.

The findings from this thesis contribute to the research on aqueous speciation of acid iron sulfate solutions, accurate determination of redox potential of the ferric/ferrous couple in acidic iron sulfate solutions, the reduction kinetics of the ferric/ferrous couple and the understanding of the iron chemistry of industrial processes for hydrometallurgical production of copper.

2. LITERATURE REVIEW

From the Introduction part, it can be seen that leaching, SX, and EW processes are the most important procedure of the copper extraction industry and Cu EW is the key component in producing the best quality copper. The traditional copper electrowinning process generates oxygen gas and corrosive acid mist with the water hydrolysis reaction as the anode reaction. What's more, both the cell voltage and its related energy consumption are high. The addition of ferrous sulfate into traditional Cu EW electrolyte and the use of corrosion resistant catalytic anode surface are investigated in past 20 years. The new technology of novel Cu EW has made lots of progress and achievement, such as adopting ferric/ferrous reaction as anodic reaction and avoiding oxygen evolution anodic reaction in order to lower electricity energy cost.

2.1 Heap leaching, Solvent Extraction, and Traditional Copper Electrowinning

2.1.1 Heap Leaching and PLS

There are lots of publishment about electrodes of copper electrowinning. However, few papers are on electrowinning cell design and electrowinning solution composition optimization.

In addition to the compositions of copper electrowinning solutions, the PLS composition and operation in cold climates are required to better understand and establish the optimum conditions. However, few papers have been published on these two topics. To our knowledge, most of these papers are limited to modeling and high temperature. There are very few published data pertaining to a systematic study on the speciation of the aqueous H_2SO_4-$Fe_2(SO_4)_3$-$FeSO_4$- Cu_2SO_4-H_2O system, especially at low temperatures.

The percentage of the heap exposed to acid-oxidizing conditions has great influence on the amount of copper finally extracted from a more common mixed (oxide and sulfide) ore heap. Based on the above conclusion, the persistence within the leaching system of low Eh-high pH microenvironments is the primary difficulty for leaching. Iron has existence in a variety of oxide, hydroxide, sulfate, sulfide, and silicate minerals in most cases of deposits that is very easy to have chemical reaction with leaching solution. According to the relative abundance of the mentioned minerals, a significant quantity of ferric or ferrous ions is released from leaching process into leaching solution and makes the values of Eh to increase or decrease. Iron species play a key role as the redox catalyst in the dissolution of sulfide minerals. Sulfide minerals are oxidized in the 3 general mechanisms: (1) direct application of oxygen, (2) by ferric ions, and (3) the action of microbes [5, 12, 35, 72, 75].

Iron acts as an important intermediary electron carrier in sulfide oxidation reactions, and pyrite is a key source of such iron. Although the detailed mechanism of the oxidization of

sulfide minerals at the surface of a dissolving sulfide grain are still in mystery and undecided, ferric iron dissolves sulfides 100–1000 times faster than oxygen under heap leach conditions (ambient or slightly elevated temperatures) according to published literature. In heap leaching, the low solubility of oxygen in water and the obstacle in replenishing oxygen from the gas phase to leaching solution in the deeper parts of heaps make the oxidation of iron by the direct action of oxygen limited. Mineral bioleaching is a combined chemical/microbial process [56, 72]. The main approach to the heap leaching treatment of such ores has been bioleaching. The function of bacteria is mainly to enhance oxidative leaching by iron (III) ions by bio-catalysis of the reoxidation of iron (II) by oxygen [56, 74-77, 92].

The chemical environment, gangue mineralogy, and particle effects in terms of size and fracturing also have mixed effects on the leaching chemistry involved in heap leaching. Therefore, species distribution study and ORP determination provide great tools to study in detail on the chemistry involved in the heap leaching process [14, 56].

For bioleaching process, the ferrous iron produced is re-oxidized back to ferric ion by iron-oxidizing microorganisms. Then, the leaching reaction is continuous in a complete cycle. Sulfur oxidizing microbes oxidize the sulfur species to sulfuric acid. The 2 main functions of the microorganisms in the solubilization of metal sulfides are to provide sulfuric acid for proton attack and to keep the iron in the oxidized ferric state for an oxidative attack on the mineral. From the latter, the microbial ferrous-iron oxidation to ferric-iron is considered as a critical sub-process in the bioleaching of sulfide minerals [13-17].

Ferric ion plays the key role of the oxidizing agent, and the ferric/ferrous ratio are the main determinants of redox potential in the bacterial leaching of sulfide minerals. Active iron

oxidizing bacteria, such as Acidithiobacillus ferrooxidans and Leptospirillum ferrooxidans, maintain high Fe^{3+}/Fe^{2+} ratios because of continuous oxidation as part of the respiratory leaching process. Ferric ion concentration in the medium plays an important role in the bioleaching process of sulfide [85, 92]. Additional ferric ions only enhance the initial leaching rates but not the final leaching yields. Studies found in literature concluded that Fe^{3+} concentration above 0.01 M does not affect chalcopyrite bioleaching kinetics [56, 65, 66, 92]. Fe can cause precipitation and heap clogging problems, and also a high concentration of Fe in the PLS will affect the extraction process and needs to be removed before SX. The chalcopyrite's leaching rate is mainly influenced by the concentration of ferric ion at concentrations lower than 0.01 or 0.1 M. At higher concentrations of ferric ion, the effect on leaching rate is negligible [56, 65, 66, 92]. Therefore, the speciation distribution of ferric ion in sulfate solutions is of great significance for the kinetics study.

Ferric ion plays an important role in the oxidation reaction, the reversible/redox potential of the ferric/ferrous couple, determined by the ferric/ferrous concentration ratio, has a key influence on leaching rate and passivation behavior. The concentration of ferric ion had very little influence on the oxidation rate and copper extraction was mainly affected by the redox potential of the solution (a function of the ferric/ferrous ratio) [65, 66, 92]. The published literature shows that a deep understanding of the factors affecting the real redox potential in PLS can help us develop a more efficient leaching process. Besides, the speciation study of the real ferric concentration/activity in PLS can enhance the study of the reduction behavior of ferric ions and further obtain its effect on the leaching rate. Accurate speciation of PLS is necessary for investigating the mechanism of industrial leaching process [65, 66, 92].

The redox potential of acidic iron sulfate solutions is one of the key operating parameters in leaching system. However, this potential is determined by the activity ratio of free ferric ion to free ferrous ion [34, 75, 92]. Iron (ferrous ions and ferric ions) plays an important role in the heap leaching of copper sulfide minerals, especially for ferric ions which are used to serve as oxidizing agent. Heap leaching is typically operated at about 10-32°C (typically optimum ~30°C) [1, 101-103].

Heap leach operations are located in different climate and different sites with changing temperature. Several heap leach operations recorded a recovery decrease in winter. The recovery rate drops greatly when the temperature drops below 5°C, which is shown in the lab column tests. Besides, the temperature decreasing makes solution viscosity increases significantly. Low leaching temperature negatively affects both the heap and the process plant. In a word, cold heaps tie up more process solution than warm heaps. Low temperature can be a problem in heap leaching. Low temperature in winter has great negative influence on the leaching rate and recovery percentage. The kinetics, iron chemistry, solution chemistry, pH, ferric/ferrous ratio, and ORP of PLS generated during leaching process below room temperature are rarely discussed and need to be further investigated [106].

Chemical reactions proceed more rapidly at higher temperatures. The rate of decomposition is sufficiently fast at 40 or 50°C for some minerals. An increase in temperature can also improve the yield of copper because the quantity of sulfur and other oxidation products that coat the mineral surface (passivation) is reduced. In bioleaching, different types of organisms dominate mineral degradation processes as the temperature changes. A comprehensive monitoring program at an industrial bioleaching heap at the Escondida mine in Chile since 2006 indicated

that an increase in heap temperature causes variation in microbial community from predominantly mesophilic to thermo-tolerant and moderately thermophilic species [1, 60, 106].

However, the temperature distribution in the heaps under different geographic locations or in the same heap but under different seasons is varying, and so does the temperature of pregnant leaching solution (typically containing 1–7 g/L Cu and 1–5 g/L Fe). The temperature, total iron, sulfuric acid concentration, and cupric ion concentration were chosen based on the industrial data [1, 84]. The ferric/ferrous ratios ranged from 0.25 to 6 in order to include the conditions published in the previous literature [1, 84, 101, 103].

The concentration of ions in solution has an effect on the ionic strength of the solution and hence on solution thermodynamics. High overall ionic strength will depress the activity of individual ions. By the same token the presence of high ionic strength also depresses the solubility of oxygen in solution. Thermodynamic modeling study is very helpful for the further investigation and deep understanding of the leaching kinetics and iron chemistry involved in the leaching process in order to increase recovery percentage and obtain higher leaching rate. All the compositions of the solution in the present work and nominal ferric/ferrous ratios were chosen base on the literature and industrial data [1, 84].

The higher concentration of sulfuric acid or lower pH leads to the increase of leach rate [92]. Lower pH values can minimize hydrolysis reaction and reduce the precipitation of Fe(III), and the positive effect caused by low pH is more obvious when the sulfuric acid is very concentrated at 3–5 M [56, 92]. Low pH levels in combination with high temperatures increase the leaching rate of chalcopyrite. In bioleaching, maintaining the pH in the preferred range between 1 and 2 is also important for ferric ion and acid regeneration by the microbial population. Thus, the capability to accurately predict leaching solution pH and acid consumption during copper ore

leaching is important for the evaluation of leaching performance and cost. pH has a significant effect on the dissolution process, controlling the oxidative activity of microorganisms. The bioleaching performance of mesophiles tends to deteriorate with increasing acidity from pH 2.0 to 1.2. Increased acid concentrations in industrial raffinate solutions of the heap bioleaching process at Minera Escondida Ltd. (MEL)-Antofagasta, Chile, produced changes in the distribution and activity of the microbial population present in the process [56, 92, 106].

The present work was initiated to carry out a solution speciation study in order to better understand the factors affection the leaching process and explore the optimum conditions for improving the leaching rate and enhancing copper recovery. Speciation analysis of the acidic iron sulfate solution system can investigate the formation/distribution of the complexes and exert their influence on the overall leaching process through obtaining more detailed thermodynamic data for the calculation of activity coefficients and equilibrium constants, especially the data below room temperature as low as 5°C. Besides, the previously developed model was validated through the comparison of the calculated ORP based on model and experimental ORP and the comparison of the species distribution in this work and the species distribution in other published literature. The comparison of the calculated ORP based on the previously developed expression demonstrated that the expression can still be used to accurately predict the ORP of the ferric/ferrous couple in these more complex solutions and different temperature range (from 5 °C to 45 °C) for the understand the iron chemistry in the ferric-dominant or ferrous dominant solutions.

2.1.2 SX and Traditional Cu EW

After heap leaching, SX is a core process in copper hydrometallurgical industry, providing highly conductive and high concentration copper electrolyte for Cu EW circuit where high-

purity cathodic copper is deposited on the surface of the cathode. SX process are made of two primary processes of extraction and stripping. Firstly, cupric ion is loaded to organic extractants from impure leach liquors. After the loading, cupric ion is transferred to the strip circuit where copper is unloaded into aqueous phase and contacted with Cu spent electrolyte solutions (~190 g/L H_2SO_4 and ~35 g/L Cu) recirculated from Cu EW tank-house. Finally, the Cu-enriched electrolyte mixed with a bleed of recirculating electrolyte from Cu EW tank-house, known as Cu advance electrolyte solutions (~50 g/L Cu and ~170 g/L H_2SO_4), is sent forward to EW cells for the electrodeposition of high-purity metallic copper onto the cathode [1, 101, 103].

Besides the detailed composition of SX-EW industrial solutions, the iron species behavior and their valence distribution in SX-EW solution (~190 g/L H_2SO_4 and ~50 g/L Cu) has not been thoroughly investigated. Iron chemistry and ORP are important tools to study the species distribution of Fe(II and III) and Cu(II) and better understand the solution chemistry in industrial SX-EW solutions at different temperatures.

What's more, in the paper of Krishna and Das, the effect of electrolyte circulation rate and electrolyte copper concentration on the current efficiency and copper deposit quality was investigated in order to increase operating current density in the copper electrowinning cell. Krishna and Das changed the current density i from 300 to 450 A/m^2 with the copper concentration of 30, 35, 40 g/L [108]. Increasing the copper concentration in the electrolyte resulted in compact deposits. During the formation of these rough cathode, it was noted that the current efficiency fell with increasing current density at constant copper electrolyte concentrations and fell with decreasing copper concentrations at constant current densities [8].

Moreover, in the traditional copper electrowinning process, oxygen is evolved at the anode, resulting in acid mist, and copper is reduced at the cathode simultaneously. Ferric ion

concentration in the copper electrowinning electrolyte (with total iron of 1-4.4 g/L) reduces the current efficiency significantly. Based on the published results, the current efficiency decreases linearly with increasing ferric ion concentration and the energy consumption increase was mainly caused by the decrease in current efficiency. It is clear that iron chemistry is very important for the traditional Cu EW process [4, 47, 52, 59].

To reach the goals of highest current efficiency (CE) and lowest energy consumption (EC), it is necessary to understand the effect of the various parameters affecting the production of copper cathodes and the effects of the possible interactions existing between them [2]. A.M. Alfantazi's work has shown that higher copper concentration has positive effect on increasing CE and decreasing EC [7]. In Y.Khouraibchia's work, increasing ferric concentration causes a significant linear decrease in current efficiency and a linear increase in energy consumption(EC) [52]. Increasing copper concentration results in a non-linear increase in current efficiency and non-linear decrease in energy consumption (EC) [3]. In published literature, Chino SX-EW plant in New Mexico, USA, consisted of west lead anodes tank-house and east alternative anodes tank-house with its own rectifier have the current density varied from 15 to 30 amperes/square feet, electrolyte temperature 35℃, lean electrolyte of 34g/L copper, 187g/L sulfuric acid, and 3g/L iron. [1].

The composition of synthetic new energy-saving Cu EW solutions was selected according to the published work [1, 39, 47]. Based on the published data, the solutions involved in the new energy-saving Cu EW process typically contain 34–50 g/L Cu, 30 g/L iron in total and 160–200 g/L sulfuric acid with temperature ranging from 40°C to 55°C. The temperature ranging from 25°C to 60°C can include all the conditions in above-mentioned literature [101,

103]. In S. Sandoval's work supported and funded by Freeport-McMoRan, 38g/L Cu, 27g/L Fe^{2+}, 3.5g/L Fe^{3+}, 180g/L sulfuric acid, temperature 51.1 °C degree was chosen [10].

2.1.3 Anode Material and Energy Consumption

The anodes were widely investigated with the development of alternative anodes and coated conventional anodes. In 2006 Freeport-McMoRan Copper & Gold Inc. (FCX) Technology center in Safford, Arizona, tried various opportunities in its SX-EW Test Facility to replace conventional Pb-Ca-Sn anodes in copper electrowinning process with alternative anode that would decrease energy consumption and remove lead contamination for the copper electrowinning circuit [1]. Another challenge from the copper electrowinning is the huge cost of producing and recovering unusable acid in the consideration of the economics of this process. Gerald L. May and Bill Imrie investigated potential reductants and the possibility of salable acid products [2].

To search for a suitable anode alternative to conventional Pb-Ca-Sn anodes which operate at relatively high OER over-potential, resulting in significant energy consumption and corrosion during copper electrowinning, Pb-Sb and Pb-Co alloy anodes and Pb/Pb-Sb, Pb/Pb-Co and Pb/Pb-Co_3O_4 composite anodes have been prepared [53]. Aluminum has a lower cost, density, and electrical resistivity than lead which is probably to reduce the bath voltage and weight used as the substrate Al/Pb-Sn anodes [53, 54].

Sb can decrease OER overpotential of anodes for copper electrowinning. As the Sb content is sufficiently low, there is no interconnecting network of Sb and corrosion is reduced. But higher Sb content reduces corrosion resistance of Pb-Sb anodes used in copper electrowinning [53-57].

Besides the important selection of suitable anode material, energy consumption in a copper

electrowinning cell is also of significant importance for improving the industrial process of Cu EW and is affected by the composition and physicochemical properties of the electrolytes, such as density, viscosity and conductivity. Density and viscosity affect the heat and mass transfer conditions in the cell and thereby affect its energy consumption [3]. The presence of impurities not only affects the physicochemical properties of the electrolyte [4, 5], but also the deposit quality [6, 38] and its crystallographic orientation [39, 40]. The large existence of ferric ion could cause remarkable increase in energy consumption [1, 3].

As above-mentioned, the existence of ferric ion can remarkably lower the current efficiency [1]. But current efficiency could not be employed as the only predictor of Cu cathode quality. The production process of Cu EW should also take CE, cathode quality, cathode deposit morphology, crystal structure into consideration. Lots of experiments based on pure electrolytes tests should also be performed with the utilization of industrial electrolytes [9].

2.2 New Development in SX-EW Technology

2.2.1 New Development in SX and Traditional Cu EW

There is a strong tendency to research and develop the new technologies for copper extraction, such as hydrometallurgical methods from the standpoints of environmental protection and resource recycling which can be competitive with conventional pyrometallurgical processes. Nowadays, more than 20% of the world's total copper production is through solvent extraction (SX) as a desirable process for metal winning from the viewpoints of natural resources and energy conservation [1, 109].

Hydroxyoximes have been the most important and applicable extractants for copper extraction among other types. Today modified aldoximes and aldoxime–ketoxime mixtures are the most widely used copper extractant systems [109].

Kinetic investigations are of major importance for the optimization and control of extraction processes to reveal the mechanism of the extraction process [110]. Finding methods to improve the extraction rate via the investigation on kinetics is interesting. In addition, design of commercial solvent extraction process needs detailed and exact information about extraction kinetics [110].

In the traditional copper electrowinning process, the oxygen bubbles that are produced at the anodes rise to the top of the electrolyte where they burst into the atmosphere, carrying tiny droplets of sulfuric acid with them. This can create a corrosive, unpleasant, and unhealthy environment in the tank house, and may cause health problems for operators [1]. For these reasons, many researchers developed ferric/ferrous anodic reaction in order to replace oxygen emission anodic reaction and delete this acid mist [2].

A new technology, known as SELE, is in operation in Chile [3]. This comprises a plastic rack that is inserted into each cell with grooves into which each cathode slides. This avoids the need for edge strips and allows the cathodes to be kept very straight, vertical, and evenly spaced, which means that current distribution is even throughout the tank house and higher current densities can be employed [1].

New developments in EW are dominated by improving energy efficiency and producing high purity copper at higher current densities [4-6]. Advances are being made in new anode materials that minimize voltage requirements [7-10]. Developments in hardware, software, automation, and robotic control promote improved tank house management, reduced labor requirements, and consistent production of high-quality copper [11].

The anodic oxidation of sulfate ions which are formed by the dissolution of sulfur dioxide in the aqueous electrolyte results in a reduction of 1.06 V versus the Standard Hydrogen

Electrode (SHE) from the reversible half-cell potential for oxygen evolution (1.23 V versus SHE) [6].

In the traditional Cu EW process, the emission of oxygen takes places at the anode, and element copper is deposited at the cathode. As is known that iron in the electrolyte in copper electrowinning cell (with total iron of 1-4.4 g/L) plays an important role in reducing the current efficiency. According to the published results [4, 82, 91], the current efficiency decreases linearly with increasing ferric ion concentration and the energy consumption increase was mainly caused by the decrease in current efficiency.

2.2.2 New Development in Novel Cu EW

Furthermore, in recent years, a novel electrowinning technology in acidic sulfate solution has been proposed by replacing the traditional anodic reaction, oxygen evolution by the decomposition of water, with a new reaction, oxidizing ferrous to ferric [4, 10]. The major advantages involved in such a new process are lower energy consumption and complete elimination of acid mist, due to the fact that the anodic potential is much lower and no oxygen generated in the anode. Although significant progress has been made for this technology, additional studies are required to modify and improve the current technology, in order to further increase the current efficiency, decrease the cell voltage and reduce the operating costs [41].

Conventional elemental sulfur could give out to 6 electrons that is sufficient to reduce 3 ferric ions. Therefore, each elemental sulfur atom could produce 3 elemental copper atoms. This reaction also shows that the excess H^+ produced is one mole of acid for each 3 moles of Cu produced or 1/3 of the excess acids produced by the SO_2 reduction. The overall reduction reaction using elemental sulfur could be express as: $6Fe^{3+} + S + 4H_2O=H_2SO_4+6H^++6Fe^{2+}$. With the elemental sulfur as the reducing agent, orthorhombic and liquid sulfurs were used.

The results show that sulfur reduces the ferric ion concentration from 1.5g/L to approximately 0.04g/L in 2 hours at 100℃ or 0.1g/L in 4 hours at 50℃ [1, 2]. Hydrogen gas is a significant potential candidate for ferric ion reduction except for its explosion risk. Platinum-coated graphite was evaluated to determine if the presence of platinum on the graphite particles helped the ferric ion reduction process in the presence of 2% hydrogen gas in argon. The platinum was coated by electrolysis deposition. However, a complete coating was not achieved. The test results showed a significant normalized rate of reduction occurred with 2.58 grams of Fe^{3+} reduced per liter of solution per hour per meter square of catalyst surface area per liter of hydrogen gas [1-3].

Carbon anodes was not effective for the anodic oxidation of SO_2 [10]. A novel graphite anode was designed for copper electrowinning. A mixture of air and 12-15% SO_2 was sparged through porous graphite anode [11].

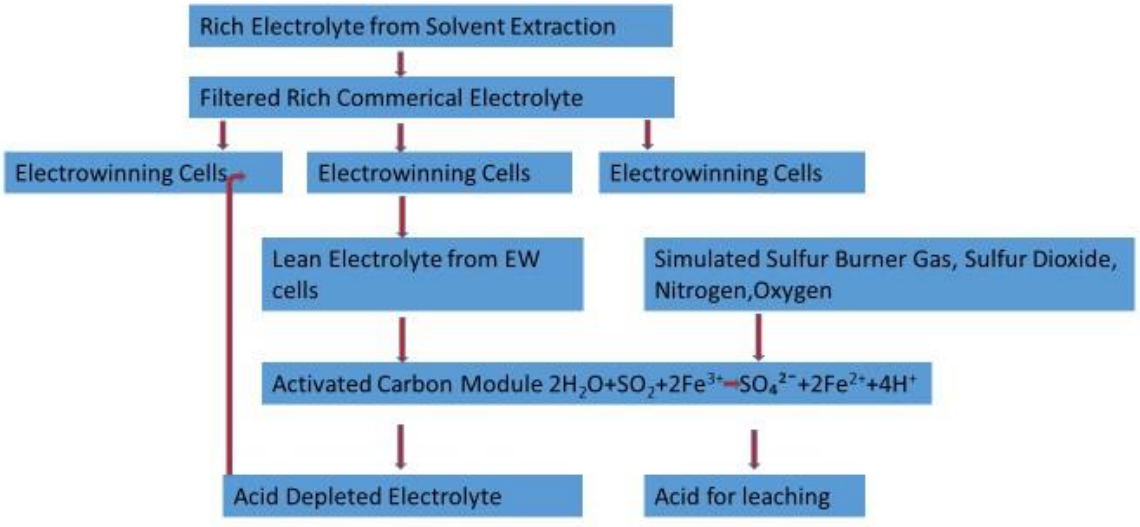

Figure 2-1 SX-EW process

3. OBJECTIVES

The overall objective of this investigation is to validate the applicability of the previously developed equation to accurately and reliably predict the ORP of ferric/ferrous couple and also conduct the species distribution study with the contribution to the understanding of iron chemistry in more complex acidic iron sulfate solutions containing cupric ion generated during the hydrometallurgical extraction of copper.

Although iron (ferrous ion and ferric ion) plays an important role in the heap leaching of copper sulfide minerals and copper electrowinning, most of the published literature is focused on the anode electrode material, the improvement of current efficiency, electrowinning cell design, and very few literatures are related to the accurate determination of ferric/ferrous couple and the iron behavior. However, it has shown that the determination of the redox potential of ferric/ferrous couple and species distribution study are highly useful to estimate and understand the iron chemistry of industrial hydrometallurgical extraction processes of copper.

In view of the preceding discussion, the specific objectives of this thesis are designed as follows:

(1) Extend the broader range of application of the previously developed equation to predict ORP of ferric/ferrous couple in the simulated more complicated solutions generated during leaching, SX, traditional Cu EW, and Novel Cu EW.

(2) Provide the developed model as a mathematical tool capable of quantifying the concentrations of free ions and complexes in terms of temperature and various solution composition under simulated industrial hydrometallurgical aqueous systems.

This thesis contributes the research on aqueous speciation study of acid iron sulfate solutions and the understanding of iron chemistry for the hydrometallurgical extraction of copper.

As mentioned in the previous section, thermodynamic modeling of Fe(II)–Fe(III)–H_2SO_4–H_2O system and Fe(II)–Fe(III)– Cu(II)–H_2SO_4–H_2O system has been carried out under conditions related to leaching and electrorefining [2, 12]. In this work, this will be further employed the methods developed previously to evaluate the possibility of extending its applicability to conditions most relevant to the industrial SX/EW process. Details for the model development could be found in the previous publication. Only the key additional information will be provided in the following.

The calculated equilibrium formation constants of main reactions in this study from 5 to 60 °C were shown in Table 2-1, Table 2-2. Information such as species concentrations and redox potentials can thus be obtained or calculated [2, 12].

Additionally, an expression Eq. (1) was developed to accurately predict redox potential in the H_2SO_4–$Fe_2(SO_4)_3$–$FeSO_4$–H_2O solutions only based on nominal ferric/ferrous ratio and temperature. From previous results it seems that this new expression could be extended to more complicated acidic iron sulfate solutions with or without copper [2], [13, 14]. Thus, this expression was applied to compare calculated potentials with experimental potentials in this work.

4. METHODOLOGY AND EXPERIMENTAL PROCEDURE

In the present study, the overall composition of both pregnant leaching solutions, solvent extraction solutions, traditional copper electrowinning solutions, and novel copper electrowinning solutions was determined according to the operating conditions of industrial processes. The largest copper ion concentration and total iron concentration were limited to 55 g/L [1]. Experimental ORP measurements of the complicated synthetic solutions based industrial processes mentioned above were carried out at experiment temperature in comparison to the calculated ORP values for model validation. The accurate measurement of ORP values is of great importance for the understanding of iron chemistry and the improvement of current efficiency for industrial hydrometallurgical processes. The applicability of the equation below is validated and extended when the concentrations of the compositions of the studied solutions, nominal ferric/ferrous ratio and temperature change a lot [95, 101-103].

4.1 Thermodynamic Modelling and Distribution of Species in Acidic Iron Sulfate Solutions

Iron (ferrous ion and ferric ion) plays an important role in the heap leaching of copper sulfide minerals and copper electrowinning. It is obvious that the distribution of iron and the redox potential in acidic iron sulfate solution is one of the most important parameters in various hydrometallurgical solutions. Hence, in a previous work, a thermodynamic model was developed and shown to reliably simulate the speciation of the H_2SO_4-$Fe_2(SO_4)_3$-$FeSO_4$-H_2O system through a wide range of solution compositions and temperatures (25°C-150°C) where most of the hydrometallurgical processes of sulfide minerals operate [56, 65, 66, 95, 101]. It is proved that ORP employed to understand the iron chemistry of industrial processes could accurately be determined solely by the variables of temperature and nominal ferric/ferrous ratio.

$$E(\mathrm{mV}) = -1\times10^{-3}\times[T(\mathrm{K})]^2 + 0.91\times T(\mathrm{K}) + \frac{2.303R}{nF}\times T(\mathrm{K})\times10^{3}\times\log\frac{C_{\text{ferric, nominal}}}{C_{\text{ferrous, nominal}}} + 492 \qquad (1)$$

There are still some interesting questions requiring further study regarding the broader range of applicability of the previously developed equation. Especially, it is of interest to determine whether this equation remains applicable under heap leaching conditions (especially for the pregnant leaching solutions in industrial operations at temperatures lower than 25 °C), and in the above-mentioned electrowinning solutions with much higher concentration of copper ion (up to 55 g/L) [95, 101-103].

When Fe and Cu sulfates are dissolved into sulfuric acid solutions, they usually distribute as soluble species including simple cations, simple anions, neutral species, charged ionic complexes, and precipitates. What's more, some existing factors have great effects on the equilibrium state of those solution systems, such as various solvents, species activities, concentrations, temperature, solubilities, and electric motive force. Due to the lack of analytical tools for in situ measurements of ions and ionic complexes, especially at too low and too high temperatures, thermodynamic modelling with experimental validation is a very helpful and important method to predict the behavior of inorganic species in complex aqueous systems and then complete the analysis of the useful data [101-103].

The Iron behavior in solutions generated during hydrometallurgical production of copper has not fully understood yet, especially with co-existence of the high concentration of cupric ion and sulfuric acid. What's more, the determination of the concentration ratio of Fe(III) to Fe(II) in simulated solutions based on industrial processes is still a challenge because of the interference from other ions and complexes, resulting in great uncertainty of the predominant

valence of Fe. There are very few publications available on the valence distribution on Fe during Leaching, SX, Cu EW processes [95, 101-103].

To determine the variables impacting on the leaching, SX, Cu EW processes from Fe and then establish the optimal conditions, it is very important and necessary to develop the solution speciation study. Although few publications have already studied the speciation of relevant aqueous solutions to quantify species distribution over a wide range of temperatures and pH by numerical thermodynamic modeling in H_2SO_4-$Fe_2(SO_4)_3$-$FeSO_4$-H_2O systems on the basis of industrial copper production processes during leaching, electrowinning, and electrorefining, the speciation study of the H_2SO_4-$CuSO_4$-$Fe_2(SO_4)_3$-$FeSO_4$-H_2O systems over a wide range of temperature has not been investigated. Therefore, a detailed speciation study of the solutions generated during hydrometallurgical production of copper is required to first quantify the species distribution of Fe and Cu in the H_2SO_4-$CuSO_4$-$Fe_2(SO_4)_3$-$FeSO_4$-H_2O systems (including concentration and valence distribution of every element) [65, 66, 95, 101-103].

Table 4-1 Standard and calculated equilibrium constants for the main species in aqueous Fe(III)-Fe(II)-Cu(II)-H_2SO_4-H_2O solutions (PLS) from 5°C to 45°C by Criss-Cobble method

Species and Formation Reactions	Log K_f° 5°C	Log K_f° 10°C	Log K_f° 15°C	Log K_f° 20°C	Log K_f° 25°C	Log K_f° 30°C	Log K_f° 35°C	Log K_f° 45°C
$H^+ + SO_4^{2-} \leftrightarrow HSO_4^-$	1.75	1.81	1.87	1.93	1.98	2.06	2.13	2.27
$Fe^{2+} + H^+ + SO_4^{2-} \leftrightarrow FeHSO_4^+$	0.34	0.53	0.72	0.90	1.08	1.25	1.42	1.75
$Fe^{2+} + SO_4^{2-} \leftrightarrow FeSO_4$°	2.09	2.13	2.17	2.21	2.25	2.29	2.33	2.42
$Fe^{3+} + H^+ + SO_4^{2-} \leftrightarrow FeHSO_4^{2+}$	1.56	1.80	2.03	2.26	2.48	2.69	2.90	3.30
$Fe^{3+} + 2SO_4^{2-} \leftrightarrow Fe(SO_4)_2^-$	1.03	1.62	2.18	2.73	5.38	3.79	4.29	5.26
$Fe^{3+} + SO_4^{2-} \leftrightarrow FeSO_4^+$	3.40	3.57	3.73	3.88	4.04	4.19	4.35	4.65
$Cu^{2+} + SO_4^{2-} \leftrightarrow CuSO4$°	2.15	2.21	2.26	2.31	2.36	2.41	2.46	2.57
$Cu^{2+} + H^+ + SO_4^{2-} \leftrightarrow CuHSO_4^+$	1.59	1.79	1.98	2.16	2.34	2.52	2.69	3.02

Table 4-2 Standard and calculated equilibrium constants for the main species in aqueous Fe(III)-Fe(II)-Cu(II)-H_2SO_4-H_2O solutions (synthetic SX, traditional Cu EW, novel Cu EW electrolytes) from 25°C to 60°C by Criss-Cobble method

Species and Formation Reactions	Log K_f° 25°C	Log K_f° 35°C	Log K_f° 40°C	Log K_f° 45°C	Log K_f° 50°C	Log K_f° 55°C	Log K_f° 60°C
$H^+ + SO_4^{2-} \leftrightarrow HSO_4^-$	1.98	2.13	2.2	2.27	2.34	2.41	2.49
$Fe^{2+} + H^+ + SO_4^{2-} \leftrightarrow FeHSO_4^+$	1.08	1.42	1.59	1.75	1.91	2.07	2.22
$Fe^{2+} + SO_4^{2-} \leftrightarrow FeSO_4$°	2.25	2.33	2.37	2.42	2.46	2.50	2.54
$Fe^{3+} + H^+ + SO_4^{2-} \leftrightarrow FeHSO_4^{2+}$	2.48	2.9	3.11	3.30	3.50	3.68	3.87
$Fe^{3+} + 2SO_4^{2-} \leftrightarrow Fe(SO_4)_2^-$	5.38	4.29	4.78	5.26	5.73	6.18	6.62
$Fe^{3+} + SO_4^{2-} \leftrightarrow FeSO_4^+$	4.04	4.35	4.50	4.65	4.79	4.94	5.08
$Cu^{2+} + SO_4^{2-} \leftrightarrow CuSO4$°	2.36	2.46	2.52	2.57	2.62	2.67	2.72
$Cu^{2+} + H^+ + SO_4^{2-} \leftrightarrow CuHSO_4^+$	2.34	2.69	2.86	3.02	3.18	3.34	3.49

The accuracy and success of speciation modelling mainly rely on the accuracy of the thermodynamic property (such as Gibbs free energy and entropy) for all related species in the studied aqueous system. These related thermodynamic properties contain standard Gibbs free energy and entropy of every species to calculate and obtain the equilibrium constants from 5 to 60 °C and the species activity coefficients to explain the non-ideal thermodynamic behavior [111-117].

This special experiment design is to validate the application of the equation to accurately and reliably to predict the redox potentials of ferric/ferrous couple in various complicated conditions of high concentration of cupric ion, acidity, total iron, and different nominal

ferric/ferrous ratios. Besides the validation of the equation, a detailed discussion related to the species distribution between 2 aqueous systems prior and after the addition of copper sulfate, addition with temperature, pH, ionic strength, and nominal ferric/ferrous ratios will be presented in this thesis. This research work will help the further investigation of speciation study of more complicated solutions in other hydrometallurgical processes [95, 101-103].

The nominal ferric/ferrous ratio in this paper is the ratio of the initial total ferric to initial total ferrous added when preparing the solution. The real ferric/ferrous ratio in the electrolyte is typically lower than its corresponding nominal ferric/ferrous ratio after speciation calculation, and details for this could be found in previous publications [56, 65, 66, 95, 101-103].

4.2 Measurements of the Oxidation-Reduction Potential of the H_2SO_4-$Fe_2(SO)_3$-$FeSO_4$-H_2O System from 5℃ to 60℃

4.2.1 Electrolyte preparation

In the present study, the overall composition of PLS, SX solutions and Cu EW solutions was determined according to the operating conditions of industrial processes. The detailed information is shown in Tables 5-1, 5-2, 5-3 and 5-4 below.

Deionized water (≥ 18MΩ), sulfuric acid (H_2SO_4, 96.1%, Fisher Chemical), iron (III) sulfate pentahydrate ($Fe_2(SO_4)_3 \cdot 5H_2O$, 97%, Acros), iron (II) sulfate heptahydrate ($FeSO_4 \cdot 7H_2O$, 99+%, Acros), copper sulfate pentahydrate ($CuSO_4 \cdot 5H_2O$, 98+%, Acros) were utilized to prepare the designed pregnant leaching solution and copper electrowinning solution. In the preparation of copper electrowinning solution, 101.8 mL H_2SO_4 (transferred by graduated pipette gradually) was dissolved in deionized water.

4.2.2 Electrode preparation

The details of the process of Pt working electrode's whole assembly, the mounting of the Pt electrode (purchased from Sigma-Aldrich) in epoxy resins (MG Chemicals), the activation in a 0.1 M sulfuric acid solution prior to electrochemical measurements could be found in the published literature [65, 66]. Prior to each test, the graphite counter electrode was immersed in ethanol for degreasing, rinsed with deionized water, and finally dried with cool air [56, 65, 66, 95, 101-103].

4.2.3 Electrochemical measurements at 5℃, 10℃,15℃, 20℃ and 25℃

In order to conduct the electrochemical experiments below room temperature, coolant polycool EG25 purchased from PolyScience (50/50 mix with deionized water) was used to fill

the tank of our PolyScience Circulating Bath and the coolant could help control cell temperature below room temperature very well [101-103].

4.2.4 Electrochemical measurements at 25℃, 30℃, 35℃, 45℃, 50℃, 55℃, and 60℃

In the present study, all of the electrochemical experiments were carried out utilizing a standard three-electrode cell with a thermostated water jacket. The pre-activated Pt electrode was the working electrode (WE) and the graphite rod served as the counter electrode (CE). A saturated Ag/AgCl electrode (saturated with KCl, Accumet* Glass Body, Fisher Scientific) was utilized as a reference electrode (RE). All potentials have been converted from Ag/AgCl to the standard hydrogen electrode (SHE). In this study, all potentials are quoted with respect to the SHE at 25 °C unless otherwise stated. Detailed information about this procedure could be found in the previous publication [56, 65, 66, 95, 101-103].

4.2.5 Correction of the measured potentials to SHE at 25℃

The measured redox potentials of the test solutions designed according to industrial process were compared with the calculated solution redox potentials by Eq. (1). Please note that all of the potentials E(mV) calculated by this equation refer to SHE at 25°C. Furtherly, the measured redox potentials should also be corrected to SHE at 25°C by the method published previously [65, 66], [95]. The two equations involved in the correction procedure are as follows:

$$E_{SHE}(T) = E_{obs} + E_{correction} = E_{obs} + E_{Ag/AgCl}(T) - \Delta E_{th} \quad (2)$$

$$E_{SHE}(25°C) = E_{SHE}(T) + \Delta E_{SHE} \quad (3)$$

Detailed values of $E_{Ag/AgCl}(T)$ (the isothermal potential of reference Ag/AgCl electrode) versus the SHE could be found in the literature. What's more, the details of Eq. (1), Eq. (2),

and Eq. (3) on electrochemical calculation could be found in the published literature [65, 66, 95].

5. VALIDATION OF EQUATION TO PREDICT THE ORP FROM 5℃ TO 60℃

5.1 Introduction

It is well-known that iron (ferric or ferrous) ions are widely involved in the hydrometallurgical production of non-ferrous metals, such as Cu, Au and Zn, mainly in the form of acidic iron sulfate solutions. As far as Cu is concerned, in a typical leaching-solvent extraction-electrowinning process, ferric ion plays a central role in the heap leaching process and is reduced to ferrous ions in the pregnant leaching solution. Ferric ion is the most important surrogate oxidant and the dissolved ferric/ferrous couple plays an important catalytic role in accelerating the leaching rate with oxygen as an oxidant [1, 65, 66, 95, 101-103].

In our previous study, a novel oxidation-reduction potential (ORP) equation only based on the variables of temperature and nominal ferric/ferrous ratio was developed to predict the redox potential of the quaternary H_2SO_4-$Fe_2(SO_4)_3$-$FeSO_4$-H_2O system, and its applicability was also extended to more complex acidic iron sulfate solutions. In this chapter, the broader range of applicability of this equation to other complicated acidic iron solutions containing cupric ions has been extended and determined. Specifically, synthetic iron-containing solutions with copper ions according to the conditions of industrial electrolyte generated during heap leaching, solvent extraction, traditional copper electrowinning and novel copper electrowinning have been used to measure the ORP and test the developed equation. It seems that this equation can still be employed to predict the redox potential of the Fe^{3+}/Fe^{2+} couple for the simulated solutions under conditions related to solvent extraction, traditional copper electrowinning, novel copper electrowinning and pregnant leaching solution generated during heap leaching over a wide range of solution concentration, nominal Fe^{3+}/Fe^{2+} ratio and temperature. It has shown that the prediction and measurement of redox potential is highly

useful to estimate and understand the iron chemistry of industrial leaching and electrowinning processes.

This thesis continues to provide new data on the extended validation of the expression developed previously, which can be used to predict the redox potential of the Fe^{3+}/Fe^{2+} couple in the acidic iron sulfate system. The heap leaching system, solvent extraction and electrowinning solutions were selected as the interest in the hydrometallurgical production of copper and development of energy-saving electrowinning technology has steadily increased. Synthetic acidic iron solutions containing copper according to the composition of industrial electrolyte generated during heap leaching, solvent extraction and electrowinning were prepared and its ORP were measured. It is demonstrated that the previously proposed expression can still be used to predict the redox potential of the Fe^{3+}/Fe^{2+} couple in the above-mentioned solutions under lower temperatures and with much higher concentration of copper.

5.2 Results and Discussion

5.2.1 Comparison between the measured potentials and calculated potentials for PLS from 5℃ to 45℃

Table 5-1 Compositions of synthetic PLS, g/L generated during heap leaching process

Test	$[H_2SO_4]$	$[Fe^{3+}]$	$[Fe^{2+}]$	$[Fe]_{total}$	$[Cu^{2+}]$	Nominal $[Fe^{3+}]/[Fe^{2+}]$
#1	4	4.2857	0.7143	5	0	6
#2	4	3.1252	1.8748	5	0	1.67
#3	4	3	2	5	0	1.5
#4	4	2	2	4	0	1
#5	4	1	4	5	0	0.25
#6	4	4.2857	0.7143	5	5	6
#7	4	3.1252	1.8748	5	3	1.67
#8	4	3.1252	1.8748	5	5	1.67
#9	4	3.1252	1.8748	5	7	1.67
#10	4	3	2	5	5	1.5
#11	2	2	2	4	5	1
#12	4	2	2	4	5	1
#13	7	2	2	4	5	1
#14	4	0.6	2.4	3	5	0.25
#15	4	1	4	5	5	0.25
#16	4	1.6	6.4	8	5	0.25

Iron (ferrous ions and ferric ions) plays an important role in the heap leaching of copper sulfide minerals, especially for ferric ions which are used to serve as oxidizing agent. Heap leaching is typically operated at about 10–32°C (typically optimum 30°C) [1].

However, the temperature distribution in the heaps under different geographic locations or in the same heap but under different seasons is varying, and so does the temperature of pregnant leaching solution (typically containing 1–7 g/L Cu and 1–5 g/L Fe). Besides the various leaching temperatures, there are very few data published about the ORP test and speciation study at the low temperature below 25°C. Therefore, it is very important and valuable to conduct the validation of Equation (1) and species distribution study below the room temperature.

The temperature, total iron, sulfuric acid concentration, and cupric ion concentration were chosen based on the industrial data from one published book [1]. The ferric/ferrous ratios ranged from 0.25 to 6 to cover the conditions published in the previous literature [1, 84].

From Eq. (1), it is shown that the redox potential of the acidic iron sulfate system can be solely determined by the nominal ferric/ferrous ratio and temperature. A comparison between the ORP measured in this work and those predicted by the Eq. (1) was used to validate the applicability of Eq. (1). All the solution compositions and temperatures are listed in Table 5-1. The measured potentials after correction to SHE at 25°C, as well as the calculated ORP by Eq. (1) are shown in Table 5-2 as well. For better comparison, those values under various conditions are demonstrated in Figure 5-1.

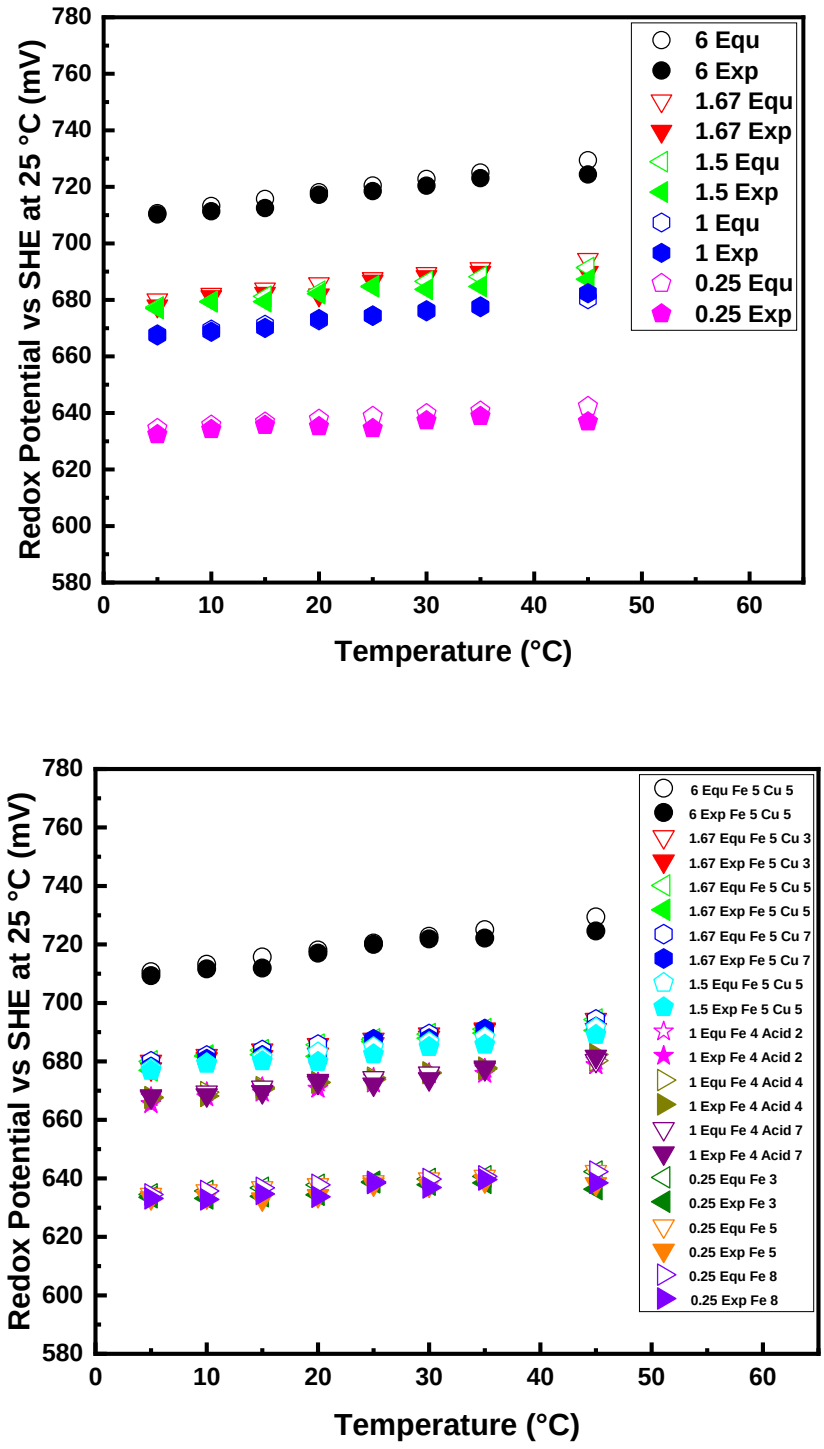

Figure 5-1 Comparison of the potentials calculated by the Equation (1) and the potentials measured by experiments (a) in the Fe(II)-Fe(III)-H_2SO_4-H_2O solutions for Test #1-#5 and (b) in the Fe(II)-Fe(III)-Cu(II)-H_2SO_4-H_2O solutions for Test #6-#11 with nominal Fe^{3+}/Fe^{2+} ratios ranging from 0.25 to 6 in the temperature range of 5-45°C. Detailed solution information about synthetic PLS was determined according to the published literature [1], [84]

Table 5-2 and Figure 5-1 clearly show that the calculated redox potentials by Eq. (1) and the measured redox potentials with various solution chemistry in the temperature range of 5-45°C are in good agreement. The differences are typically within 3 mV. These results indicate that the accuracy of the redox potential predicted by Eq. (1) is acceptable over a wider range of solution compositions and conditions, especially when temperatures are lower than 25°C. Eq. (1) can thus be used to predict the ORP for the PLS generated during heap leaching, even at low experiment temperature of 5, 10, 15, and 20 °C. The equation can be useful and applicable under lower temperature as well. It can also be potentially used to understand the iron chemistry and facilitate the study of the kinetics/mechanism analysis based on the total iron, nominal ferric/ferrous, temperature and measured ORP [56, 65, 66, 95, 101-103].

However, when employing the measured redox potential to predict the nominal ferric/ferrous ratio based on Equation (1) for the understanding the iron chemistry in the PLS, especially when temperatures are lower than 25°C, it is highly recommended that the error for the measured redox potential is within 4 mV. Otherwise, there will be a large error for the calculated nominal ferric/ferrous ratio based on the measured redox potential. Because the nominal ferric/ferrous ratio is more sensitive. Even a very small deviation in measured redox potential will cause a large error for the predicted nominal ferric/ferrous ratio. More attention should be paid to the experimental measurement of the redox potential in the lab when considering for the utilization of Equation (1) to understand the iron chemistry in the PLS. For example, the nitrogen gas should be purged into the PLS for at least 25 minutes before any electrochemical test in order to ensure that there is almost no existing dissolved oxygen molecule inside the PLS; the temperature controller should be working steadily, reliably and accurately; the Pt working electrode should be kept in the excellent no-dust environment and be completely cleaned before running

electrochemical test; the reference electrode should be calibrated by standard solution every time; the systematic error should be eliminated [56, 65, 66, 95, 101-103].

It has been published that the nominal Fe^{3+}/Fe^{2+} ratio and temperature are the only 2 variables in the previously developed expression in easily and accurately determining the values of ORPs in the aqueous $FeSO_4$-$Fe_2(SO_4)_3$-H_2SO_4 system and $FeSO_4$-$Fe_2(SO_4)_3$-$CuSO_4$-H_2SO_4 system up to 150 °C [56, 65, 66, 101-103]. Compared with those previously published results, much lower acidity (2-7 g/L sulfuric acid), lower copper concentration (3-7 g/L cupric ion), different total iron (3-8 g/L), and lower temperature (as low as 5 °C) were employed in the present work in order to validate and extend the applicability of the previously developed expression.

In Figure 5-1 a and Figure 5-1 b, the results show that the measured ORPs are always in good agreement with those calculated by the previously developed expression for both aqueous Fe(II)-Fe(III)-H_2SO_4-H_2O solutions and Fe(II)-Fe(III)-Cu(II)-H_2SO_4-H_2O solutions in all the conditions. The deviation of the redox potential between expression prediction and experimental measurements in both solution systems is usually less than 3 mV under all the solution condition. It is suggested that the addition of Cu(II), different concentration of sulfuric acid, different total iron has no obvious influence on the applicability of this expression.

It is proved that the addition of cupric ion or not, different total iron, different concentrations of sulfuric acid/cupric ion have no obvious contribution to ORPs based on the above discussion.

5.2.2 Comparison between the measured potentials and calculated potentials for SX solutions from 25℃ to 60℃

SX provides the method for producing pure, concentrated Cu electrolytes from dilute, impure leach liquors, which is very crucial process for the more and more important combined technology of SX-EW for hydrometallurgy extraction of copper. SX flowsheets employed in

purifying of copper leach liquors consist of 2 essential continuous processes of extraction and stripping. In the stripping process, the Cu-loaded organic phase is contacted with a strong acid spent electrolyte with the sulfuric acid concentration of 175-190 g/L from the EW circuit, which strips Cu from the organic phase into the electrolyte [1]. The solutions involved in SX process typically contain 30-40 g/L cupric ion with temperature ranging from 25 to 40°C. In present work, the experiment temperature ranging from 25 to 60°C and various compositions of prepared synthetic SX solutions can cover all the conditions in above mentioned literature.

Table 5-2. Compositions of synthetic SX solution

Sample	$[H_2SO_4]$	$[Fe^{3+}]$	$[Fe^{2+}]$	$[Fe]_{total}$	$[Cu^{2+}]$	Nominal $[Fe^{3+}]/[Fe^{2+}]$
#1	200	0.01	1	1.01	0	0.01
#2	200	0.05	3	3.05	0	0.0167
#3	200	1	1	2	0	1
#4	200	2	1	3	0	2
#5	200	4	0.1	4.1	0	40
#6	200	30	0.3	30.3	0	100
#7	200	0.01	1	1.01	30	0.01
#8	200	0.01	1	1.01	40	0.01
#9	200	0.05	3	3.05	30	0.0167
#10	200	0.05	3	3.05	40	0.0167
#11	200	1	1	2	30	1
#12	200	1	1	2	40	1
#13	200	2	1	3	30	2
#14	200	2	1	3	40	2
#15	200	4	0.1	4.1	30	40
#16	200	4	0.1	4.1	40	40
#17	200	30	0.3	30.3	36	100
#18	200	30	0.3	30.3	38	100

However, the composition of solutions from the Cu-depleted organic phase/the Cu-enriched aqueous phase (both from strip circuit) and the raffinate (from extraction circuit). The temperature, total iron, sulfuric acid concentration, and cupric ion concentration were chosen based on the industrial data from one published book [1]. The ferric/ferrous ratios ranged from 0.25 to 6 to cover the conditions published in the previous literature [1, 84].

According to the chapter 2 and equation (1), the redox potential of the acidic iron sulfate system can be accurately determined by 2 variables of the nominal ferric/ferrous ratio and experiment temperature. A comparison between the ORP values measured in chapter 5 of this thesis and those predicted by the equation (1) was employed to validate the applicability of this previously developed equation. All the solution compositions and temperatures are listed in Table 5-3. The measured potentials shown in Figure 5-2 are plotted after correction to SHE at 25°C, as well as the calculated ORP by Equation (1). For better comparison and analysis, those values under various conditions are demonstrated in Figure 5-2.

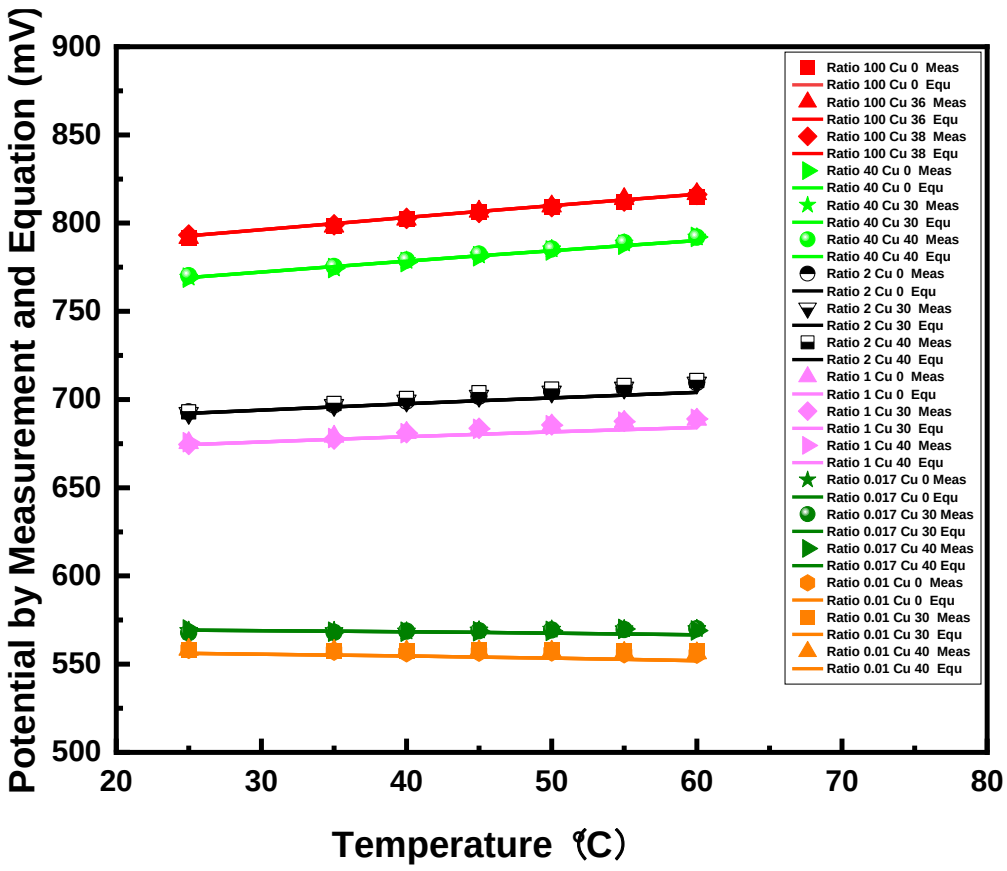

Figure 5-2 Comparison of the potentials calculated by the Equation in this work and measured by 18 experiments in synthetic solvent extraction (SX) solutions containing 0-40 g/L cupric ion, 200 g/L sulfuric acid, 1.01-30.3 g/L total iron with 6 different nominal Fe^{3+}/Fe^{2+} ratios in the temperature range of 25-60°C. Solution information was determined according to published literature [1]

Table 5-3 and Figure 5-2 clearly show that the calculated redox potentials by Eq. (1) and the measured redox potentials with various solution chemistry in the temperature range of 25-60°C are in good agreement. The deviation of the calculated ORP based on Equation (1) does not exceed 3 mV. The differences are typically within 3 mV. Furthermore, it is shown that the co-existence of cupric ion up to 40 g/L does not exert any obvious influence on the accurate prediction of redox potentials calculated by Equation (1). Based on the above analysis, the equation and the results could be used to understand iron chemistry and kinetics based on the measure ORP during SX

process. These results indicate that the accuracy of the redox potential predicted by Eq. (1) is acceptable over a wider range of solution compositions and conditions.

According to the analysis of Table 5-3 and Figure 5-2, Equation (1) can thus be used to predict the ORP for the complicated acidic solutions generated during solvent extraction. It can also be potentially used to understand the iron chemistry based on the total iron, nominal ferric/ferrous ratio, temperature and measured ORP [56, 65, 66, 95, 101-103].

5.2.3 Comparison between the measured potentials and calculated potentials for Traditional Cu EW solutions from 25℃ to 60℃

Table 5-3 Compositions of synthetic Traditional EW solution, g/L

Sample	$[H_2SO_4]$	$[Fe^{3+}]$	$[Fe^{2+}]$	$[Fe]_{total}$	$[Cu^{2+}]$	Nominal $[Fe^{3+}]/[Fe^{2+}]$
#1	180	3.5	1	4.5	0	3.5
#2	180	2.4	0.4	2.8	0	6
#3	180	3.5	1	4.5	45	3.5
#4	180	3.5	1	4.5	50	3.5
#5	180	3.5	1	4.5	55	3.5
#6	180	2.4	0.4	2.8	45	6
#7	180	2.4	0.4	2.8	50	6
#8	180	2.4	0.4	2.8	55	6
#9	180	1.2	0.1	1.3	45	12
#10	180	1.2	0.1	1.3	50	12
#11	180	1.2	0.1	1.3	55	12

Table 5-4. Results for solution in the traditional Cu EW process from 25 to 60°C

Chemical Analysis		Experimental results measured in the lab							Calculated redox potential by Equation		E_{SHE} (25°C) E_h
Tests	Assays	Fe_{total} g/L	Fe^{3+} g/L	Fe^{2+} g/L	Cu^{2+} g/l	H_2SO_4 g/l	T (°C)	E_h (obs) mV	Fe^{3+} /Fe^{2+} (nominal)	E (Calc) mV	E (Meas) mV
1	1	1.3	1.2	0.1	45	200	25	542.87	12	738.27	739.87
	2	1.3	1.2	0.1	45	200	35	555.14	12	743.45	744.41
	3	1.3	1.2	0.1	45	200	40	562.50	12	745.97	747.77
	4	1.3	1.2	0.1	45	200	45	569.25	12	748.43	750.51
	5	1.3	1.2	0.1	45	200	50	576.91	12	750.85	754.08
	6	1.3	1.2	0.1	45	200	55	583.36	12	753.21	756.41
	7	1.3	1.2	0.1	45	200	60	590.72	12	755.53	759.55
2	8	2.8	2.4	0.4	45	200	25	526.00	6	720.46	723.00
	9	2.8	2.4	0.4	45	200	35	537.35	6	725.05	726.62
	10	2.8	2.4	0.4	45	200	40	544.40	6	727.26	729.67
	11	2.8	2.4	0.4	45	200	45	550.88	6	729.43	732.15
	12	2.8	2.4	0.4	45	200	50	556.98	6	731.54	734.14
	13	2.8	2.4	0.4	45	200	55	563.11	6	733.61	736.16
	14	2.8	2.4	0.4	45	200	60	568.63	6	735.62	737.47
3	15	4.5	3.5	1	45	200	25	510.05	3.5	706.61	707.05
	16	4.5	3.5	1	45	200	35	522.63	3.5	710.73	711.90
	17	4.5	3.5	1	45	200	40	528.76	3.5	712.71	714.03
	18	4.5	3.5	1	45	200	45	535.51	3.5	714.65	716.77
	19	4.5	3.5	1	45	200	50	541.34	3.5	716.53	718.50
	20	4.5	3.5	1	45	200	55	548.08	3.5	718.36	721.14
	21	4.5	3.5	1	45	200	60	554.22	3.5	720.15	723.05
4	22	4.5	3.5	1	50	200	25	509.75	3.5	706.61	706.74
	23	4.5	3.5	1	50	200	35	522.93	3.5	710.73	712.21
	24	4.5	3.5	1	50	200	40	529.68	3.5	712.71	714.95
	25	4.5	3.5	1	50	200	45	535.51	3.5	714.65	716.77
	26	4.5	3.5	1	50	200	50	541.95	3.5	716.53	719.11
	27	4.5	3.5	1	50	200	55	548.70	3.5	718.36	721.75
	28	4.5	3.5	1	50	200	60	554.83	3.5	720.15	723.67
5	29	4.5	3.5	1	55	200	25	510.67	3.5	706.61	707.66
	30	4.5	3.5	1	55	200	35	521.71	3.5	710.73	710.98
	31	4.5	3.5	1	55	200	40	528.45	3.5	712.71	713.72
	32	4.5	3.5	1	55	200	45	535.82	3.5	714.65	717.08
	33	4.5	3.5	1	55	200	50	542.56	3.5	716.53	719.72
	34	4.5	3.5	1	55	200	55	549.00	3.5	718.36	722.06
	35	4.5	3.5	1	55	200	60	556.06	3.5	720.15	724.89

The advance electrolyte from SX usually contains 45 g/L Cupric ion and 170 g/L sulfuric acid. This advance electrolyte is mixed with a bleed of spent electrolyte leaving the Cu EW cells to generate the recirculating electrolyte that is the feed to the Cu EW cells. The spent electrolyte consists of -5 g/L cupric ion less that the recirculating electrolyte, because a single pass through an EW cell takes a bite of 5 g/L cupric ion from the electrolyte. The spent electrolyte acid concentration is generally limited to 190-200 g/L. Although higher acidities can improve

electrolyte conductivity, too high acidity can accelerate the hydrolytic degradation of the organic phase in SX and higher acidities also increase the corrosivity of acid mist causing the decreasing of anode lifetime.

A temperature of 45-55°C for Cu EW solution is the optimized option for the expected high conductivity that is an important factor for minimizing energy consumption.

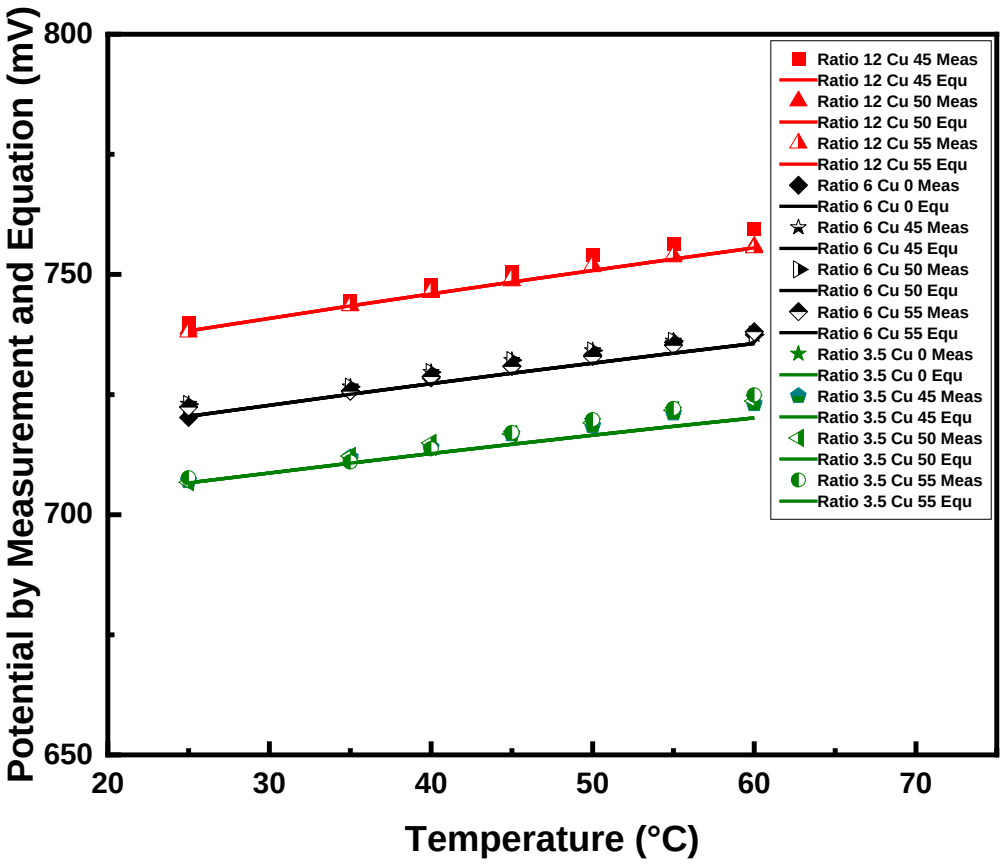

Figure 5-3. Comparison of the potentials calculated by the Equation in this work and measured by experiments in acidic iron sulfate solutions from traditional Cu EW containing 0-55 g/L cupric ion, 180 g/L sulfuric acid, 1.3-4.5 g/L total iron with 3 different nominal Fe^{3+}/Fe^{2+} ratios in the temperature range of 25-60°C. Parameters were determined according to the literature [1]

Based on the published industrial data on worldwide copper mines in the book (Schlesinger et al., 2011), the selected cupric ion concentrations and the different nominal Fe^{3+}/Fe^{2+} ratios are shown in Table 3. The nominal Fe^{3+}/Fe^{2+} ratio ranges from 0.25 to 12 with the various concentration of cupric ion from 45 g/L to 55 g/L.

In Figure 5-3, it should be emphasized that a wider range of nominal Fe^{3+}/Fe^{2+} ratio from 0.25 to 12 is used and the solution composition was totally different from those shown in Figure 5- 1 and Figure 5-2. The concentration of sulfuric acid is 200 g/L and a higher concentration of cupric ion from 45 g/L to 55 g/L was used.

From Table 5-4, Table 5-5 and Figure 5-3, over a wider range of solution conditions, the measured redox potentials were in good agreement with the calculated redox potentials, with a deviation typically lower 3 mV. It should be noted that a wide range of nominal Fe^{3+}/Fe^{2+} ratio (3.5:1, 6:1, and 12:1) is employed. The above analyses of the experimental results from Table 5-5 and Figure 5-3 further strongly support the wide applicable range of Eq. (1) in acidic iron sulfate solutions containing different cupric ion concentrations in the range of 45 g/L to 55 g/L. Based on this analysis, it can be shown that the concentration of cupric ion has almost no effect on measured potentials.

5.2.4 Comparison between the measured potentials and calculated potentials for Novel Cu EW solutions from 25℃ to 60℃

Table 5-5 Compositions of synthetic Novel EW solution, g/L

Sample	$[H_2SO_4]$	$[Fe^{3+}]$	$[Fe^{2+}]$	$[Fe]_{total}$	$[Cu^{2+}]$	Nominal $[Fe^{3+}]/[Fe^{2+}]$
#1	180	1	50	51	0	0.02
#2	180	1.1	28.8	29.9	0	0.0382
#3	180	3.4	26.5	29.9	0	0.1283
#4	180	6	40	46	0	0.15
#5	180	6	30	36	0	0.2
#6	180	6	20	26	0	0.3
#7	180	1	44.3	45.3	38	0.0226
#8	180	1	35	36	36	0.0286
#9	180	1	35	36	40	0.0286
#10	180	1	35	36	44	0.0286
#11	180	1.1	28.8	29.9	38	0.0382
#12	180	1.1	28.8	29.9	40	0.0382
#13	180	3.4	26.5	29.9	38	0.1283
#14	180	3.4	26.5	29.9	40	0.1283
#15	180	6	20	26	36	0.3
#16	180	6	20	26	38	0.3
#17	180	6	20	26	40	0.3
#18	180	6	20	26	44	0.3

Table 5-6 Results for solutions based on the novel energy-saving Cu EW process from 25 to 60°C

Chemical Analysis		Experimental results measured in the lab							Calculated redox potential by Equation		E_{SHE} (25°C) E_h
Tests	Assays	Fe_{total} g/L	Fe^{3+} g/L	Fe^{2+} g/L	Cu^{2+} g/l	H_2SO_4 g/l	T (°C)	E_h (obs) mV	Fe^{3+} /Fe^{2+} (nominal)	E (Calc) mV	E (Meas) mV
1	1	29.9	3.4	26.5	38	180	25	425.40	0.038	621.66	622.40
	2	29.9	3.4	26.5	38	180	35	434.30	0.038	622.93	623.57
	3	29.9	3.4	26.5	38	180	40	439.51	0.038	623.49	624.78
	4	29.9	3.4	26.5	38	180	45	444.72	0.038	623.99	625.99
	5	29.9	3.4	26.5	38	180	50	450.24	0.038	624.45	627.41
	6	29.9	3.4	26.5	38	180	55	456.07	0.038	624.86	629.12
	7	29.9	3.4	26.5	38	180	60	460.98	0.038	625.22	629.81
2	8	29.9	3.4	26.5	40	180	25	429.49	0.038	621.66	626.48
	9	29.9	3.4	26.5	40	180	35	438.25	0.038	622.93	627.52
	10	29.9	3.4	26.5	40	180	40	442.93	0.038	623.49	628.20
	11	29.9	3.4	26.5	40	180	45	447.62	0.038	623.99	628.88
	12	29.9	3.4	26.5	40	180	50	452.15	0.038	624.45	629.31
	13	29.9	3.4	26.5	40	180	55	456.61	0.038	624.86	629.66
	14	29.9	3.4	26.5	40	180	60	460.99	0.038	625.22	629.82
3	15	29.9	1.1	28.8	38	180	25	393.54	0.128	590.52	590.54
	16	29.9	1.1	28.8	38	180	35	402.09	0.128	590.75	591.36
	17	29.9	1.1	28.8	38	180	40	407.31	0.128	590.78	592.57
	18	29.9	1.1	28.8	38	180	45	412.52	0.128	590.77	593.78
	19	29.9	1.1	28.8	38	180	50	416.20	0.128	590.71	593.42
	20	29.9	1.1	28.8	38	180	55	421.41	0.128	590.59	594.47
	21	29.9	1.1	28.8	38	180	60	426.02	0.128	590.43	594.85
4	22	29.9	1.1	28.8	40	180	25	394.73	0.128	590.52	591.73
	23	29.9	1.1	28.8	40	180	35	402.40	0.128	590.75	591.67
	24	29.9	1.1	28.8	40	180	40	407.00	0.128	590.78	592.27
	25	29.9	1.1	28.8	40	180	45	411.60	0.128	590.77	592.86
	26	29.9	1.1	28.8	40	180	50	416.20	0.128	590.71	593.36
	27	29.9	1.1	28.8	40	180	55	420.80	0.128	590.59	593.85
	28	29.9	1.1	28.8	40	180	60	425.40	0.128	590.43	594.24

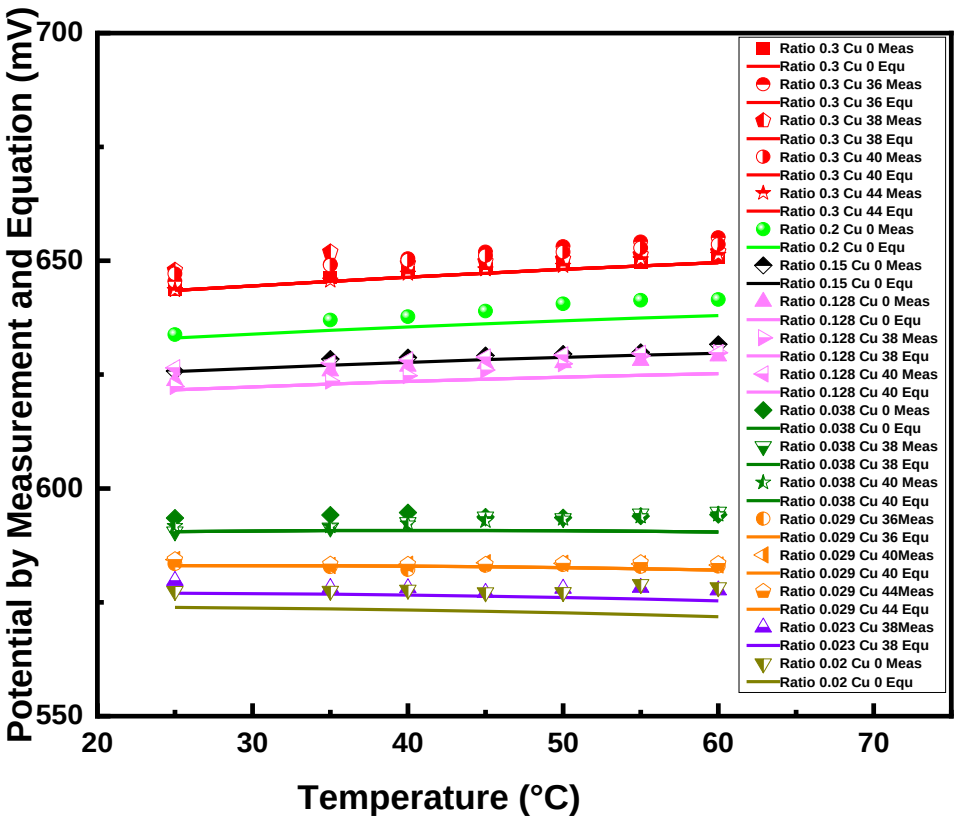

Figure 5-4. Comparison of the potentials calculated by the Equation in this work and measured by experiments in novel copper electrowinning (Cu EW) solutions containing 0-44 g/L cupric ion, 180 g/L sulfuric acid, 26-51 g/L total iron with 8 different nominal Fe^{3+}/Fe^{2+} ratios in the range of 25-60°C. Detailed information could be found in the literature [1], [86]

The applicability of the developed Eq. (1) is also investigated in synthetic copper electrowinning solutions based on the novel energy-saving technology in terms of ion concentration, nominal ferric/ferrous ratios, cupric ion concentration, sulfuric acid concentration and temperature. The solution composition was selected according to the published work [1, 86].

Based on the industrial data from the reference [1] and the previously published literature [86], the solutions involved in the new energy-saving Cu EW process typically contain 34-50 g/L Cu, 30 g/L iron and 160-200 g/L sulfuric acid with temperature ranging from 40°C to 55°C. The temperature ranging from 25°C to 60°C can include all the conditions in above-mentioned literature [1].

Table 5-7 shows the measured potentials and calculated potentials with the same total iron concentration of 29.9 g/L containing the same sulfuric acid concentration of 180 g/L with different nominal ferric/ferrous ratios and copper ion concentration. Figure 5-4 clearly shows the comparison of the potentials in the prepared solutions predicted by the developed Eq. (1) and measured by experiments in this work at various cupric ion concentrations and nominal ferric/ferrous ratios in the temperature range of 25-60°C. Although cupric ion concentration changes from 38 g/L to 44 g/L under the same nominal ferric/ferrous ratio, the experimental measured potentials almost do not change.

From the results in Table 5-7 and Figure 5-4, the applicability of Eq. (1) in acidic iron sulfate solutions containing cupric ions under electrowinning conditions was confirmed by the fact that the difference between measured potential and calculated potential was always lower than 4.8 mV under the same temperature and the same nominal ferric/ferrous ratio, and in most cases was within 3 mV.

From above analysis, it seems that the potentials depend significantly on the nominal ferric/ferrous ratio and temperature even with a much higher cupric ion concentration up to 44 g/L.

5.2.5 Comparison between the measured potentials and calculated potentials for several special nominal ferric/ferrous ratios from 5℃ to 60℃

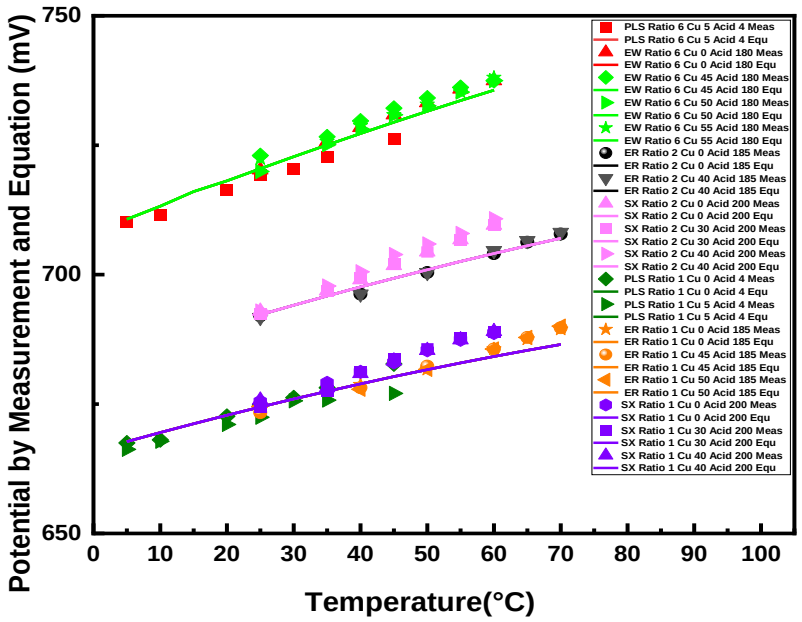

Figure 5-5 Comparison of the potentials calculated by the Equation in this work and measured by experiments in acidic iron sulfate solutions from synthetic PLS, synthetic SX solutions, traditional Cu EW solutions and Cu ER solutions with 3 different nominal Fe^{3+}/Fe^{2+} ratios of 6:1, 2:1, and 1:1 in the temperature range of 5-70°C. Parameters were determined according to the literature [1]

As shown in Figure 5-5, under the same nominal Fe^{3+}/Fe^{2+} ratio of 6:1 at temperature 25 °C, 35 °C and 45 °C, the two different series of measured potentials agreed with each other very well with different sulfuric acid concentration of 3 g/L and 200 g/L, respectively, and different cupric ion concentration of 4 g/L and 45 g/L, respectively.

It is observed that the measured redox potentials were in good agreement with the calculated redox potentials at the same nominal ferric/ferrous ratio and experiment temperature. The deviation between the measured redox potential and the calculated redox potential are with 3-6 mV. The above analysis of the experimental result from Figure 5-5 further strongly supports the wide applicable range of Equation (1) in acidic iron sulfate solutions containing different cupric

ion concentrations in the range of 0-55 g/L and various sulfuric acid concentrations in the range of 3-200 g/L. Based on this analysis, it can be shown that the concentration of cupric ion and sulfuric acid has almost no effect on the accuracy of measured potentials. Those facts strongly support our conclusion that the potential could be easily and accurately determined solely based on nominal Fe^{3+}/Fe^{2+} ratio and temperature, and not affected by the change of the concentrations of iron, copper and sulfuric acid [101-103].

5.3 Summary

Based on the published industrial data on worldwide copper mines in the book [1], the selected cupric ion concentrations and the different nominal Fe^{3+}/Fe^{2+} ratios are shown in Table 5-1, 5-3, 5-4, 5-6.

The Fe^{3+}/Fe^{2+} ratio ranges from 0.01 to 100 with the various concentration of cupric ion from 1 g/L to 55 g/L.

In Figure 5-3, it should be emphasized that a wider range of nominal Fe^{3+}/Fe^{2+} ratio from 03.5 to 12 is used and the solution composition was totally different from those shown in Figure 5-1 and Figure 5-2. The concentration of sulfuric acid is 200 g/L and a higher concentration of cupric ion from 45 g/L to 55 g/L was used.

From Table 5-4, Table 5-5 and Figure 5-3, over a wider range of solution conditions, the measured redox potentials were in good agreement with the calculated redox potentials, with a deviation typically lower than 3 mV. It should be noted that a wide range of nominal Fe^{3+}/Fe^{2+} ratio (3.5:1, 6:1, and 12:1) is employed. The above analyses of the experimental results from Table 3 and Figure 3 further strongly support the wide applicable range of Eq. (1) in acidic iron sulfate solutions containing different cupric ion concentrations in the range of 45 g/L to 55 g/L. Based on

this analysis, it can be shown that the concentration of cupric ion has almost no effect on measured potentials.

The data in the tables and figures in chapter 5 is clearly shown that Eq. (1) can be employed to predict the redox potential of the ferric/ferrous couple in complicated pregnant leaching solutions generated from heap leaching, SX solutions and Cu EW solutions. It may also be used to understand iron chemistry and kinetics analysis based on the measured redox potential during Cu EW process. As shown above, in such a case, the deviation of measured redox potential should be no more than 4 mV generally [56, 65, 66, 95, 101-103].

In the pure quaternary H_2SO_4-$Fe_2(SO_4)_3$-$FeSO_4$-H_2O system, the applicability of Eq. (1) is proved in a pH range of 0.55-1.5 [56], [65, 66]. It should be noted that the solution with the highest nominal sulfuric acid concentration was about 1.02 mol/L, corresponding to an even lower pH value [95]. In our present study, the nominal sulfuric acid concentration is as high as 1.84 mol/L, corresponding to a nominal pH value of about -0.26 (the actual pH values of the solutions should be different based on the solution composition). Furthermore, it is shown that the co-existence of cupric ion up to 0.87 mol/L does not exert an obvious influence on the accurate prediction of redox potentials calculated by Eq. (1). Based on the above analysis, a conclusion can be drawn that Eq. (1) is applicable across a wide range of pH, copper concentration and temperature, even at the temperature as low as 5 °C.

The aim of this study was to investigate the applicability of the equation developed previously in different solution compositions with various temperatures (especially lower than 25°C) and higher copper concentration for the pregnant leaching solutions, SX solutions and copper electrowinning solutions. The comparison of experimental and calculated results suggested that Eq. (1) is quantitatively validated with nominal ferric/ferrous ratios from 0.01 to 100, temperature

ranging from 5 °C to 60 °C, various concentrations of cupric ion from 1 g/L to 55 g/L, iron from 1 to 30.3 g/L and sulfuric acid from 3 to 200 g/L. It could be concluded that the redox potentials depend significantly on the nominal ferric/ferrous ratio and temperature, but it is almost unaffected by the various concentrations of cupric ion and sulfuric acid. The equation can still be used under lower temperatures as well. It is expected that the findings in this work could facilitate the understanding of iron chemistry and the kinetics/mechanism analysis in the above-mentioned industrial processes, and potentially other processes for hydrometallurgical production of copper [95, 101-103].

.

6. SPECIATION STUDY AND IRON CHEMISTRY FOR PLS FROM 5℃ TO 45℃

6.1 Introduction

The previous publication has shown that, iron sulfates present in sulfuric acid solution are distributed as soluble species including simple metal ions, neutral or charged complexes, as well as precipitates such as Fe_2O_3 formed at high temperatures, and therefore, a speciation model is required to quantify the distribution of Fe in acidic iron sulfate solutions and, further, to predict the redox potentials of the Fe^{3+}/Fe^{2+} couple via the Nernst equation [56, 65, 66, 95]. The speciation results and the obtained redox potentials of the Fe^{3+}/Fe^{2+} couple (by using the relative amounts of free ferric and ferrous and the accompanying activity coefficients in the solution) could be then employed to carry out mechanistic analyses and attendant optimization studies of industrial processes [65].

There are very few data published about speciation study and iron chemistry research at the low temperatures below 25℃.

6.2 Results and Discussion

6.2.1 Speciation Distribution Calculated in the Aqueous H_2SO_4-$Fe_2(SO_4)_3$-FeSO4-H_2O System

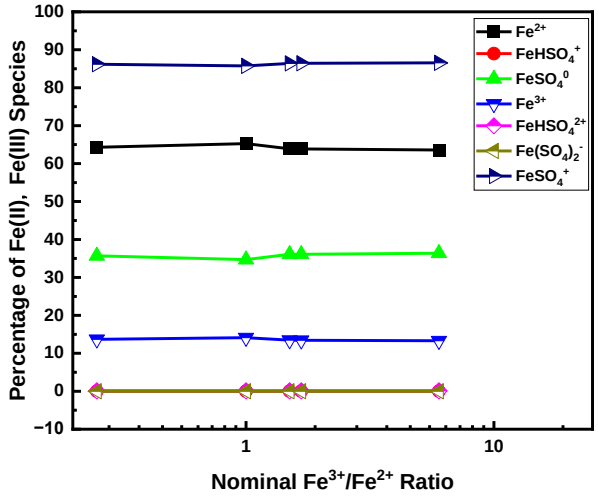

(a)

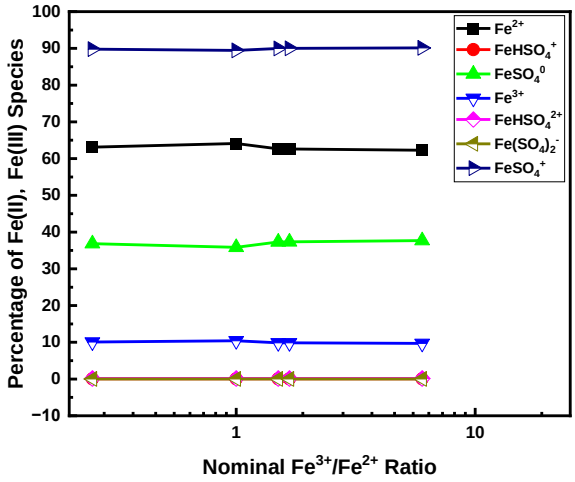

(b)

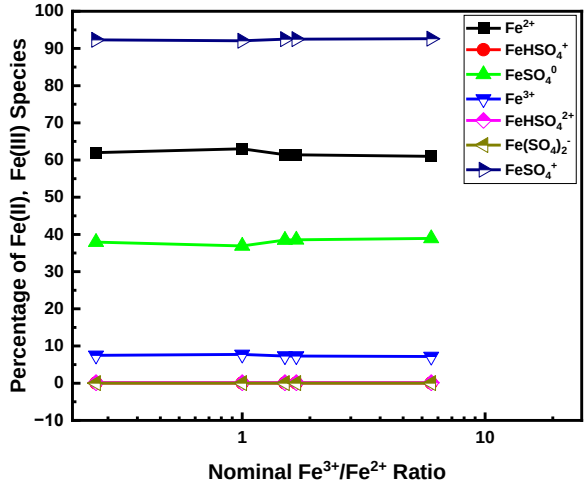

(c)

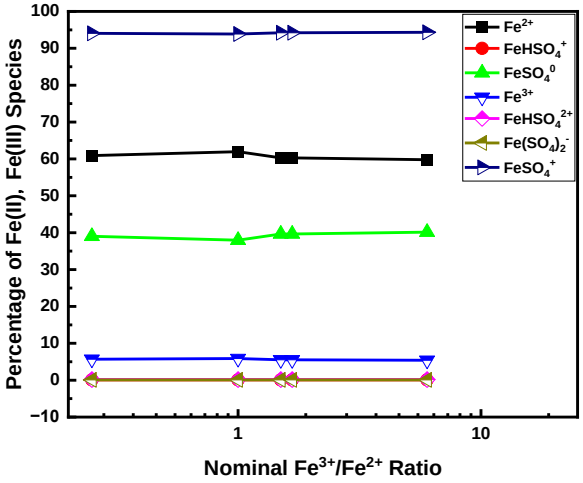

(d)

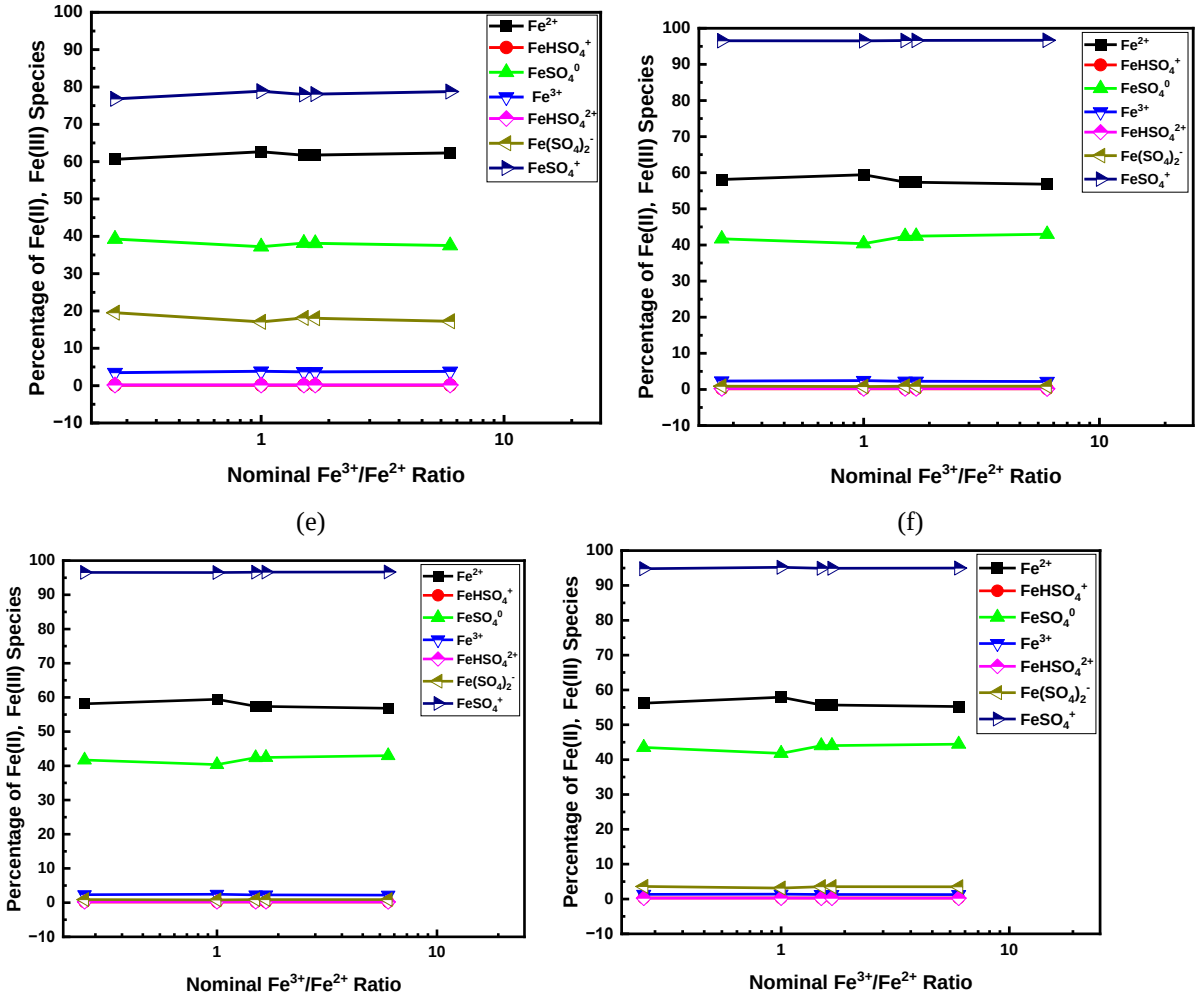

Fig. 6-1. Calculated aqueous speciation diagram of the main ferric and ferrous species in the Fe(II)-Fe(III)-H_2SO_4 solutions (synthetic PLS) with nominal Fe^{3+}/Fe^{2+} ratio from 0.25 to 6 from 5°C to 45°C from Test #1 to Test #5 with (a) 5°C; (b) 10°C; (c) 15°C; (d) 20°C; (e) 25°C; (f) 30°C; (g) 35°C; (h) 45°C. Please note that the sum of the percentage values of both Fe(II) species (filled symbols) and Fe(III) species (half-filled symbols) are 100%.

Figure 6-1 presents the results of the aqueous speciation (expressed as a percentage of the total ferric or ferrous) for tests #1−#5 in Table 5-1 in Fe(II)−Fe(III)−H_2SO_4−H_2O solutions with different nominal Fe^{3+}/Fe^{2+} ratios (the ratio of total Fe(III) to total Fe(II) initially added to the solution) from 5 to 45 °C. In this part, the thermodynamic model of the Fe(II)−Fe(III)−H_2SO_4−H_2O system will be first employed to evaluate the possibility of extending its applicability to the acidic iron sulfate solutions with a much lower acid concentration (3-7 g/L sulfuric acid) and different

iron chemistry. As observed under each testing temperature (5, 10, 15, 20, 25, 30, 35, and 45 °C), there is no apparent fluctuation of the percentage for each species, and the distribution curves tend to be very stable at 5 different nominal Fe^{3+}/Fe^{2+} ratios.

Fig.6-1 a to h show the speciation results from modeling calculation in aqueous Fe(II, III)-H_2SO_4 solutions with nominal Fe^{3+}/Fe^{2+} ration of 0.25:1, 1:1, 1.5:1, 1.67:1 and 6:1 from 5 °C to 45 °C for test #1-#5. The solution compositions are listed in Table 5-2 (#1–5). It can be seen that under each temperature, the distribution percentage of each species of Fe(II) and Fe(III) tends to be very stable at different.

For Fe(II) species, free Fe^{2+} is the predominant species of total Fe (II), followed by $FeSO^{o}_{4}$, with their percentages accounting for 55.25–65.26% and 34.71–44.44%, respectively. $FeHSO^{+}_{4}$ is the least abundant Fe (II) species, with a proportion of 0.03–0.31% from 5 to 45 °C. For Fe(III) species, $FeSO^{+}_{4}$ ion complex is the major species of total Fe(III), taking up 76.81–96.68%, with the percentage of free Fe^{3+} ions as 1.26–13.68%, $Fe(SO_4)^{-}_{2}$ as 0.01–3.61% and $FeHSO^{2+}_{4}$ as 0.11–0.26% from 5 to 45 °C, respectively. The single free ferric ion accounts for only a small amount of total Fe(III), and its percentage keeps decreasing with temperature.

The distribution results in aqueous Fe(II, III)-H_2SO_4-H_2O solutions are similar to those in literature [56, 65, 66, 95, 101-103]. Evidently, from the above modeling results, changing the nominal Fe^{3+}/Fe^{2+} ratio from 0.25 to 6 does not exert any significant influence on the distribution of the dissolved species. Temperature plays a major role in affecting the species distribution.

Consequently, a conclusion can be drawn that the previously developed model is still applicable at low temperature (as low as 5 °C) when changing the iron chemistry and acid concentration in this work compared with the previous results in related leaching conditions.

6.2.2 Speciation Distribution Calculated in the Aqueous H_2SO_4-$CuSO_4$-$Fe_2(SO_4)_3$-$FeSO_4$-H_2O System

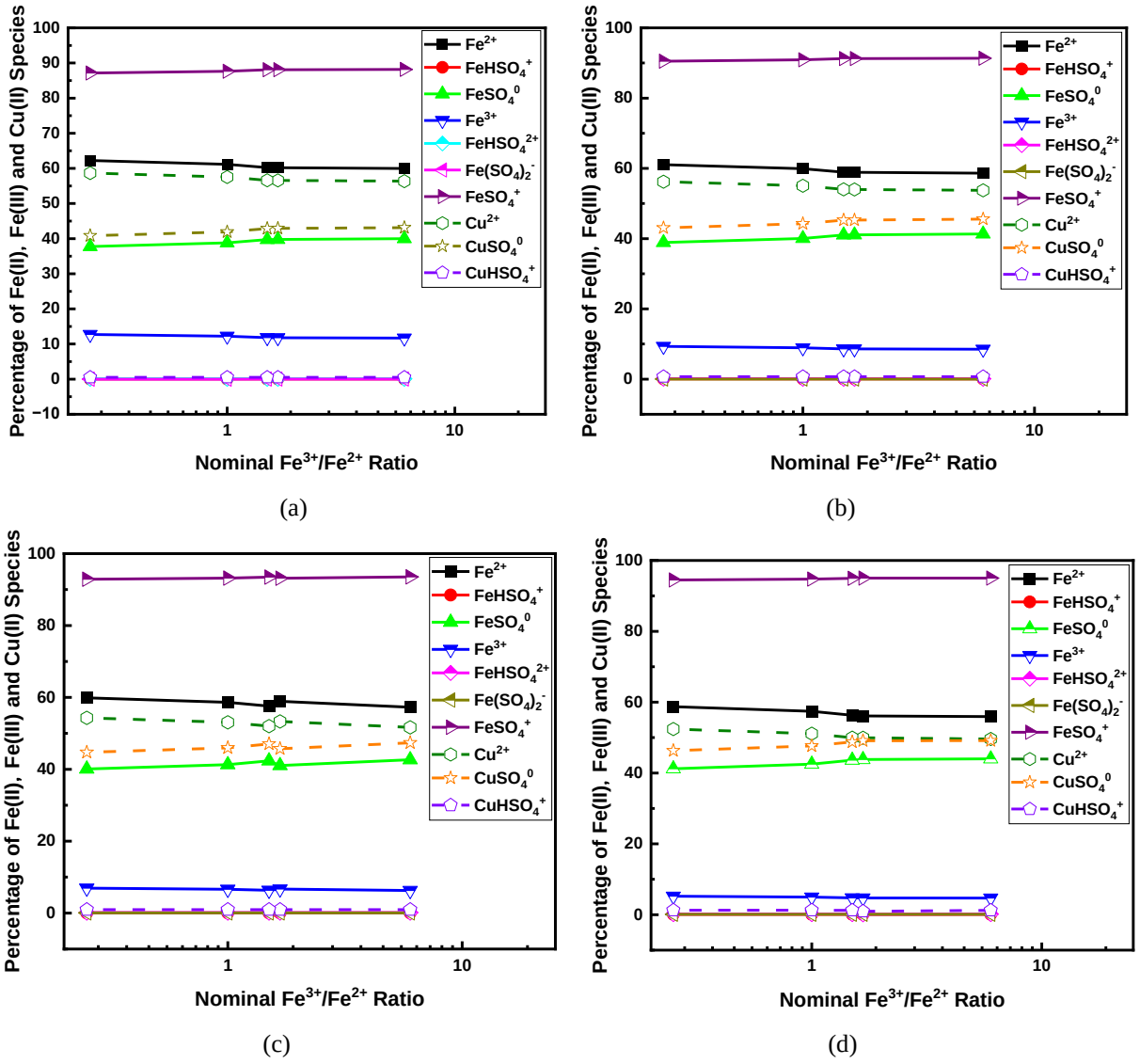

(a) (b)

(c) (d)

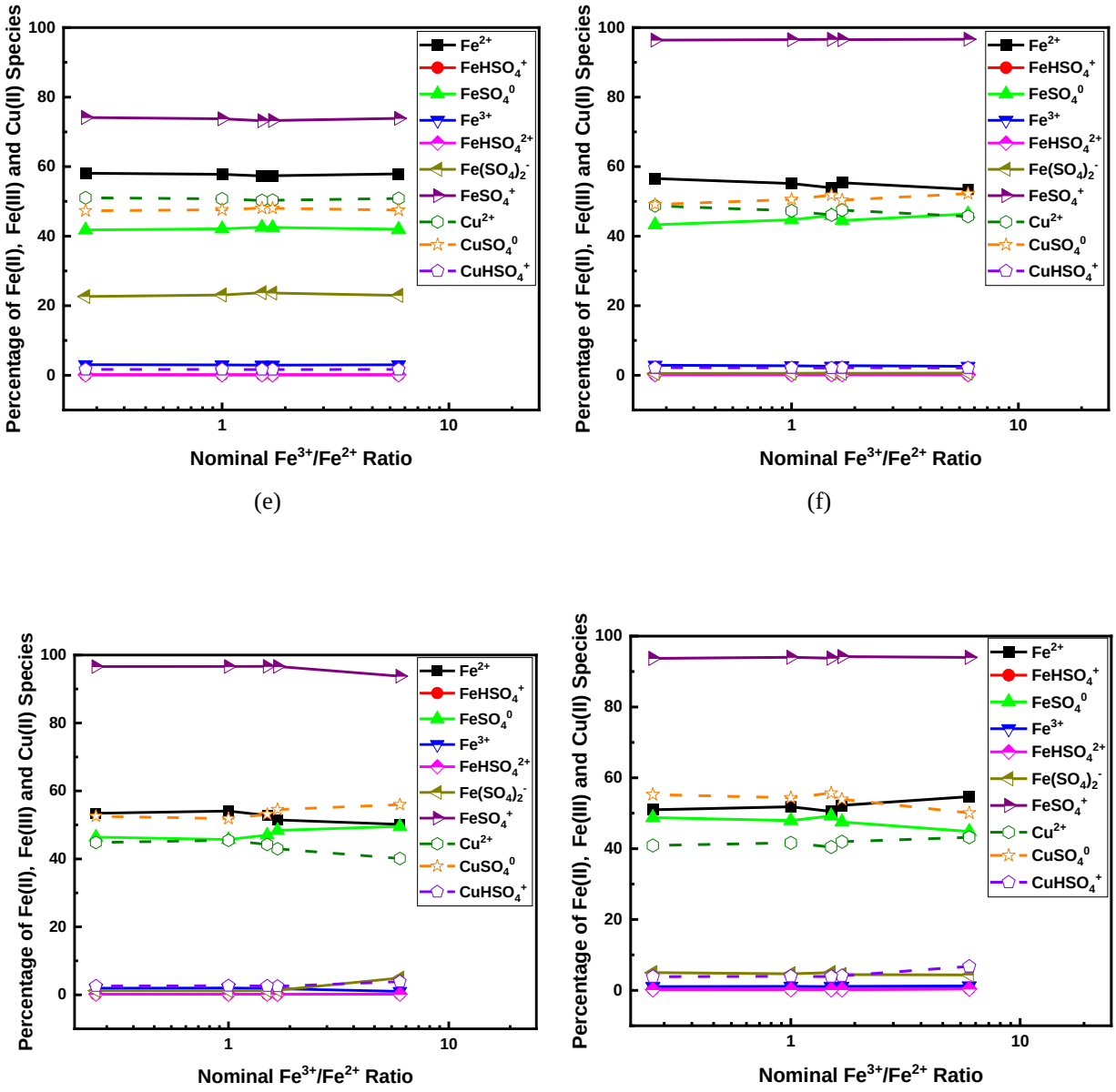

Fig. 6-2. Calculated aqueous species distribution diagram in the Fe(II)-Fe(III)-Cu(II)-H_2SO_4-H_2O solutions (synthetic PLS) with nominal Fe^{3+}/Fe^{2+} ratio ranging from 0.25 to 6 with Test #6, #8, #10, #12 and #15 with (a) 5°C; (b) 10°C; (c) 15°C; (d) 20°C; (e) 25°C; (f) 30°C; (g) 35°C; (h) 45°C. Please note that the sum of the percentage values of Fe(II) species(filled symbols), Fe(III) species (half-filled symbols) and Cu(II) species (unfilled symbols) are 100%.

Fig. 6-2 a to h show the speciation results from modeling calculation in aqueous Fe(II, III)-Cu(II)-H_2SO_4-H_2O solutions with nominal Fe^{3+}/Fe^{2+} ration of 0.25:1, 1:1, 1.5:1, 1.67:1 and 6:1 from 5 °C to 45 °C for test #6, #8, #10, #12, and #15. The solution compositions are listed in Table

5-2. In the comparison of test # 1 and test #6, test #2 and test #8, test #3 and test #10, test #4 and test #12, test #5 and test #15, the difference is the addition of the cupric ion (5 g/L). In the comparison of test #7, test #8, test #9, the difference is the concentration of the cupric ion (3 g/L, 5 g/L, 7 g/L). In the comparison of test #11, test #12, test #13, the difference is the concentration of the sulfuric acid (2 g/L, 4 g/L, 7 g/L). In the comparison of test #14, test #15, test #16, the difference is the concentration of the total iron (3 g/L, 5 g/L, 8 g/L). It can be seen in Figure. 6-2 that under each temperature, the distribution percentage of each species of Fe(II), Fe(III), and Cu(II) tends to be very stable at different temperature.

For Fe(II) species, free Fe^{2+} is the predominant species of total Fe (II), followed by $FeSO^{o}_{4}$, with their percentages accounting for 48.24–62.49% and 37.45–51.52%, respectively. $FeHSO^{+}_{4}$ is the least abundant Fe (II) species, with a proportion of 0.02–0.46% from 5 to 45 °C. The percentage of free Fe(II) in Figure 6-2 is slightly lower than that of the Fe(II)-Fe(III)-H_2SO_4-H_2O solutions shown in the Figure 6-1.

For Fe(III) species, $FeSO^{+}_{4}$ ion complex is the major species of total Fe(III), taking up 69.56–96.83%, with the percentage of free Fe^{3+} ions as 0.95–12.84%, $Fe(SO_4)^{-}_{2}$ as 0.02–27.86% and $FeHSO^{2+}_{4}$ as 0.11–0.42% from 5 to 45 °C, respectively. The results show that the proportion of free ferric ion decreases as a function of temperature. The percentage of $Fe(SO_4)^{-}_{2}$ is much larger than those of Fe(II)-Fe(III)-H_2SO_4-H_2O solutions shown in the figure 6-1. These results are in good agreement with the Fe(II)-Fe(III)-H_2SO_4-H_2O solutions.

In addition, most of Cu (II) species distributes as free Cu^{2+}, with a proportion of 38.43–58.71%. $CuHSO^{+}_{4}$ accounts for 0.50–6.73% and the percentage of $CuSO^{o}_{4}$ is in the range of 41.59–57.98% ranging from 5 °C to 45 °C. The species distribution of Cu(II) is different from the published literature that shows that free cupric ion is the sole predominant species[56, 65, 66, 95, 101-103].

According to the above discussion, changing the nominal Fe^{3+}/Fe^{2+} ratio from 0.25 to 6, different total iron, different sulfuric acid concentration, and the addition of Cu(II) do not exert any significant influence on the distribution of the dissolved species. Temperature is the only variation shows an important influence on the distribution of Fe(II), Fe(III), and Cu(II). The thermodynamic modeling has been proven as an effective tool to describe aqueous behavior of Fe(II), Fe(III), and Cu(II) at or below 25 °C.

6.2.3 Model Validity by Comparison of the Redox Potential between Speciation Results and Experimental Measurements from 5 °C to 45 °C

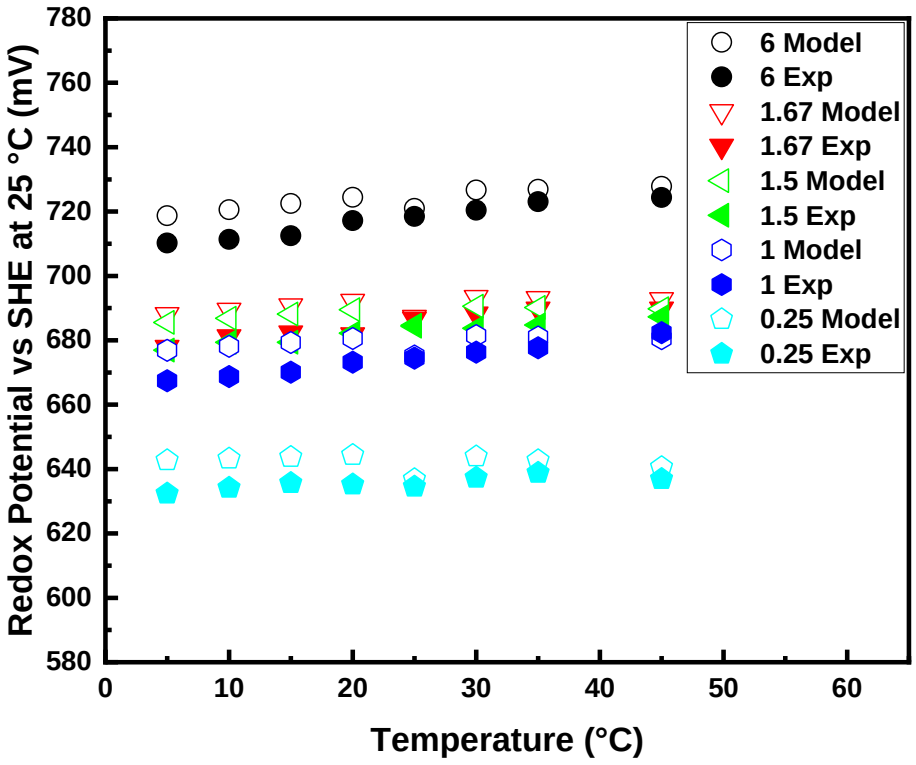

(a)

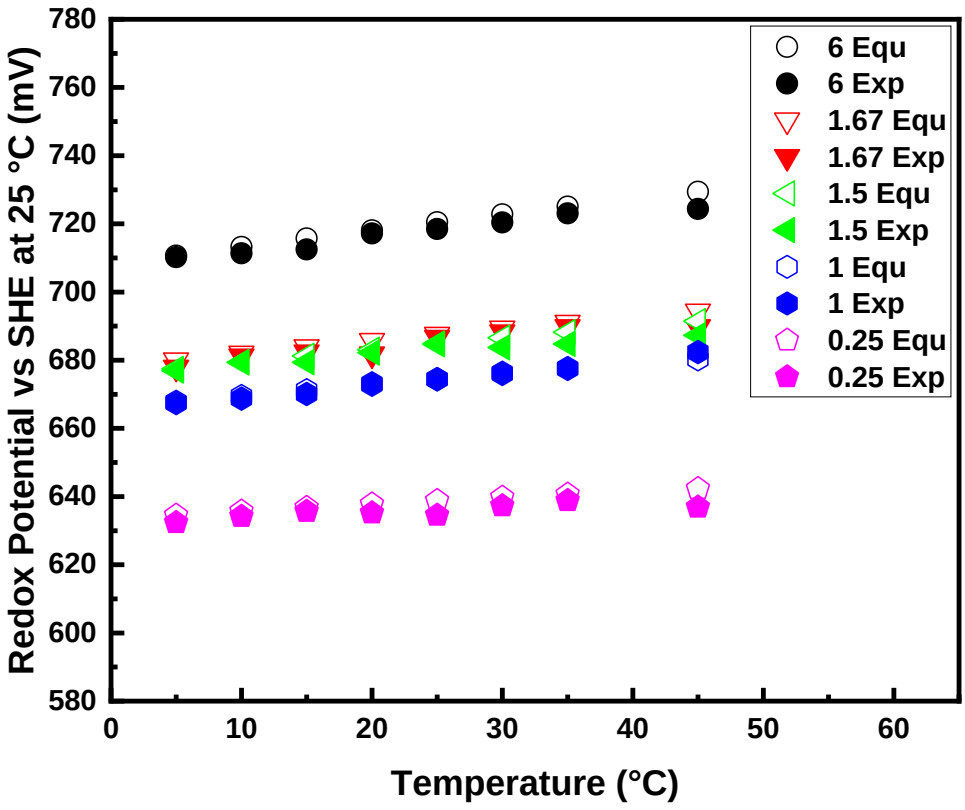

(b)

Fig. 6-3. Comparison of potentials (a) calculated by thermodynamic modeling and measured by experiments, and (b) calculated by Equation (1) in this work and measured by experiments vs SHE at 25°C with various nominal ratios and different temperature ranging from 5°C to 45°C from Test #1 to Test #5 in the Fe(II)-Fe(III)-H_2SO_4-H_2O solutions (synthetic PLS) from Table 5-1.

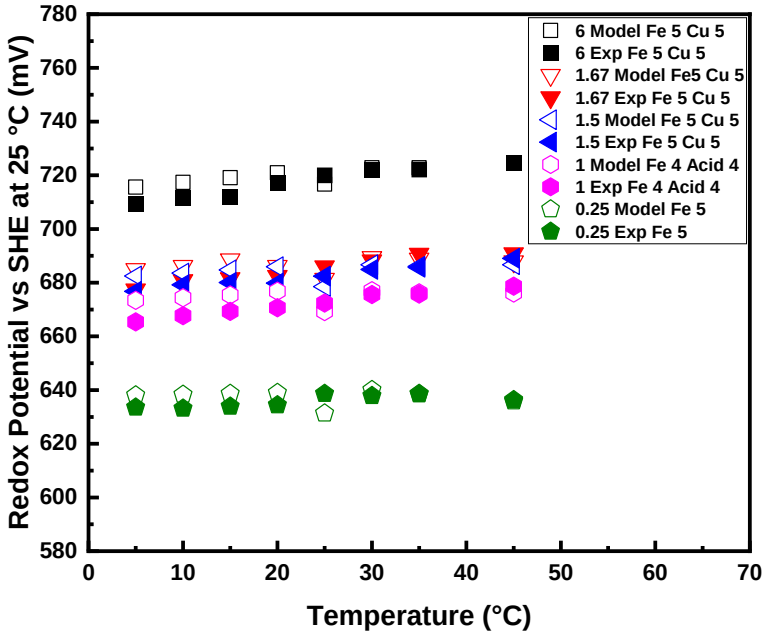

(a)

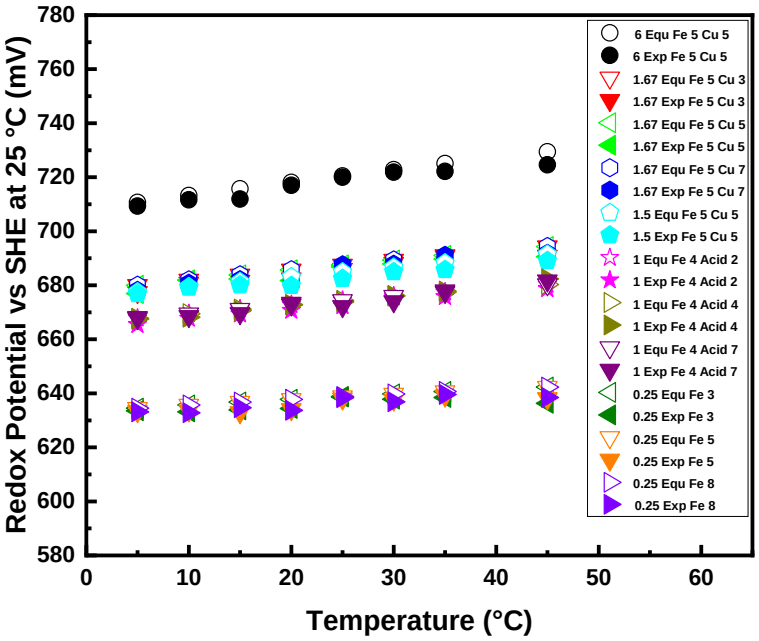

(b)

Fig. 6-4. Comparison of potentials (a) calculated by thermodynamic modeling and measured by experiments with Test #6, #8, #10, #12 and #15, and (b) calculated by Equation (1) in this work and measured by experiments vs SHE at 25°C from Test #6 to Test #16 with various nominal ratios and different temperature ranging from 5°C to 45°C in the Fe(II)-Fe(III)-Cu(II)-H_2SO_4-H_2O solutions (synthetic PLS) from Table 5-1.

In order to validate the thermodynamic speciation model, the comparison of the values of ORP from model calculation by Nernst equation and experimental measurements was employ in the present work. Figure 6-3 and Figure 6-4 shows that the ORP values predicted by the previously developed model and measured from the experiments with nominal ferric/ferrous ratio ranging from 0.25 to 6 in both Fe(II)-Fe(III)-H_2SO_4-H_2O solutions and Fe(II)-Fe(III)-Cu(II)-H_2SO_4-H_2O solutions investigated in the present work are in good agreement from 5 °C to 45 °C. The deviation of the redox potential between modeling prediction and experimental measurements is usually less than 7 mV under all the solution condition.

The deviation of the redox potential between modeling prediction and experimental measurements in Fe(II)-Fe(III)-Cu(II)-H_2SO_4-H_2O solutions from 5 °C to 45 °C is smaller than that of Fe(II)-Fe(III)-H_2SO_4-H_2O solutions from 5 °C to 45 °C. Besides, the deviation of the redox potential between modeling prediction and experimental measurements from 25 °C to 45 °C is always smaller than that from 5 °C to 25 °C in both solution systems. The thermodynamic modeling research and its accuracy could be improved and need to be further investigated, especially below room temperature.

The deviation of the redox potential between modeling prediction and experimental measurements in Fe(II)-Fe(III)-H_2SO_4-H_2O solutions from 5 °C to 25 °C is within 6 mV. But the deviation of the redox potential between modeling prediction and experimental measurements in Fe(II)-Fe(III)-Cu(II)-H_2SO_4-H_2O solutions from 5 °C to 25 °C is smaller and is within 5 mV. The comparison results show that the addition of cupric ion has positive effect on the accuracy of the modeling prediction on the values of ORP, especially at the temperature below 25 °C.

The discussion above could prove the qualitative and quantitative validation to the previously developed speciation model by experimental measurements. The conclusion also could be drown here that the predicted distribution and concentration of each species are correct for either aqueous Fe(II)-Fe(III)-H_2SO_4-H_2O solutions or aqueous Fe(II)-Fe(III)-Cu(II)-H_2SO_4-H_2O solutions in all the conditions.

6.2.4 Effect of Lower Acid Concentration, Lower Cupric Ion Concentration and Low Temperature on the Accuracy of Calculated ORP Based on Model for PLS

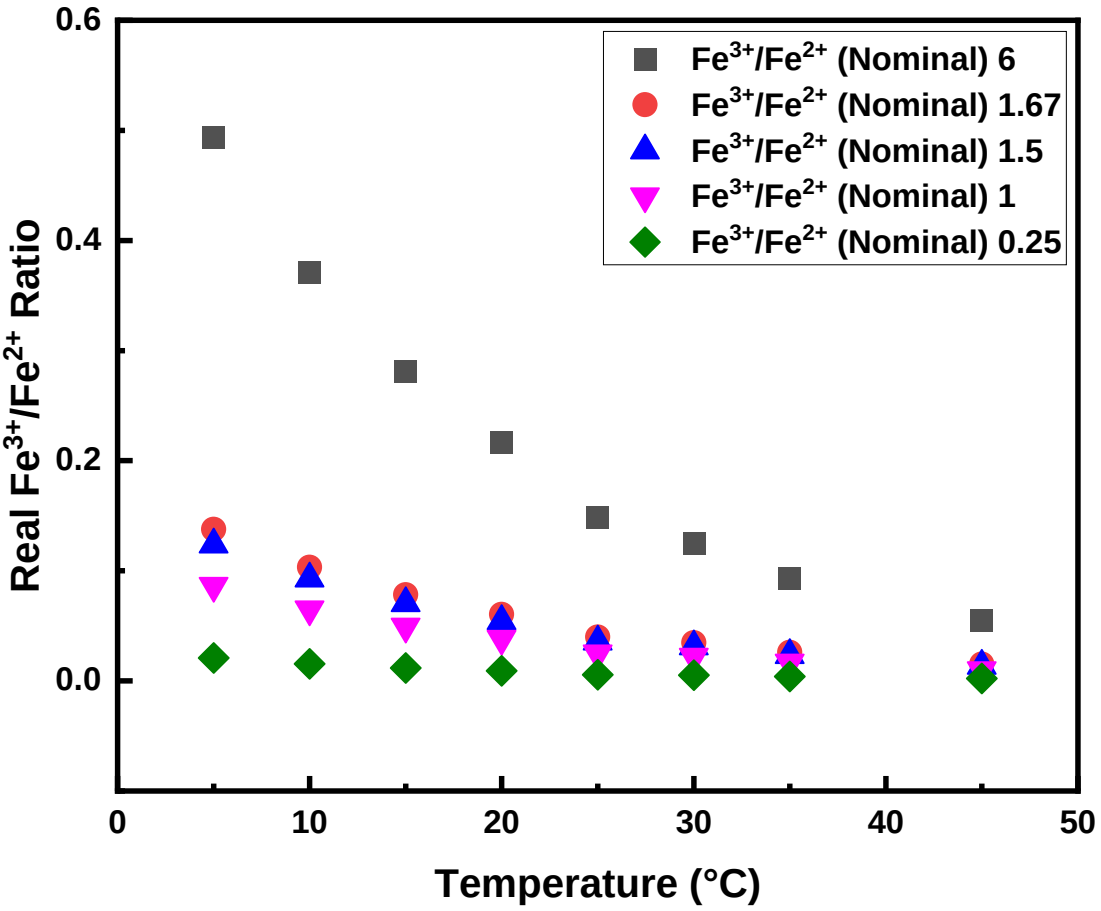

Fig.6-5. Calculated real Fe^{3+}/Fe^{2+} ratios in the Fe(II)-Fe(III)-Cu(II)-H_2SO_4-H_2O solutions (synthetic PLS) with different nominal Fe^{3+}/Fe^{2+} ratios in the temperature range from Test #1 to Test #5 from 5°C to 45°C.

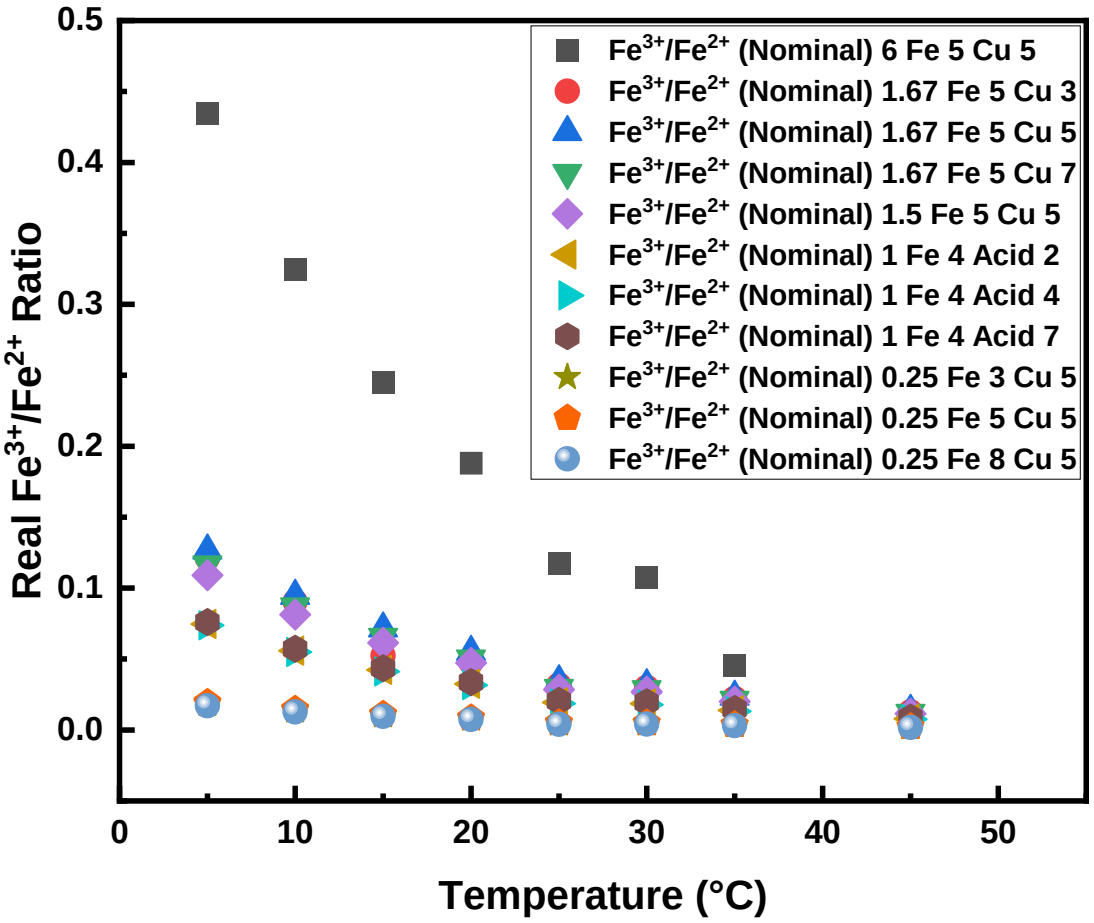

Fig.6-6. Calculated real Fe^{3+}/Fe^{2+} ratios in the Fe(II)-Fe(III)-Cu(II)-H_2SO_4-H_2O solutions (synthetic PLS) with different nominal Fe^{3+}/Fe^{2+} ratios in the temperature range from Test #6 to Test #16 from 5°C to 45°C.

According to the discussion in the previous sections, it shows that either with a lower acid concentration (2-7 g/L) or with the coexistence of a much smaller amount of cupric ion (3-7 g/L), the redox potential can still be solely determined by the ferric/ferrous couple at the set temperature. Changing of the concentrations of sulfuric acid and cupric ion exerts no apparent influence on the prediction of redox potentials. The addition of a small amount of cupric ion has no influence on the accurate prediction of the redox potential for the above-mentioned acid iron sulfate solution systems either calculated from model results or measured by experiment. It shows that either with

much lower acid concentration or with or without the coexistence of a small amount of cupric ion, the redox potential can still be solely determined by the nominal ferric/ferrous couple. The following discussion will explain the reason and theory supporting this phenomenon.

The temperature dependence of the calculated real ferric/ferrous ratio (the concentration of free ferric to free ferrous from speciation study results) in the H_2SO_4-$Fe_2(SO_4)_3$-$FeSO_4$-H_2O system and H_2SO_4-$CuSO_4$-$Fe_2(SO_4)_3$-$FeSO_4$-H_2O system with various solution compositions in the temperature range of 5-60℃ under different nominal ferric/ferrous ratios is presented in Figure 6-5 and Figure 6-6. The nominal ferric/ferrous ratios ranging from 0.25 to 6 are presented in test #1−#16 in Table 5-2. It shows that all the real ferric/ferrous ratios calculated from thermodynamic model are significantly lower than nominal ferric/ferrous ratios in both systems at all temperatures. Besides, the calculated real ferric/ferrous ratios for the tests #1−#5 in the Fe(II)−Fe(III)−H_2SO_4−H_2O system shown in Figure 6-5 and for the tests #6−#16 in the Fe(II)−Fe(III)−Cu(II)−H_2SO_4−H_2O system shown in Figure 6-6 decrease significantly with the increasing temperature from 5 to 45 ℃ under the same initial ferric/ferrous ratio.

6.2.5 Analysis of Calculated pH

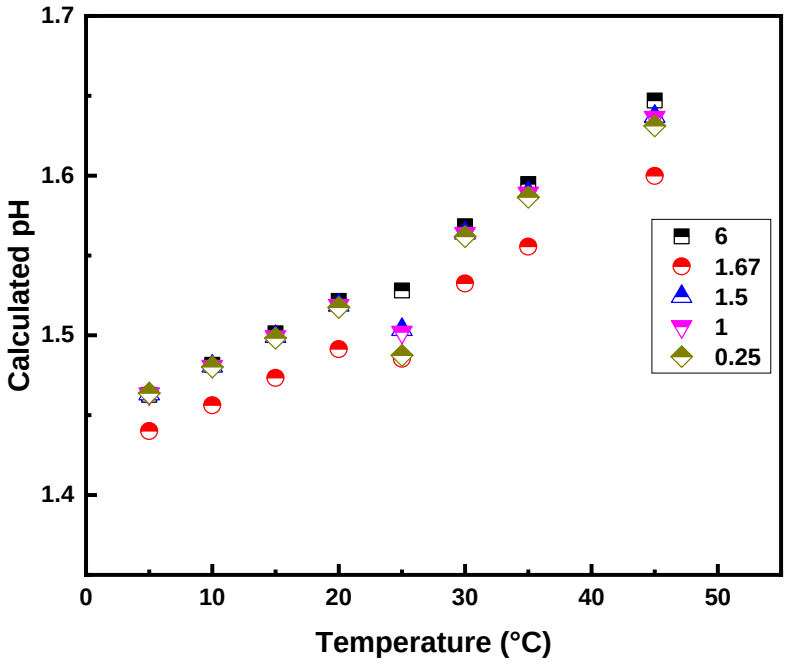

(a)

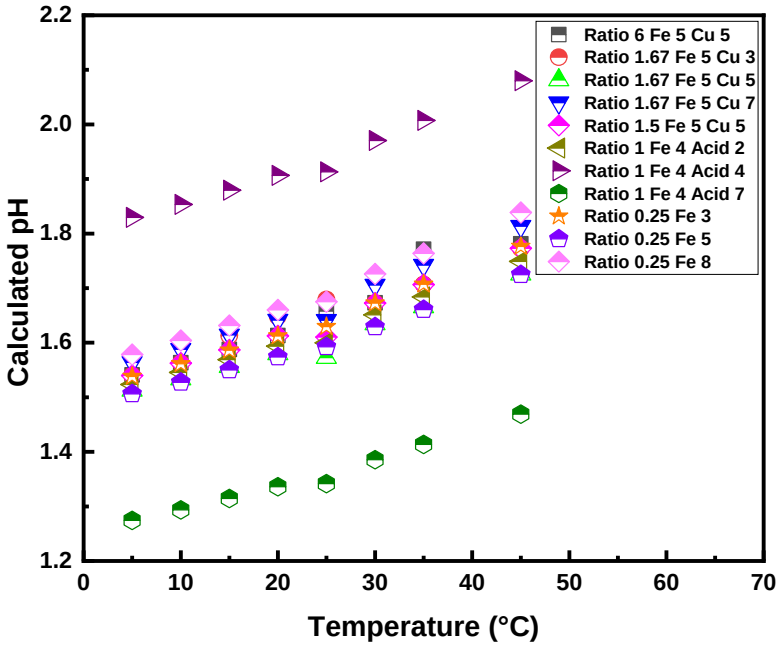

(b)

Fig.6-7. Calculated pH of (a) the Fe(II)-Fe(III)-H_2SO_4 solutions (synthetic PLS) from Test #1 to Test #5 and (b) the Fe(II)-Fe(III)-Cu(II)-H_2SO_4 solutions (synthetic PLS) from Test # 6 to Test # 16 with nominal Fe^{3+}/Fe^{2+} ratio ranging from 0.25 to 6 in the temperature range of 5°C-45°C.

It is always a great challenge for measuring pH in industrial leaching solutions due to their high acidity (typically pH < 2). From the validated thermodynamic modeling results, it can provide the needed concentration and activity coefficient of H^+ ion to calculate pH values in the test #1-#16 in table 5-2. Thermodynamic modeling is a great tool to study the pH of the synthetic solutions involved in this work.

Fig. 6-7 a and b show the estimated pH for various solution compositions in the present study. The pH increases slightly from 1.4 to 1.6 in the temperature range of 5 to 45 °C under all studied nominal Fe^{3+}/Fe^{2+} ratios in Fe(II)-Fe(III)-H_2SO_4-H_2O solutions shown in Fig. 6-7 . The pH increases slightly from 1.4 to 2.1 in the temperature range of 5 to 45 °C under all studied nominal Fe^{3+}/Fe^{2+} ratios in Fe(II)-Fe(III)-Cu(II)-H_2SO_4-H_2O solutions shown in Fig. 6-7. The slight increase of pH over temperature is caused by the fact that more complex species form, such as $FeHSO^+_4$, $FeHSO^{2+}_4$, and $CuHSO^+_4$. In fact, more protons are consumed by combining with free metal ions to form more thermodynamically stable ionic complexes and neutral species, giving the reason to the declining concentration of H^+ ions or slight increase of pH value. This can also explain why the distribution of dissolved aqueous species is highly dependent on pH and temperature.

6.2.6 Analysis of Calculated Ionic Strength

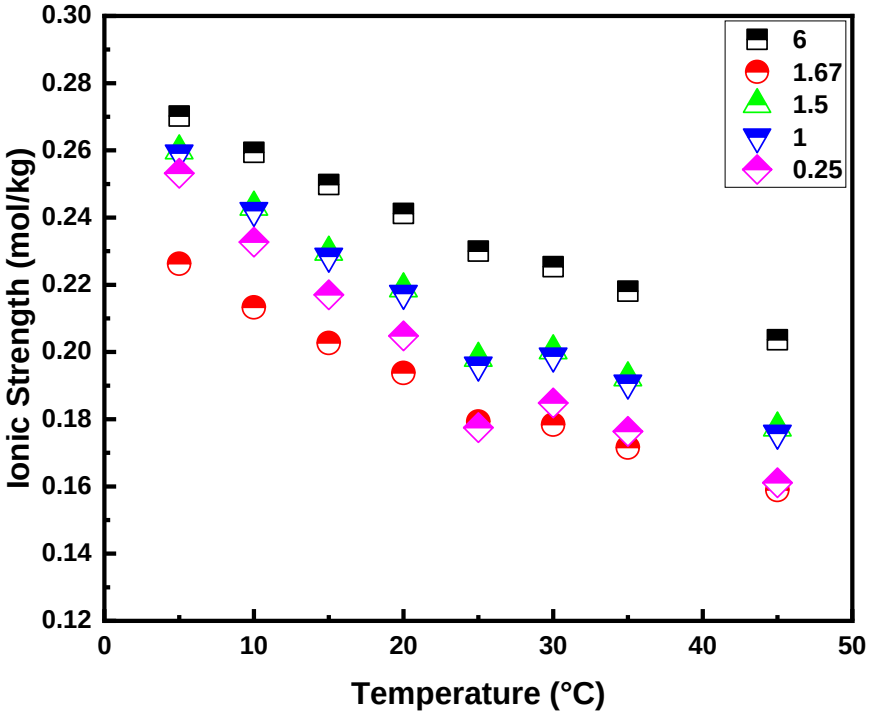

(a)

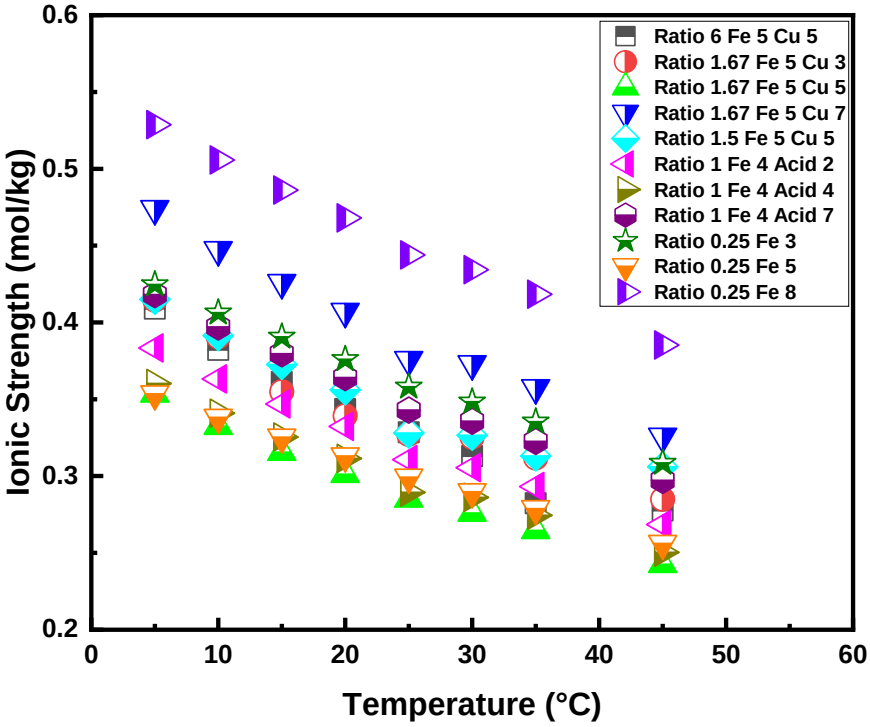

(b)

Fig.6-8. Calculated real ionic strength of (a) the Fe(II)-Fe(III)-H_2SO_4 solutions (synthetic PLS) from Test #1 to Test #5 and (b) the Fe(II)-Fe(III)-Cu(II)-H_2SO_4 solutions (synthetic PLS) from Test # 6 to Test # 16 with nominal Fe^{3+}/Fe^{2+} ratios ranging from 0.25 to 6 in the temperature range of 5°C-45°C.

The effective ionic strengths of the present solutions calculated from modeling results are shown in Fig. 8 a and b, which are generally lower than 0.5 mol/kg H_2O with a tendency of declining over temperature. The drop of ionic strength with temperature is caused by the fact that the ion association of higher charged ions (such as Fe^{2+}, Fe^{3+} and Cu^{2+}) in solutions leads to the formation of more stable and less charged ionic complexes (such as $FeHSO^{+}_4$, $FeHSO^{2+}_4$, $FeSO^{+}_4$, $Fe(SO_4)^{-}_2$ and $CuHSO^{+}_4$), and neutral species (such as $FeSO^{o}_4$, and $CuSO^{o}_4$), as indicated in Figs. 6-2.

6.3 Summary

In this work, thermodynamic model study and its speciation distribution investigation of aqueous Fe(II)-Fe(III)-H_2SO_4-H_2O solutions and aqueous Fe(II)-Fe(III)-Cu(II)-H_2SO_4-H_2O solutions under different conditions most relevant to the current industrial heap leaching process from 5 to 45 °C provide a great tool to quantify the species distribution and facilitate the deep understanding of Fe(II), Fe(III), and Cu(II) behavior with the help of fundamental data.

The results of the species distribution study of Fe(III), Fe(II), and Cu(II) in the both aqueous Fe(II)-Fe(III)-H_2SO_4-H_2O solutions and Fe(II)-Fe(III)-Cu(II)-H_2SO_4-H_2O solutions in all the conditions reveal that for Fe(II) species, free Fe^{2+} is the predominant species of total Fe (II), followed by $FeSO^{o}_4$ and the least abundant $FeHSO^{+}_4$; for Fe(III) species, Fe(III) is mainly distributed as $FeSO^{+}_4$ (the major species), free Fe^{3+} ions (second major species), $Fe(SO_4)^{-}_2$ and $FeHSO^{2+}_4$; Cu(II) is mainly dissolved as $CuSO^{o}_4$ (the major species), free Cu^{2+}, and the least abundant $CuHSO^{+}_4$. What's more, temperature is the only variation shows an important influence

on the distribution of Fe(II), Fe(III), and Cu(II) and the addition of Cu(II) (3-8 g/L) do not exert any substantial effects on the distribution of the dissolved species.

The reliable and accurate prediction of the measured redox potential for all solution conditions validates the previously developed model. The good agreement between experimental ORPs and the calculated ones shows that this expression can still be employed to predict the redox potential in the studied solutions with a much lower sulfuric acid concentration (2-7 g/L) and copper concentration (3-8 g/L). The results that the experimental ORPs in both 2 solution systems are almost identical to each other strongly prove that the redox potential of acidic iron sulfate solutions with a much lower sulfuric acid concentration and a lower cupric ion concentration can still be solely determined by the nominal ferric/ferrous ration and temperature. The speciation distribution model and previously developed expression could explain the change of the redox potential with temperature for all nominal ferric/ferrous ratios in studied synthetic PLS. The present work could help the deeper understanding and further investigation of the kinetics, iron chemistry, solution chemistry, pH, ferric/ferrous ratio, and ORP of PLS generated during heap leaching process, especially below room temperature.

The present work also provides an alternative method of estimating the pH value through the validated modeling results under extreme acidic conditions, generally less than 2 over the studied conditions.

The model study provides a promising method for the speciation studies of the Fe(II)-Fe(III)-Cu(II)-H_2SO_4-H_2O solutions over a wide range of solution compositions, various temperatures, allowing a comprehensive explaining of Fe(II), Fe(III), and Cu(II) behavior, such as the valence distribution, redox potential prediction, and pH estimation in Fe(II)-Fe(III)-Cu(II)-H_2SO_4-H_2O solutions. The reliable prediction of the ORPs by the speciation model and the previously

developed expression with high accuracy is very helpful and valuable for the further investigation and deep understanding of the leaching kinetics and iron chemistry involved in the leaching process in order to increase recovery percentage and obtain higher leaching rate.

7. SPECIATION STUDY AND IRON CHEMISTRY FOR SX SOLUTION FROM 25℃ TO 60℃

7.1 Introduction

A better understanding of species distribution for iron (ferrous and ferric) and copper in solutions generated during SX process is of great importance for the production of high-purity $CuSO_4$–H_2SO_4 electrolyte and for minimizing iron concentration. Therefore, a detailed speciation study is required here to quantitatively describe the species distribution in SX solutions.

7.2 Results and Discussion

7.2.1 Speciation Distribution Calculated in the aqueous H_2SO_4-$Fe_2(SO_4)_3$-$FeSO_4$-H_2O system

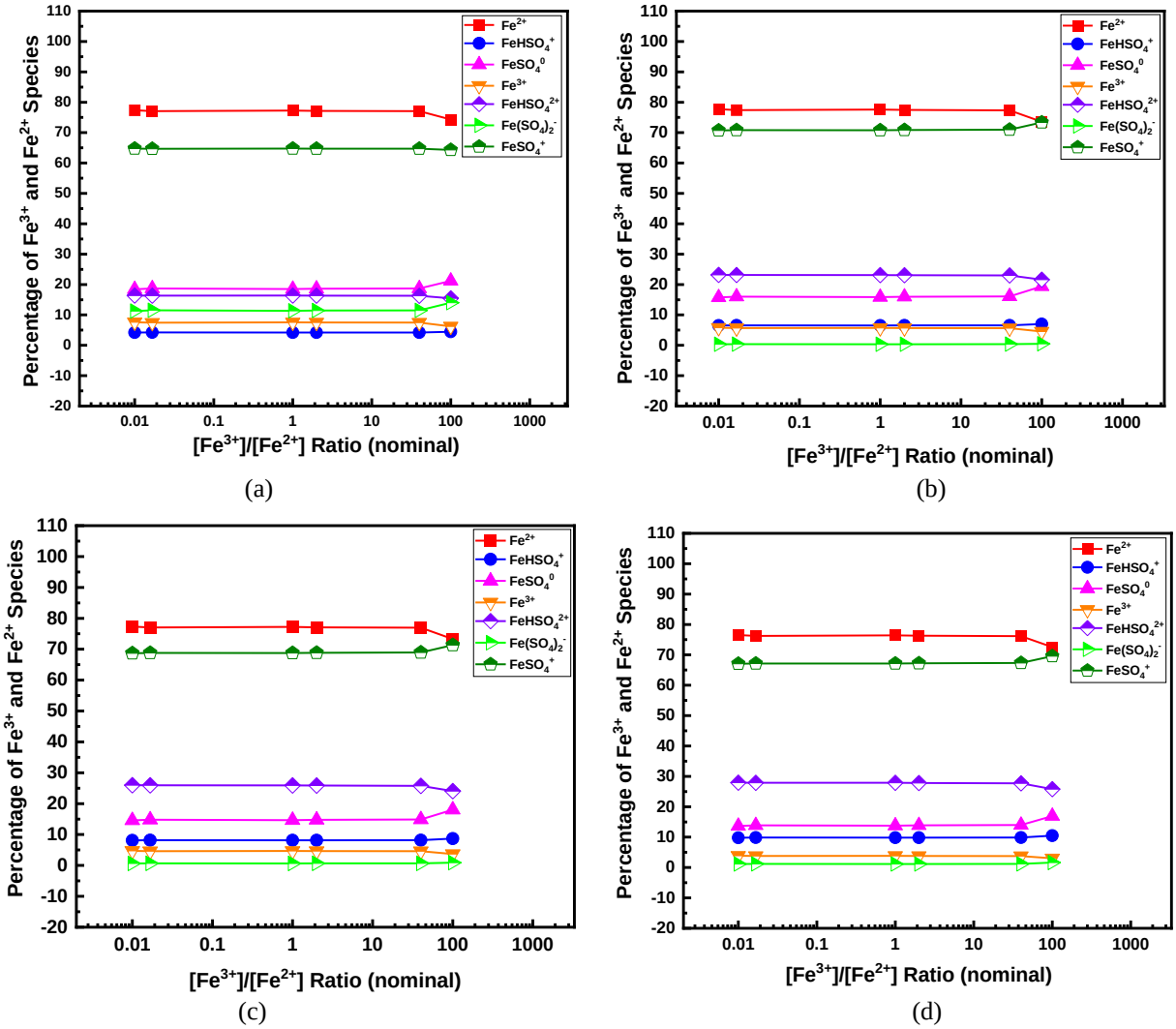

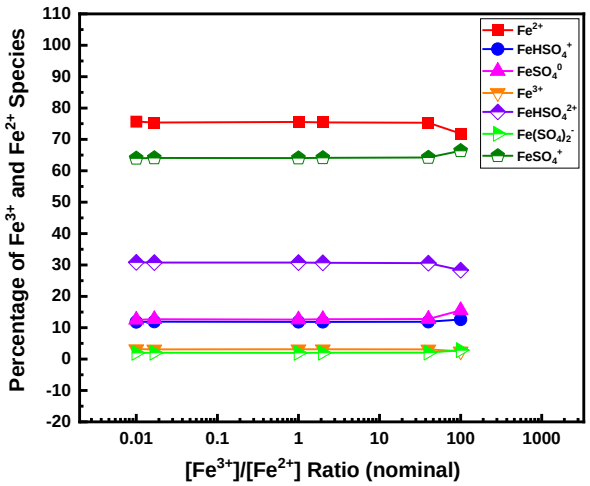

(e)

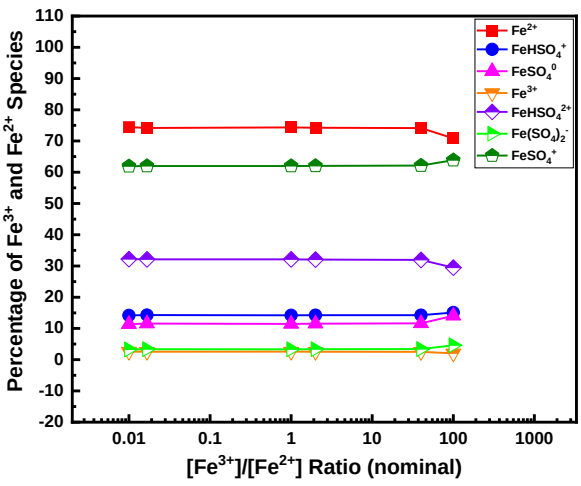

(f)

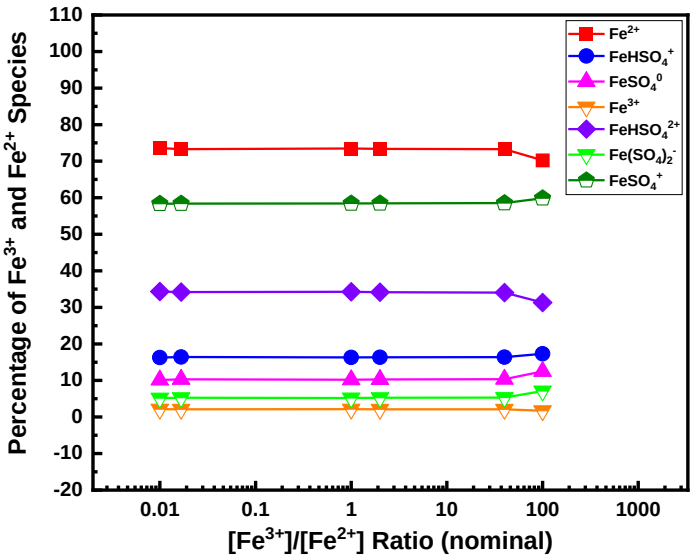

(g)

Figure 7-1 Calculated aqueous speciation diagram of the main ferric and ferrous species in the Fe(II)-Fe(III)-H_2SO_4-H_2O solutions (synthetic SX) from 25°C to 60°C with (a) temperature 25°C; (b) temperature 35°C; (c) temperature 40°C; (d) temperature 45°C; (e) temperature 50°C; (f) temperature 55°C; (g) temperature 60°C. Please note that the sum of the percentage values of both Fe(II) species (filled symbols) and Fe(III) species (half-filled symbols) are 100%.

The results of the aqueous speciation (expressed as the percentage of the total ferric or ferrous) in aqueous Fe(II)–Fe(II)–H_2SO_4 solution from 25 to 60 °C are presented in Figure 7-1. The results of species distribution for the solutions with four different nominal Fe^{3+}/Fe^{2+} ratios are similar to each other. Fe(II) species mainly distribute as free Fe^{2+} cations which account for 70.23-77.73% of the total Fe(II). $FeHSO_4^+$ is in the smallest proportion 4.2% at 25 °C, and then gradually increases up to 17.29% at 60 °C. $FeSO_4^o$ is the second dominant species at 25 °C initially (about 21.21%), and then decreases to about 10.14% eventually at 60 °C.

For Fe(III) species, free Fe^{3+} accounts for only 1.69–7.6%. The percentage of $FeHSO_4^{2+}$ ranges from 16.3% to 34.34%. The percentage of $Fe(SO_4)_2^-$ is around 0.35%–14.01%. However, the distribution of this species strongly is dependent on temperature and total amount of Fe(III). Similar observation was also found in the published literature [2, 8, 9, 12]. $FeSO_4^+$ is the predominant species for Fe(III) and takes the proportion of 58.36-73.35% of total Fe(III).

Additionally, the predominant species of Fe(II) and Fe(III) are free Fe^{2+} and $FeSO_4^+$, which is similar to the results from the literature published previously [2, 12].

7.2.2 Speciation Distribution Calculated in the aqueous H_2SO_4-$CuSO_4$-$Fe_2(SO_4)_3$-$FeSO_4$-H_2O system

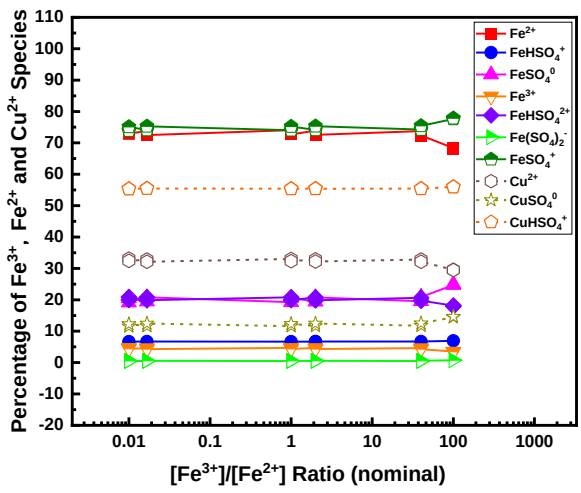

(a)

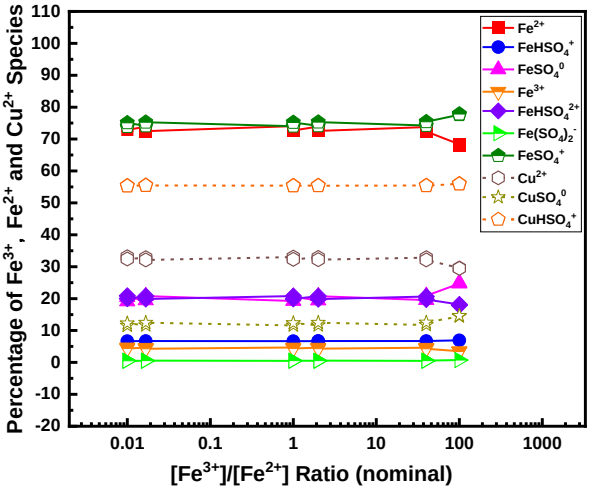

(b)

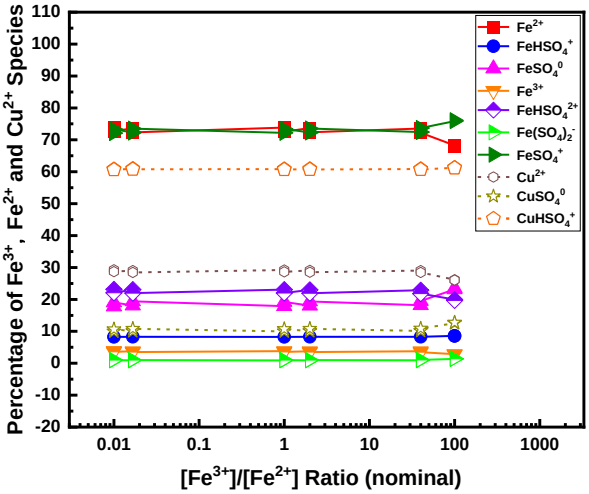

(c)

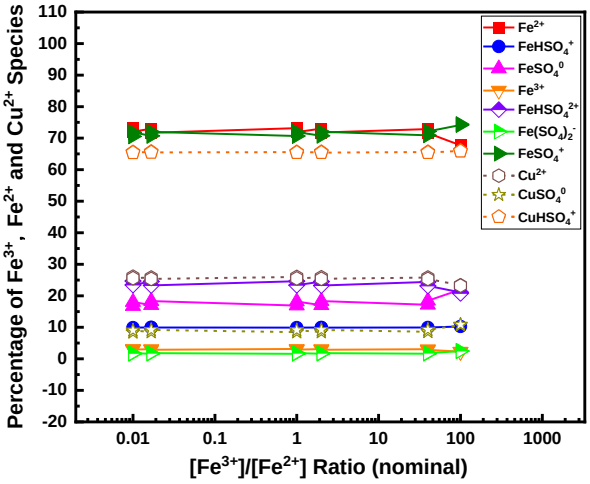

(d)

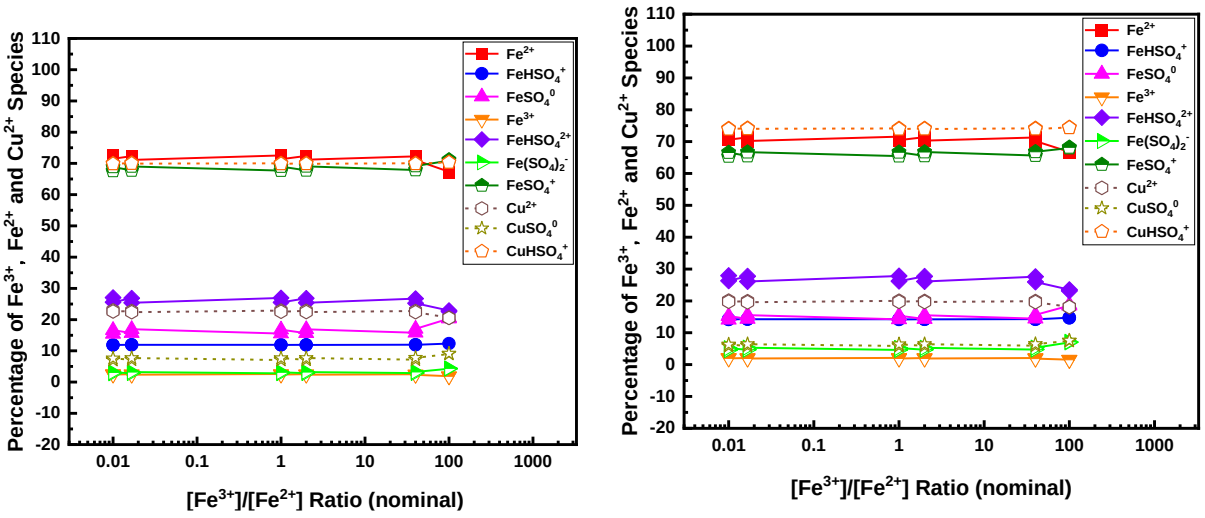

(e) (f)

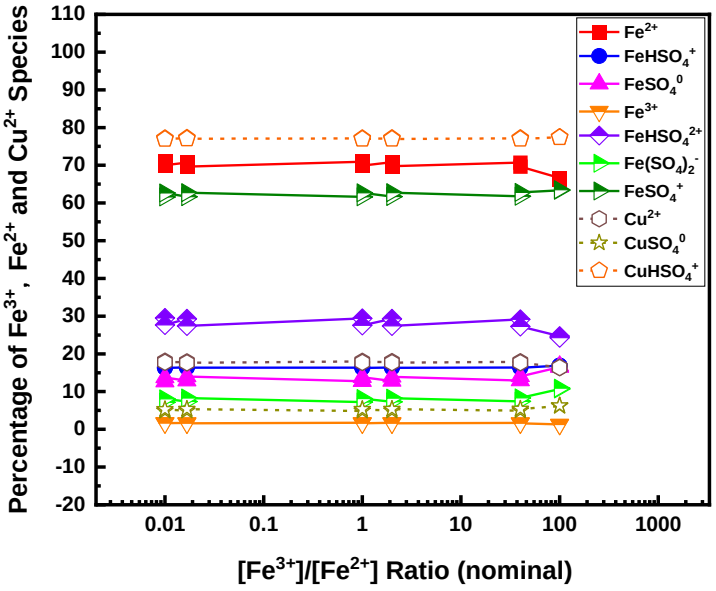

(g)

Figure 7-2 Calculated aqueous species distribution diagram in the Fe(II)-Fe(III)-Cu(II)-H_2SO_4-H_2O solutions (synthetic SX) from sample # 7 to sample # 18 with nominal Fe^{3+}/Fe^{2+} ratio ranging from 0.01 to 100 with (a) temperature 25°C; (b) temperature 35°C; (c) temperature 40°C; (d) temperature 45°C; (e) temperature 50°C; (f) temperature 55°C; (g) temperature 60°C. Please note that the sum of the percentage values of Fe(II) species (filled symbols), Fe(III) species (half-filled symbols) and Cu(II) species (unfilled symbols) are 100%

Figure 7-2 shows the results of the aqueous speciation in Fe(II)-Fe(III)-Cu(II)-H_2SO_4-H_2O solutions for synthetic SX with various solution composition from 25 to 60 °C. It shows that the overall percentage trend of each Fe(II) and Fe(III) species does not have any substantial change

after $CuSO_4$ was added. The percentage of free ferrous cations is within 66.38-74.22%, which is slightly lower than that in Fe(II)-Fe(III)-H_2SO_4-H_2O system. The proportion of $FeHSO_4^+$ is within 4.28-16.88% which is nearly equal to that of Fe(II)-Fe(III)-H_2SO_4-H_2O solution. The percentage of $FeSO_4^o$ is in the range of 12.63-25.84% and is slightly larger than that in the Fe(II)-Fe(III)-H_2SO_4-H_2O system.

For Fe(III) species, free ferric cations and $FeHSO_4^{2+}$ only account for a minor proportion, about 2.27-6.12% and 12.81-29.51%, which are slightly lower than those in Fe(II)-Fe(III)–H_2SO_4-H_2O system. $FeSO_4^+$ remains the predominant species of Fe(III), with a percentage of 61.59-77.86%. The percentage of $Fe(SO_4)_2^-$ is in the range of 0.48-18.67%, which is similar to the results from the literature published previously [2, 12].

Cu(II) species mainly distributes as Cu^{2+}, $CuSO_4^o$and $CuHSO_4^+$, with the proportion of 16.37%-41.14%, 16.37-18.1%, and 43.31%-77.36%, respectively. $CuSO_4^o$ is the least abundant species and its proportion decreases when increasing temperature. The second most abundant Cu(II) species is free Cu^{2+} and its percentage decreases when increasing temperature.

A considerable proportion of Cu(II) exists as $CuHSO_4^+$ and its proportion increases with temperature.

7.2.3 Model Validity by Comparison of the Redox Potential between Speciation Results and Experimental Measurements from 25 °C to 60 °C

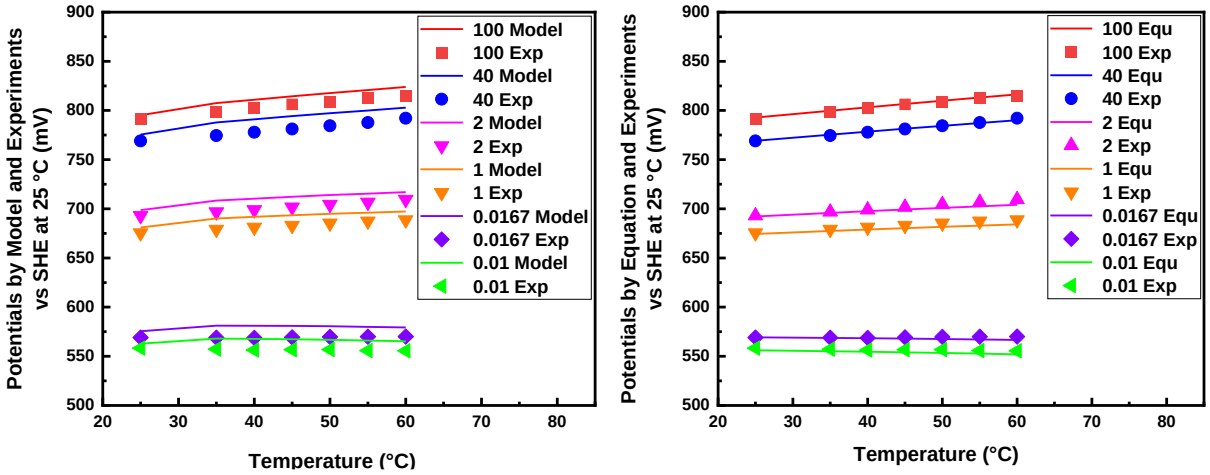

(a) (b)

Figure 7-3 Comparison of potentials (a) calculated by thermodynamic modeling and measured by experiments, and (b) calculated by Equation (1) in this work and measured by experiments vs SHE at 25°C with various nominal ratios and different temperature ranging from 25°C to 60°C in the Fe(II)-Fe(III)-H_2SO_4-H_2O solutions (synthetic SX) from Table 5-3

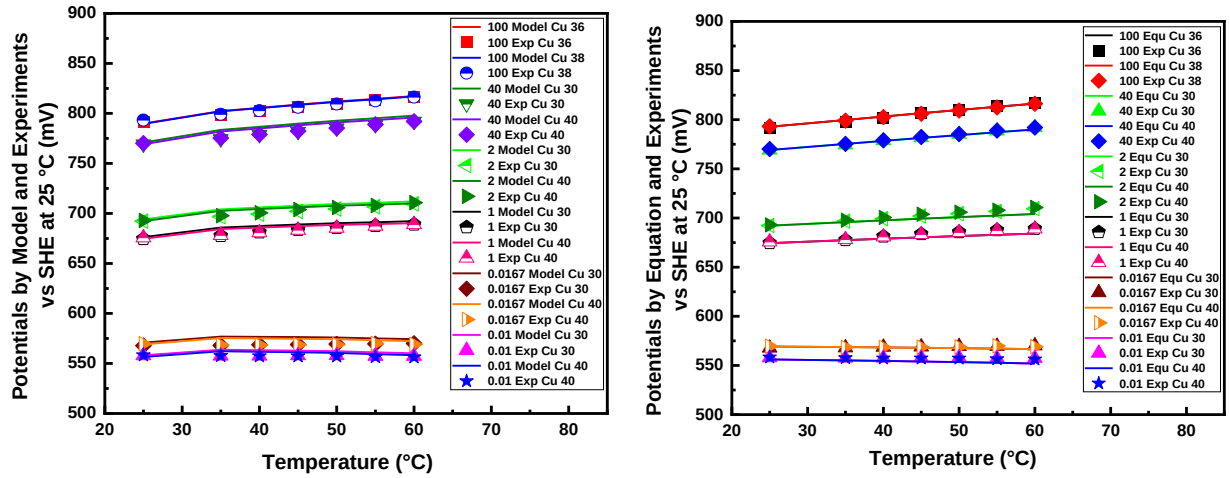

(a) (b)

Figure 7-4 Comparison of potentials (a) calculated by thermodynamic modeling and measured by experiments, and (b) calculated by Equation (1) in this work and measured by experiments vs SHE at 25°C with various nominal ratios and different temperature ranging from 25°C to 60°C in the Fe(II)-Fe(III)-Cu(II)-H_2SO_4-H_2O solutions (synthetic SX) from Table 5-3.

A comparison of the reversible potentials between experimental measurement and model calculation was employed to validate the model. As shown in Figure 7-3 and Figure 7-4, the redox potentials predicted by the model and measured by experiment are in good agreement under different nominal Fe^{3+}/Fe^{2+} ratios in both synthetic Fe(II)-Fe(III)-H_2SO_4-H_2O solution and Fe(II)-Fe(III)-Cu(II)-H_2SO_4-H_2O solution from 25 to 60 °C. The difference between experimental and calculated values was typically around ±5 mV depending on solution composition and temperature. This proves that the model is qualitatively and quantitatively validated. Therefore, a conclusion can be drawn that the predicted species distribution are correct for both Fe(II)-Fe(III)-H_2SO_4-H_2O and Fe(II)-Fe(III)-Cu(II)-H_2SO_4-H_2O solutions in the temperature and composition ranges investigated in the present work.

In addition, Eq. (1) has been proved to accurately predict redox potential in Fe(II)–Fe(III)–H_2SO_4–H_2O system over a wide range of solution composition [2, 14]. The comparison of measured potential by experiment and calculated potential by Eq. (1) in the present study are employed to validate its broad applicability as well. Figure 7-3 and Figure 7-4 show that the experimental potentials in the present study are in an excellent agreement with those calculated by Eq. (1). The potential difference is generally less than 1.5 mV under nominal Fe^{3+}/Fe^{2+} ratios ranging from 0.01 to 100 with the concentrations of copper concentration varying from 30 to 40 g/L and with the sulfuric acid same concentration of 200 g/L, respectively. Therefore, a conclusion could be drawn that the expression developed previously can also be employed to accurately predict the redox potential in complicated solutions for SX process in this thesis.

7.2.4 Calculated Real Ferric/Ferrous Ratio Based on Model for SX Solutions

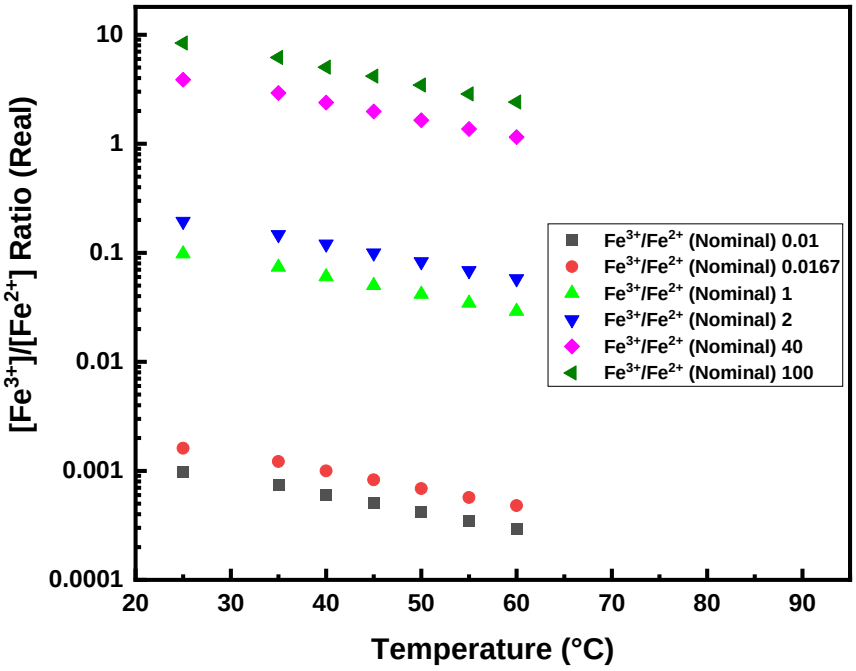

Figure 7-5 Calculated real Fe^{3+}/Fe^{2+} ratios in the Fe(II)-Fe(III)-H_2SO_4-H_2O solutions (synthetic SX) with different nominal Fe^{3+}/Fe^{2+} ratios in the temperature range from 25°C to 60°C.

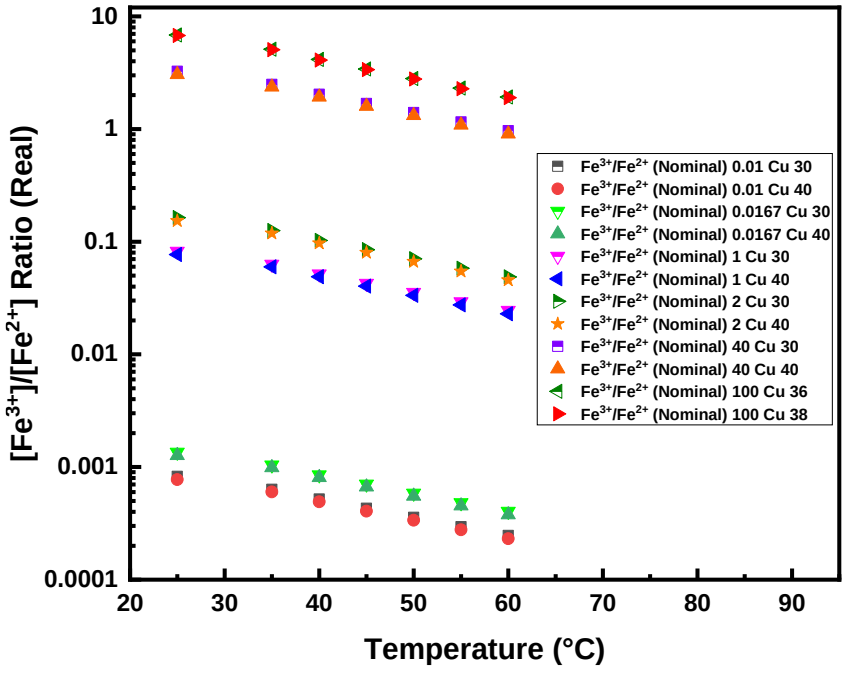

Figure 7-6 Calculated real Fe^{3+}/Fe^{2+} ratios in the Fe(II)-Fe(III)-Cu(II)-H_2SO_4-H_2O solutions (synthetic SX) with different nominal Fe^{3+}/Fe^{2+} ratios in the temperature range from 25°C to 60°C.

In Figure 7-5 an Figure 7-6, the real ferric/ferrous ratios calculated from thermodynamic model are shown for the tests #1−#6 in the Fe(II)−Fe(III)−H_2SO_4−H_2O system and for the tests #7−#18 in the Fe(II)−Fe(III)−Cu(II)−H_2SO_4−H_2O system. The 6 different nominal ferric/ferrous ratios ranging from 0.01 to 100 are presented in test #1−#18 in Table 5-2. As is shown in Figure 7-5 and Figure 7-6, all the nominal ferric/ferrous ratios are remarkably higher than the responding nominal ferric/ferrous ratios calculated from thermodynamic model at all 7 temperatures ranging from 25 to 60°C in both two systems. What's more, the real ferric/ferrous ratios calculated based on model for the tests #1−#6 in the Fe(II)−Fe(III)−H_2SO_4−H_2O system and for the tests #7−#18 in the Fe(II)−Fe(III)−Cu(II)−H_2SO_4−H_2O system both decrease significantly with the temperature increasing from 5 to 45 °C under the same nominal ferric/ferrous ratio shown in Figure 7-5 and Figure 7-6.

7.2.5 Analysis of Calculated pH

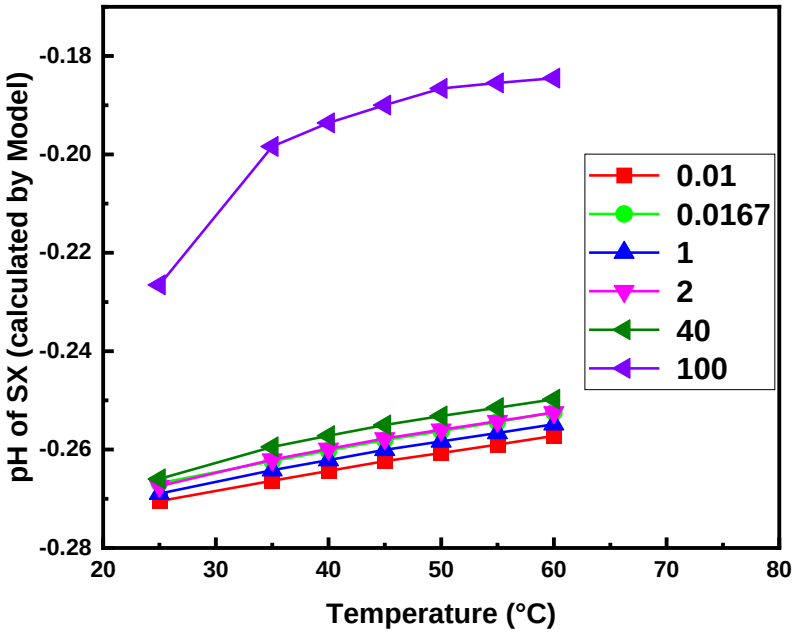

Figure 7-7 Calculated pH of the Fe(II)-Fe(III)-H_2SO_4-H_2O solutions (synthetic SX) from sample #1 to sample #6 with different nominal Fe^{3+}/Fe^{2+} ratios in the temperature range of 25°C-60°C.

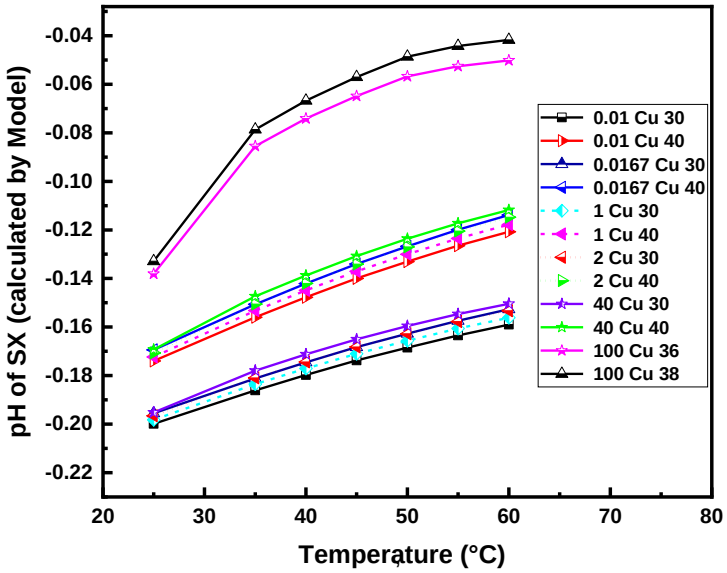

Figure 7-8 Calculated pH of the Fe(II)-Fe(III)-Cu(II)-H_2SO_4-H_2O solutions (synthetic SX) from sample # 7 to sample # 18 with nominal Fe^{3+}/Fe^{2+} ratio ranging from 0.01 to 100 in the temperature range of 25°C-60°C.

From the validated thermodynamic modeling results, the pH values for the solutions in tests #1−#18 can be calculated by the obtained activity of hydrogen ions in this thesis. This provides an indirect way to study the pH of the involved solution in this thesis. The calculated pH's for various solution compositions are shown in Figure 7-7 and Figure 7-8. It can be observed that the pH values of iron sulfate/iron−copper sulfate solutions are generally less than 0, in the range of -0.19 to -0.27 and -0.04 to -0.2over the studied temperatures and nominal Fe^{3+}/Fe^{2+} ratios. In both systems, under the same nominal Fe^{3+}/Fe^{2+} ratio, the pH increases gradually with temperature up to 60 °C. The increased pH values show that the concentrations of H^+ ions in the 2 systems slightly decrease when the solution temperatures gradually increase from 25 to 60 °C. The results above implies that more protons are combined with free metal ions and sulfate anions to form more thermodynamically stable ionic complexes at higher temperatures, resulting in the declining concentration of H^+ ions.

7.2.6 Analysis of Calculated Ionic Strength

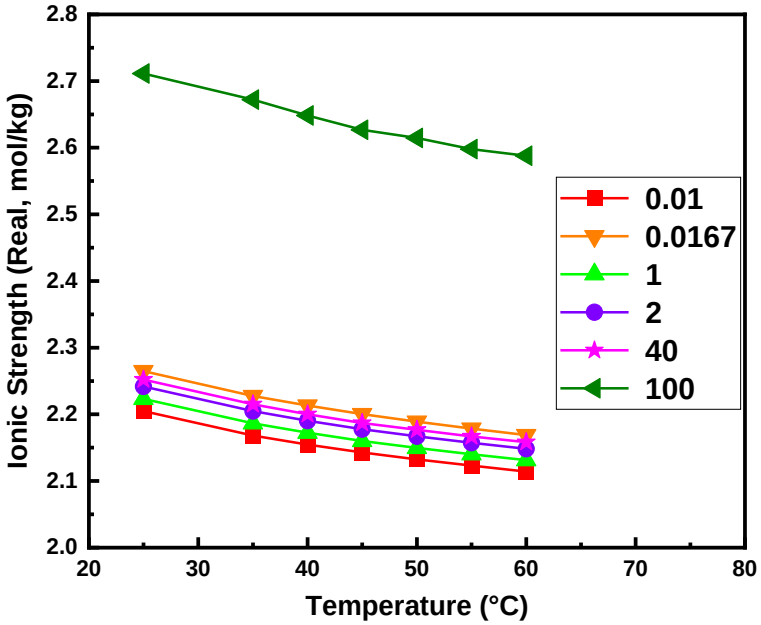

Figure 7-9 Calculated real ionic strength of the Fe(II)-Fe(III)-H_2SO_4-H_2O solutions (synthetic SX) from sample #1 to sample #6 with different nominal Fe^{3+}/Fe^{2+} ratios in the temperature range of 25°C-60°C.

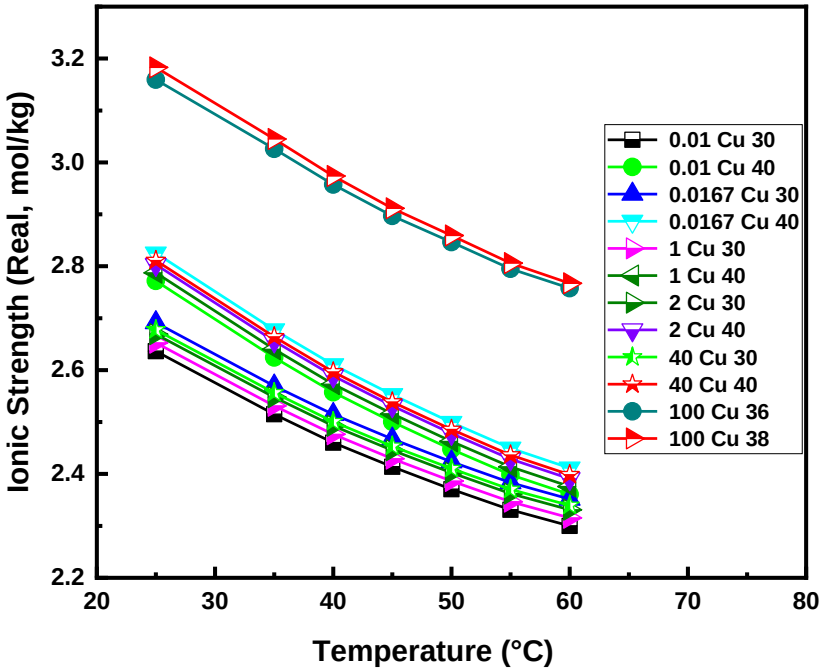

Figure 7-10 Calculated real ionic strength of the Fe(II)-Fe(III)-Cu(II)-H_2SO_4-H_2O solutions (synthetic SX) from sample # 7 to sample # 18 with nominal Fe^{3+}/Fe^{2+} ratio ranging from 0.01 to 100 in the temperature range of 25°C-60°C.

As can be observed, under the same nominal Fe^{3+}/Fe^{2+} ratio, increasing temperatures from 25 to 60 °C results in a gradual decrease of the real ionic strength. This may be explained by the fact that ion association of higher charged ions such as Fe^{2+}, Fe^{3+}, and Cu^{2+} in solutions leads to the formation of more stable and less charged ionic complexes such as $FeHSO_4^+$, $FeHSO_4^{2+}$, $FeSO_4^+$, $Fe(SO_4)_2^-$, and $CuHSO_4^+$ when increasing the temperature, as can be clearly observed in Figure 8-1 and Figure 8-2.

The nominal ionic strengths for all nominal Fe^{3+}/Fe^{2+} ratios are in the range of 2.14-2.72 mol/kg H_2O for the Fe(II)-Fe(III)-H_2SO_4-H_2O solutions and 2.3-3.2 mol/kg H_2O for the Fe(II)-Fe(III)-Cu(II)-H_2SO_4-H_2O solutions. It is evident that the values of the real ionic strength of the present solutions by using the calculated ionic concentration of charged species from modeling results are much lower than those by using nominal species concentration in the two systems. This is because the concentration of higher charged ions such as Fe^{2+}, Fe^{3+}, Cu^{2+}, and SO_4^{2-} decreases significantly, and at the same time, they are employed to form lower charged ionic complexes (HSO_4^-, $FeHSO_4^+$, $FeHSO_4^{2+}$, $FeSO_4^+$, $Fe(SO_4)_2^-$, and $CuHSO_4^+$) and neutral species ($FeSO_4°$ and $CuSO_4°$).

7.3 Summary

The speciation of Fe(II)-Fe(III)-H_2SO_4-H_2O and Fe(II)-Fe(III)-Cu(II)-H_2SO_4-H_2O solutions was investigated by thermodynamic modeling under conditions related to SX. Results reveal that most of the Fe(III) is distributed as complexes and the free Fe^{3+} accounts for only a minor percentage, whereas a large amount of Fe(II) exists in the form of free Fe^{2+}. The Cu(II) species mainly distributes as Cu^{2+}, $CuSO_4^o$ and $CuHSO_4^+$, and a considerable proportion of Cu(II) exists as $CuHSO_4^+$.

The validity of the proposed model was confirmed by reliable prediction of measured redox potential from 25 to 60 °C. The fact that there exists an excellent agreement between the redox potential calculated by previously developed and measured by this work, further extends its applicability and provides an alternative method of predicting redox potential. It is expected that the findings in this work will facilitate the development of combined SX/EW technology to achieve higher current efficiency.

Based on the discussion in Chapter 7 and the previous Chapter 6, it seems that either with a much higher acid concentration or with the coexistence of a higher amount of copper ions, the redox potential can still be solely determined by the Fe^{3+}/Fe^{2+} couple. Changing of those two parameters exerts no apparent influence on the prediction of redox potentials. Particularly, the addition of a high amount of copper does not affect the redox potential for the abovementioned two systems either calculated from model results or measured by experiment. The following discussion will explain in more details regarding this phenomenon.

From the modeling results, it was found that adding 30 or 40 g/L Cu(II) in copper sulfate does not significantly change the distribution of each species in various solution compositions over studied temperatures. It also should be noted that due to the interference of high concentration of

H_2SO_4, the percentage of Fe(II), Fe(III), Cu(II) species fluctuates a bit at nominal Fe^{3+}/Fe^{2+} ratio 100, but overall remains stable under each studied temperature and nominal Fe^{3+}/Fe^{2+} ratio range. Temperature exerts a substantial influence on species distribution rather than solution compositions. By using speciation model, the concentration (represented in percentage) of each studied Fe(II), Fe(III), Cu(II) species as a function of temperature can be quantified. It may be helpful to employ the above speciation results in Cu spent electrolyte to better define iron control and removal strategies.

Speciation of Fe(II)−Fe(III)−Cu(II)−H_2SO_4−H_2O aqueous systems was developed by thermodynamic modeling under conditions most relevant to the current industrial SX electrolyte from 25 to 60 °C. The model can help quantify the species distribution and provide fundamental data for a deeper understanding of Fe (II and III) and Cu behavior during SX process.

The calculated distribution of each Fe(II and III) and Cu(II) species in the Fe(II)-Fe(III)-H_2SO_4-H_2O and Fe(II)-Fe(III)-Cu(II)-H_2SO_4-H_2O systems reveals that Fe(II) is primarily distributed as free Fe^{2+}, $FeHSO_4^+$ and $FeSO_4$°; Fe(III) is mainly distributed as free Fe^{3+}, $FeSO_4^+$, $FeHSO_4^{2+}$, and $Fe(SO_4)_2^-$; Cu(II) is mainly dissolved as Cu^{2+}, $CuSO_4$°, and $CuHSO_4^+$. Especially, after the addition of a high amount of copper (30-40 g/L), the overall distribution trends of each Fe(II) and Fe(III) species do not have substantial changes.

The validity of the proposed model was confirmed by reliable and accurate prediction of the measured redox potential throughout all solution conditions. The excellent agreement between measured potentials and those calculated proves that this expression can also be employed to predict the redox potential in SX solutions with a higher acid and cupric ion concentration. A detailed analysis of the model-calculated results in terms of the free ferric and ferrous ion concentration ratios and their accompanying activity coefficients, together with the fact that the

experimental ORP values in the two solution systems are almost identical to each other, strongly supports that the redox potential of acidic iron sulfate solutions with a much higher acid concentration and a high amount of copper can still be solely determined by the Fe^{3+}/Fe^{2+} couple. The speciation model and developed expression explain the change of the redox potential with temperature for all nominal Fe^{3+}/Fe^{2+} ratios.

Furthermore, this work provides an alternative method of estimating the pH by the validated modeling results under extreme acidic conditions. As expected, the pH values of iron sulfate/iron-copper sulfate solutions are generally less than 0 over the studied conditions and increase gradually with temperature. The pH values in iron sulfate solutions are overall lower than those in iron-copper sulfate solutions. It is also worth noting that the real ionic strength calculated by the concentrations of ionic species based on modeling results is significantly lower than the nominal ionic strength calculated by nominal species concentrations. Although the effective ionic strength is still relatively high, the excellent agreement of redox potentials between experimental measurements and model prediction justifies the reasonable use of the B-dot model for the calculation of activity coefficients of dissolved species.

It should be emphasized that this work provides a reliable set of thermodynamic data, and the model developed in this study is a feasible and promising method for the studies on the speciation of the Fe(II)-Fe(III)-Cu(II)-H_2SO_4-H_2O system over a wide range of solution conditions, allowing a comprehensive description of Fe and Cu behavior, such as the valence distribution, redox potential calculation, and pH estimation in the acidic iron sulfate solution with copper. The reliable prediction of the redox potential by the speciation model and the developed expression with high accuracy is particularly valuable and attractive. Therefore, it can be expected that the findings in the present work will facilitate our further investigation on the speciation of more

complicated acidic iron sulfate solutions as well as solutions in other copper hydrometallurgical processes

8. SPECIATION STUDY AND IRON CHEMISTRY FOR IRON CHEMISTRY FOR TRADITIONAL EW SOLUTION FROM 25℃ TO 60℃

8.1 Introduction

A thermodynamic model was developed and proved to reliably simulate the speciation of H_2SO_4-$Fe_2(SO_4)_3$-$FeSO_4$-H_2O system through a wide range of solution compositions and temperatures [2]. The model was validated by accurate prediction of measured redox potential, and a novel redox potential equation was also developed. Additionally, when $CuSO_4$ is further dissolved in the acidic iron sulfate solution, species such as Cu^{2+}, $CuSO_4^o$, $CuHSO_4^+$ will be formed according to the literature [7-9]. Hence, the related thermodynamic data were collected and reviewed for model calculation [7-12]. Especially, in our previous publication, thermodynamic modeling of Fe(II)-Fe(III)-Cu(II)-H_2SO_4-H_2O system was carried out under conditions most relevant to the copper electrorefining [12, 101-103].

8.2 Results and Discussion

8.2.1 Speciation Distribution Calculated in the aqueous H_2SO_4-$Fe_2(SO_4)_3$-$FeSO_4$-H_2O system

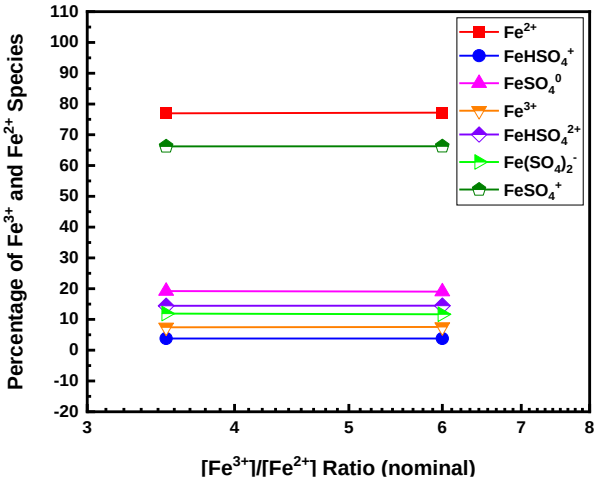

(a)

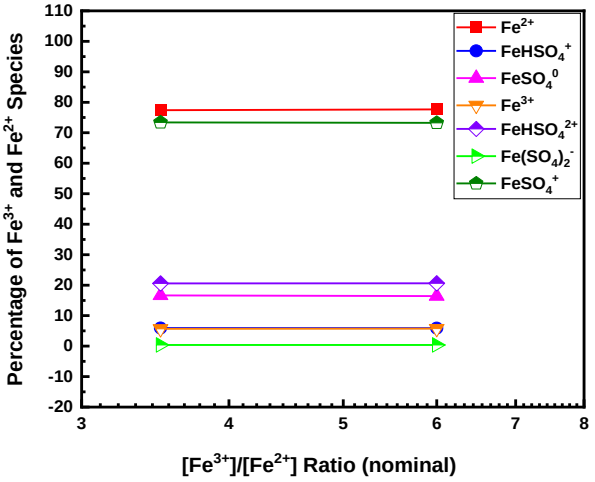

(b)

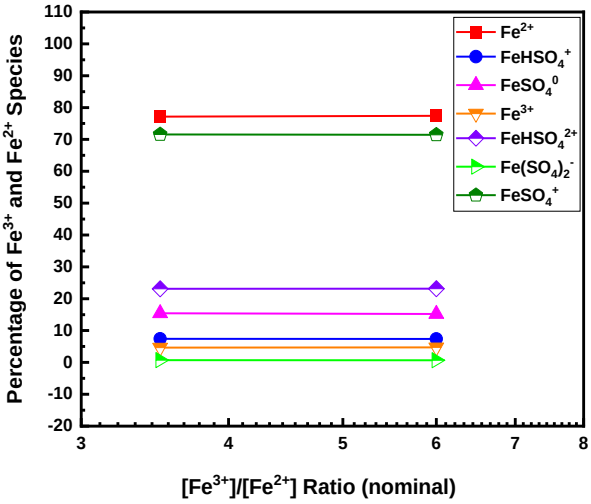

(c)

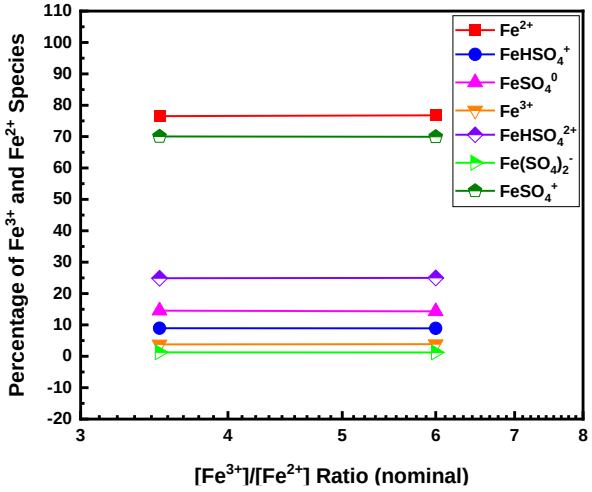

(d)

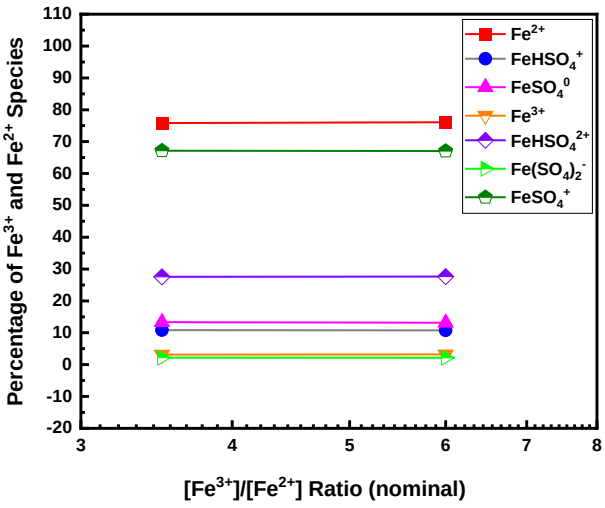

(e)

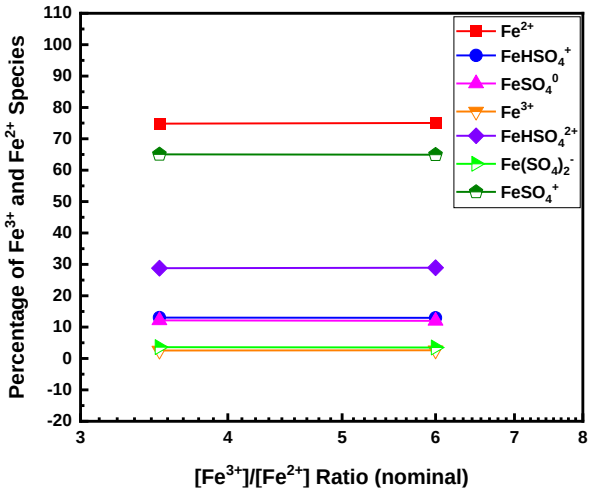

(f)

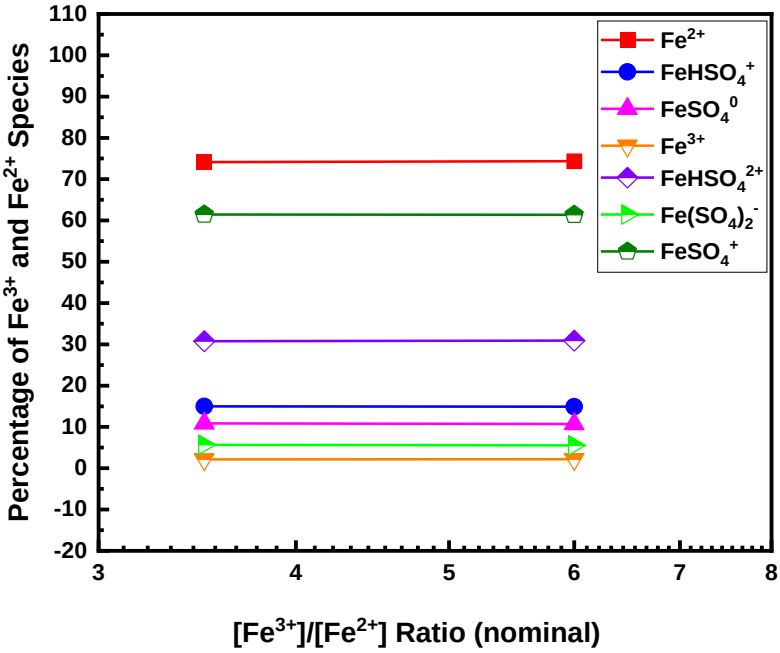

(g)

Figure 8-1 Calculated aqueous speciation diagram of the main ferric and ferrous species in the Fe(II)-Fe(III)-H_2SO_4-H_2O solutions (synthetic Traditional EW) from 25°C to 60°C with (a) temperature 25°C; (b) temperature 35°C; (c) temperature 40°C; (d) temperature 45°C; (e) temperature 50°C; (f) temperature 55°C; (g) temperature 60°C. Please note that the

sum of the percentage values of both Fe(II) species (filled symbols) and Fe(III) species (half-filled symbols) are 100%.

The results of the aqueous speciation (expressed as the percentage of the total ferric or ferrous) in aqueous Fe(II)-Fe(II)-H_2SO_4 solution from 25 to 60 °C are presented in Figure 8-1. The results of species distribution for the solutions with 3 different nominal Fe^{3+}/Fe^{2+} ratios are similar to each other. Fe(II) species mainly distribute as free Fe^{2+} cations which account for 74.14-77.67% of the total Fe(II). $FeHSO_4^+$ is in the smallest proportion 3.79% at 25 °C, and then gradually increases up to 14.99% at 60 °C. $FeSO_4^o$ is the second dominant species at 25 °C initially (about 19.02%), and then decreases to about 10.72% eventually at 60 °C.

For Fe(III) species, free Fe^{3+} accounts for only 2.14-7.56%. The percentage of $FeHSO_4^{2+}$ ranges from 14.44% to 30.9%. The percentage of $Fe(SO_4)_2^-$ is around 0.37%-11.89%. However, the distribution of this species strongly is dependent on temperature and total amount of Fe(III). Similar observation was also found in the published literature [2, 8, 9, 12]. $FeSO_4^+$ is the predominant species for Fe(III) and takes the proportion of 61.38–73.39% of total Fe(III).

Additionally, the predominant species of Fe(II) and Fe(III) are free Fe^{2+} and $FeSO_4^+$, which is similar to the results from the literature published previously [2, 12].

8.2.2 Speciation Distribution Calculated in the aqueous H_2SO_4-$CuSO_4$-$Fe_2(SO_4)_3$-$FeSO_4$-H_2O systems

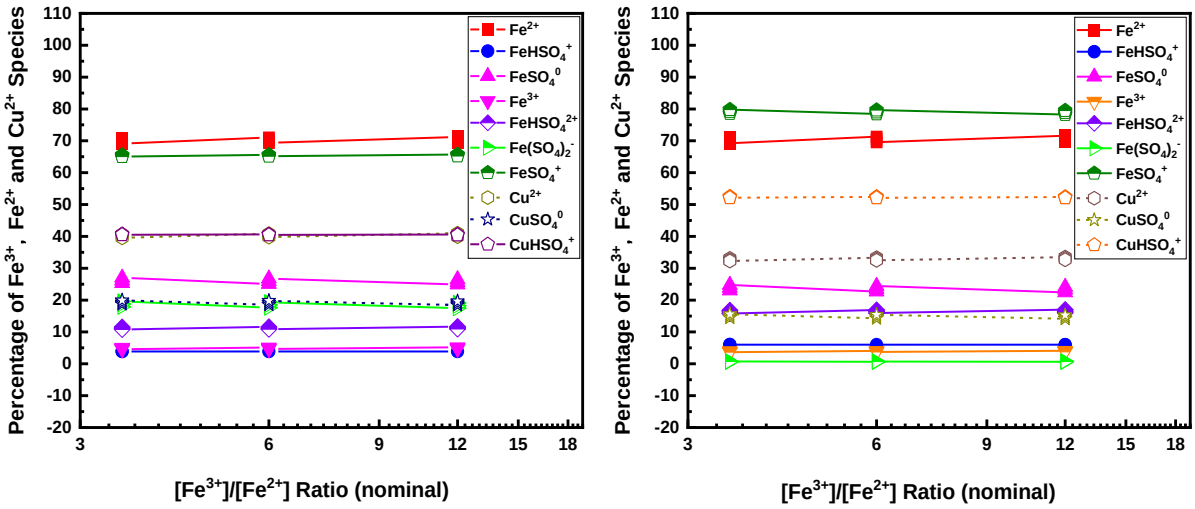

(a) (b)

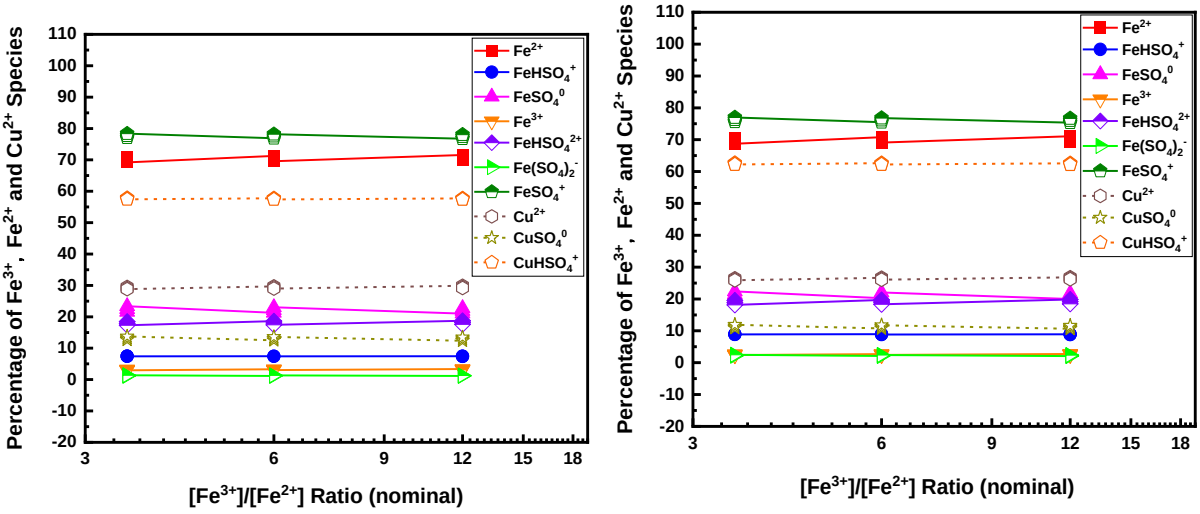

(c) (d)

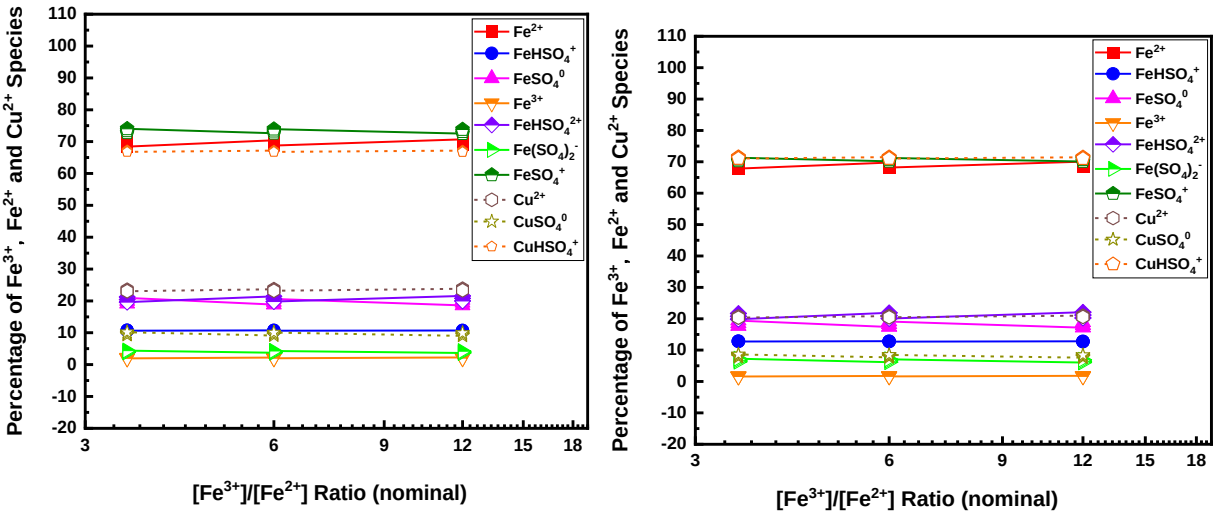

(e) (f)

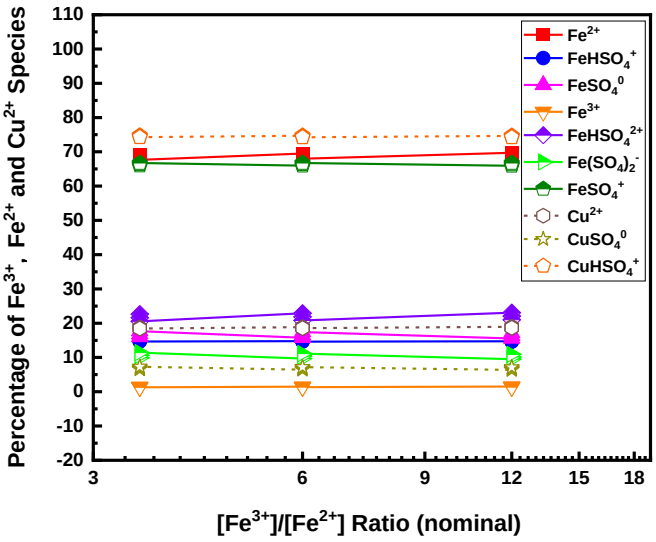

(g)

Figure 8-2 Calculated aqueous species distribution diagram in the Fe(II)-Fe(III)-Cu(II)-H_2SO_4-H_2O solutions (synthetic Traditional EW) from sample # 3 to sample # 11 with nominal Fe^{3+}/Fe^{2+} ratio ranging from 3.5 to 12 with (a) temperature 25°C; (b) temperature 35°C; (c) temperature 40°C; (d) temperature 45°C; (e) temperature 50°C; (f) temperature 55°C; (g) temperature 60°C. Please note that the sum of the percentage values of Fe(II) species (filled symbols), Fe(III) species (half-filled symbols) and Cu(II) species (unfilled symbols) are 100%.

Figure 7-2 shows the results of the aqueous speciation in Fe(II)–Fe(III)–Cu(II)–H_2SO_4–H_2O solutions for synthetic SX with various solution composition from 25 to 60 °C. It shows that the overall percentage trend of each Fe(II) and Fe(III) species does not have any substantial change after $CuSO_4$ was added. The percentage of free ferrous cations is within 67.68-71.59%, which is slightly lower than that in Fe(II)-Fe(III)-H_2SO_4-H_2O system. The proportion of $FeHSO_4^+$ is within 3.87-14.82% which is nearly equal to that of Fe(II)-Fe(III)-H_2SO_4-H_2O solution. The percentage of $FeSO_4^o$ is in the range of 15.99-27.00% and is slightly larger than that in the Fe(II)-Fe(III)-H_2SO_4-H_2O system.

For Fe(III) species, free ferric cations and $FeHSO_4^{2+}$ only account for a minor proportion, about 1.29-5.21% and 10.78-23.09%, respectively, which are slightly lower than those in Fe(II)-Fe(III)-H_2SO_4-H_2O system. $FeSO_4^+$ remains the predominant species of Fe(III), with a percentage of 65.03~79.81%. The percentage of $Fe(SO_4)_2^-$ is in the range of 0.63-19.59%, which is similar to the results from the literature published previously [2, 12].

Cu(II) species mainly distributes as Cu^{2+}, $CuSO_4^o$and $CuHSO_4^+$, with the proportion of 18.43-40.98%, 6.39-19.90%, and 40.46-74.71%, respectively. $CuSO_4^o$ is the least abundant species and its proportion decreases when increasing temperature. The second most abundant Cu(II) species is free Cu^{2+} and its percentage decreases when increasing temperature. A considerable proportion of Cu(II) exists as $CuHSO_4^+$ and its proportion increases with temperature.

8.2.3 Model Validity by Comparison of the Redox Potential between Speciation Results and Experimental Measurements from 25 °C to 60 °C

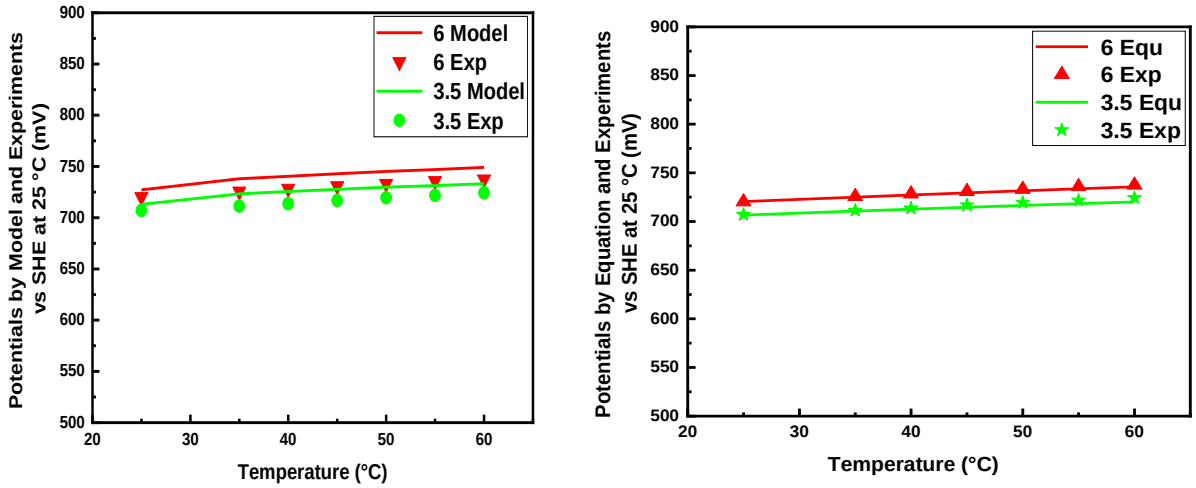

(a) (b)

Figure 8-3 Comparison of potentials (a) calculated by thermodynamic modeling and measured by experiments, and (b) calculated by Equation (1) in this work and measured by experiments vs SHE at 25°C with various nominal ratios and different temperature ranging from 25°C to 60°C in the Fe(II)-Fe(III)-H_2SO_4-H_2O solutions (synthetic Traditional EW) from Table 5-6.

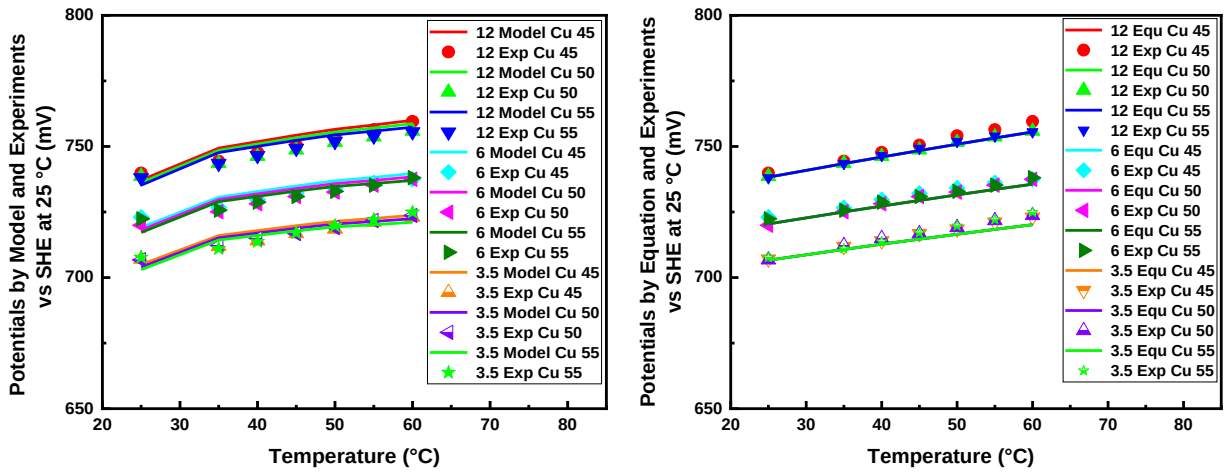

Figure 8-4 Comparison of potentials (a) calculated by thermodynamic modeling and measured by experiments, and (b) calculated by Equation (1) in this work and measured by experiments vs SHE at 25°C with various nominal ratios and different temperature ranging from 25°C to 60°C in the Fe(II)-Fe(III)-Cu(II)-H_2SO_4-H_2O solutions (synthetic Traditional EW) from Table 5-6.

A comparison of the reversible potentials between experimental measurement and model calculation was employed to validate the model. As shown in Figure 8-3 and Figure 8-4, the redox potentials predicted by the model and measured by experiment are in good agreement under different nominal Fe^{3+}/Fe^{2+} ratios in both synthetic Fe(II)-Fe(III)-H_2SO_4-H_2O solution and Fe(II)–Fe(III)– Cu(II)–H_2SO_4–H_2O solution from 25 to 60 °C. The difference between experimental and calculated values was typically around ±4 mV depending on solution composition and temperature. The results above proves that the model is qualitatively and quantitatively validated. Therefore, a conclusion can be drawn that the predicted species distribution are correct and useful for both Fe(II)-Fe(III)-H_2SO_4-H_2O and Fe(II)-Fe(III)-Cu(II)-H_2SO_4-H_2O solutions in the temperature and composition ranges investigated in this thesis.

In addition, Eq. (1) has been proved to accurately predict redox potential in Fe(II)–Fe(III)–H_2SO_4–H_2O system over a wide range of solution composition [2, 14]. The comparison of measured potential by experiment and calculated potential by Eq. (1) in the present study are employed to validate its broad applicability as well. Figure 8-3 and Figure 8-4 show that the experimental potentials in the present study are in an excellent agreement with those calculated by Eq. (1). The potential difference is generally less than 2 mV under nominal Fe^{3+}/Fe^{2+} ratios ranging from 3.5 to 12 with the concentrations of copper concentration varying from 45 to 55 g/L and with the sulfuric acid same concentration of 180 g/L, respectively. Therefore, a conclusion could be drawn that the expression developed previously can also be employed to accurately predict the redox potential in complicated solutions for traditional Cu EW process in this thesis.

From the above analysis of the model-calculated results, together with the fact that the experimental ORP values in the 2 solution systems are almost identical to each other, it seems that the redox potential of acidic iron sulfate solutions with a much higher acid concentration and a high amount of copper can still be solely determined by the Fe^{3+}/Fe^{2+} couple. Based on the above discussion, the proposed model was validated by reliable and accurate prediction of measured redox potentials. It proves that either with much higher acid concentration with or without the coexistence of a higher amount of copper ions, the redox potential can still be solely determined by the Fe^{3+}/Fe^{2+} couple. There is no apparent influence on the prediction of redox potentials caused by those two parameters. The expression developed previously can also be employed to predict the redox potential in much more complicated solutions. The speciation model and developed expression explain the change of the redox potential with temperature for all nominal Fe^{3+}/Fe^{2+} ratios.

It should be emphasized that the current work provides a set of thermodynamic data which has proved to be reliable to simulate the distribution of a simple ion, ion complex, and neutral molecule by thermodynamic modeling for the abovementioned solutions, thus providing a new method to understand the behavior of species involved in the acidic iron sulfate solution with copper.

Validation of the studied thermodynamic model is limited to the range of solution compositions and temperatures in this work as a broader range may lead to the generation or presence of additional species. Additional experimental and theoretical work is needed to better understand the 2 solution systems.

8.2.4 Calculated Real Ferric/Ferrous Ratio Based on Model for Traditional EW Solutions

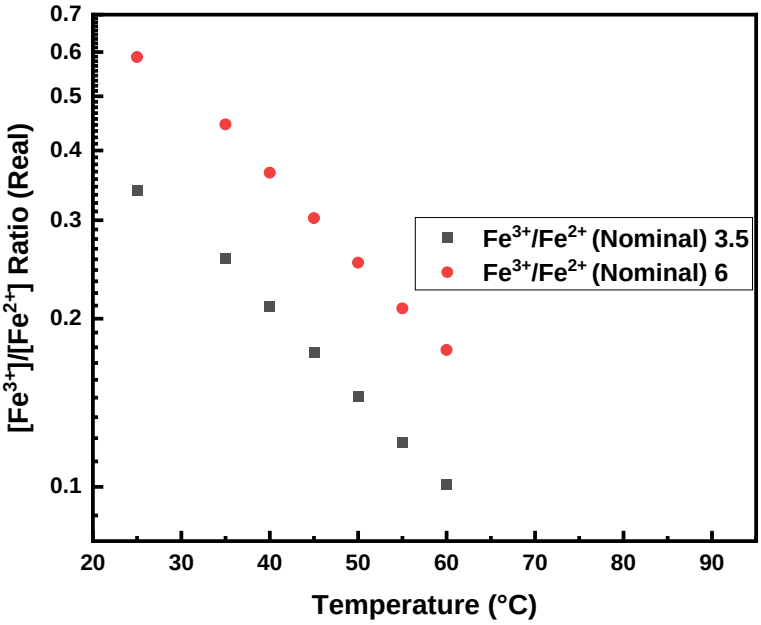

Figure 8-5 Calculated real Fe^{3+}/Fe^{2+} ratios in the Fe(II)-Fe(III)-H_2SO_4-H_2O solutions (synthetic Traditional EW) with different nominal Fe^{3+}/Fe^{2+} ratios in the temperature range from 25°C to 60°C.

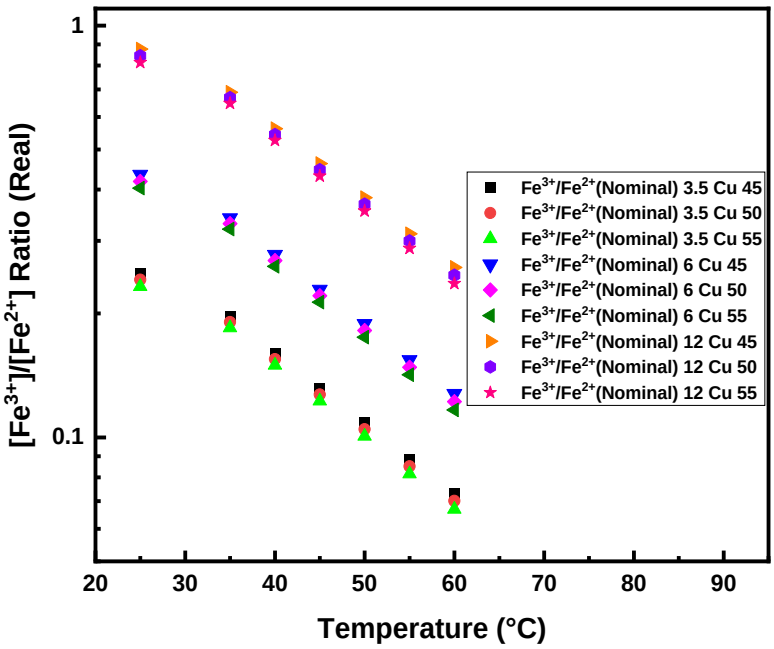

Figure 8-6 Calculated real Fe^{3+}/Fe^{2+} ratios in the Fe(II)-Fe(III)-Cu(II)-H_2SO_4-H_2O solutions (synthetic Traditional EW) with different nominal Fe^{3+}/Fe^{2+} ratios in the temperature range from 25°C to 60°C.

As is shown in Figure 8-5 an Figure 8-6, the real ferric/ferrous ratios calculated from thermodynamic model for the tests #1−#2 in the Fe(II)−Fe(III)−H_2SO_4−H_2O system and for the tests #3−#11 in the Fe(II)−Fe(III)−Cu(II)−H_2SO_4−H_2O system. The 3 different nominal ferric/ferrous ratios ranging from 3.5 to 12 are presented in test #1−#11 in Table 5-3. In Figure 8-5 and Figure 8-6, all the nominal ferric/ferrous ratios are remarkably higher than the responding nominal ferric/ferrous ratios calculated from thermodynamic model at all 7 temperatures ranging from 25 to 60°C in the Fe(II)−Fe(III)−H_2SO_4−H_2O system and in the Fe(II)−Fe(III)−Cu(II)−H_2SO_4−H_2O system. What's more, the real ferric/ferrous ratios calculated based on model for the tests #1−#2 in the Fe(II)−Fe(III)−H_2SO_4−H_2O system and for the tests #3−#11 in the Fe(II)−Fe(III)−Cu(II)−H_2SO_4−H_2O system both decrease significantly with the

temperature increasing from 5 to 45 °C under the same nominal ferric/ferrous ratio shown in Figure 8-5 and Figure 8-6.

The nominal ferric/ferrous ratio in this paper is the ratio of the initial total ferric to initial total ferrous added when preparing the solution. The real ferric/ferrous ratio in the electrolyte is typically lower than its corresponding nominal ferric/ferrous ratio after speciation calculation, and details for this could be found in our previous publication [1, 92, 101-103].

8.2.5 Analysis of Calculated pH

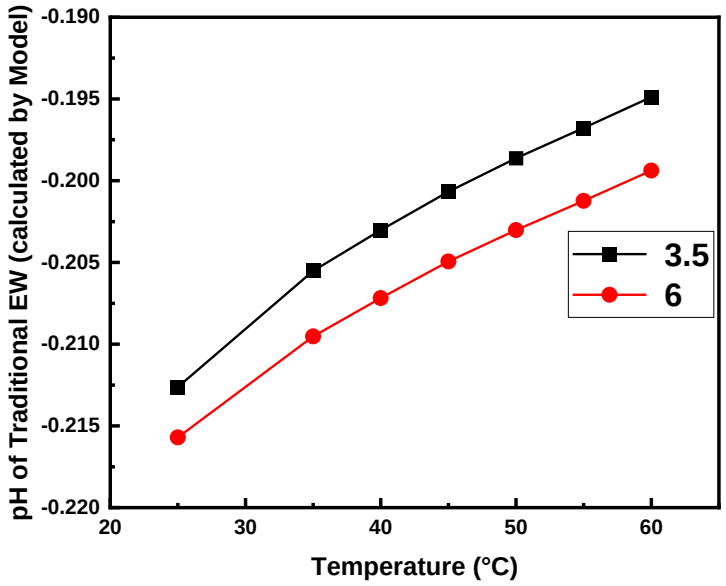

Figure 8-7 Calculated pH of the Fe(II)-Fe(III)-H_2SO_4-H_2O solutions (synthetic Traditional EW) from sample #1 to sample #2 with different nominal Fe^{3+}/Fe^{2+} ratios in the temperature range of 25°C-60°C.

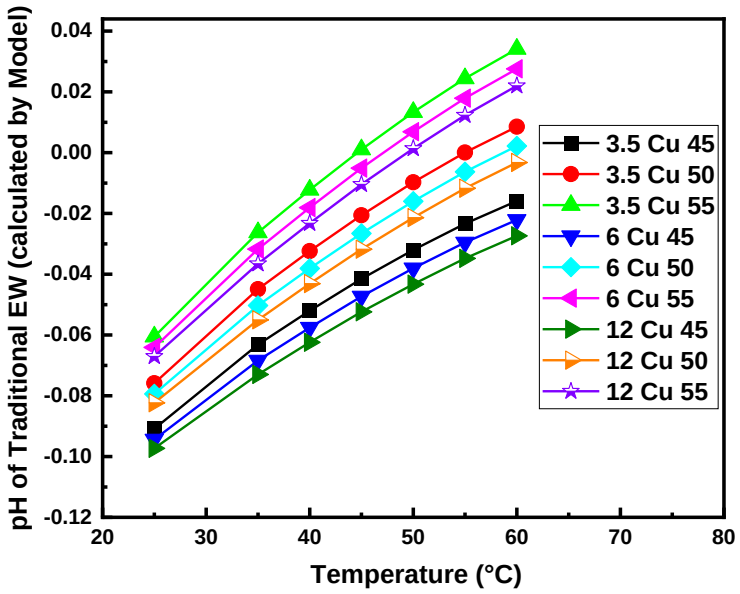

Figure 8-8 Calculated pH of the Fe(II)-Fe(III)-Cu(II)-H_2SO_4-H_2O solutions (synthetic Traditional EW) from sample # 3 to sample # 11 with nominal Fe^{3+}/Fe^{2+} ratio ranging from 0.01 to 100 in the temperature range of 25°C-60°C.

pH is one of the key parameters in the industrial solutions. However, owing to the extreme acidic conditions, it is very challengeable to measure pH directly in the studied solutions. From the validated thermodynamic modeling results, the pH values for the solutions can be calculated by the obtained activity of hydrogen ions in this thesis. This provides an indirect way to study the pH of the involved solution in this thesis. The calculated pH for various solution compositions are shown in Figure 8-7 and Figure 8-8. It can be observed that the pH values of iron sulfate/iron−copper sulfate solutions are generally less than 0, in the range of -0.217 to -0.197 and -0.11 to 0.36 over the studied temperatures and nominal Fe^{3+}/Fe^{2+} ratios. In both systems, under the same nominal Fe^{3+}/Fe^{2+} ratio, the pH increases gradually with temperature up to 60 °C. The increase of pH values shows the concentrations of H^+ ions in the 2 systems slightly decrease when the solution temperatures gradually increase from 25 to 60 °C. This implies that more protons are

combined with free metal ions and sulfate anions to form more thermodynamically stable ionic complexes at higher temperatures, resulting in the declining concentration of H^+ ions.

Moreover, under the same nominal Fe^{3+}/Fe^{2+} ratio, the pH values in iron sulfate solutions are overall lower than those in iron−copper sulfate solutions at studied temperatures. This means that the addition of copper sulfate results in an increase of pH, in other words, a decrease in concentration of H^+ ions. This is mainly due to the fact that the addition of a sulfate anion leads to the ion association to form a stable ionic complex which causes a decrease in the free H^+ concentration in the solution.

8.2.6 Analysis of Calculated Ionic Strength

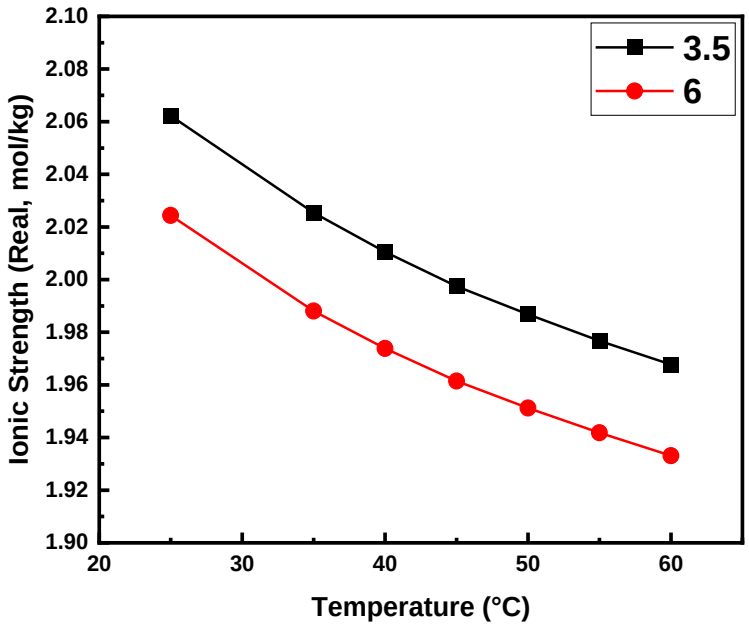

Figure 8-9 Calculated real ionic strength of the Fe(II)-Fe(III)-H_2SO_4-H_2O solutions (synthetic Traditional EW) from sample #1 to sample #2 with different nominal Fe^{3+}/Fe^{2+} ratios in the temperature range of 25°C-60°C.

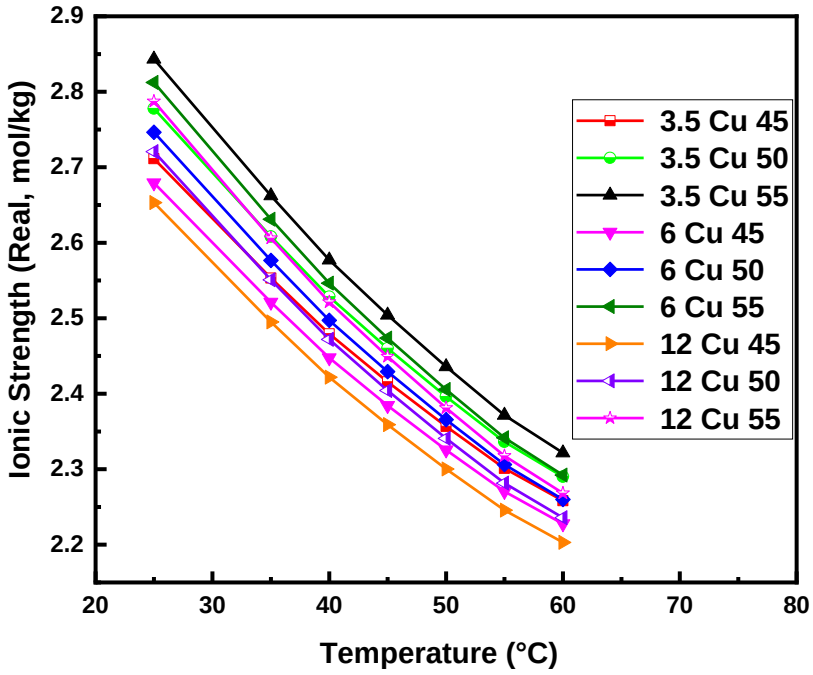

Figure 8-10 Calculated real ionic strength of the Fe(II)-Fe(III)-Cu(II)-H_2SO_4-H_2O solutions (synthetic Traditional EW) from sample # 3 to sample # 11 with nominal Fe^{3+}/Fe^{2+} ratio ranging from 3.5 to 12 in the temperature range of 25°C-60°C.

As can be observed, under the same nominal Fe^{3+}/Fe^{2+} ratio, increasing temperatures from 25 to 60 °C results in a gradual decrease of the real ionic strength. This may be explained by the fact that ion association of higher charged ions such as Fe^{2+}, Fe^{3+}, and Cu^{2+} in solutions leads to the formation of more stable and less charged ionic complexes such as $FeHSO_4^+$, $FeHSO_4^{2+}$, $FeSO_4^+$, $Fe(SO_4)_2^-$, and $CuHSO_4^+$ when increasing the temperature, as can be clearly observed in Figure 8-1 and Figure 8-2.

The nominal ionic strengths for all nominal Fe^{3+}/Fe^{2+} ratios are in the range of 1.94-2.06 mol/kg H_2O for the Fe(II)-Fe(III)-H_2SO_4-H_2O solutions and 2.2-2.7 mol/kg H_2O for the Fe(II)-Fe(III)-Cu(II)-H_2SO_4-H_2O solutions. It is evident that the values of the real ionic strength of the present solutions by using the calculated ionic concentration of charged species from modeling results are much lower than those by using nominal species concentration in the two systems. This

is because the concentration of higher charged ions such as Fe^{2+}, Fe^{3+}, Cu^{2+}, and SO_4^{2-} decreases significantly, and at the same time, they are employed to form lower charged ionic complexes (HSO_4^-, $FeHSO_4^+$, $FeHSO_4^{2+}$, $FeSO_4^+$, $Fe(SO_4)_2^-$, and $CuHSO_4^+$) and neutral species ($FeSO_4°$ and $CuSO_4°$).

The overall concentration trend as a function of temperature for each studied species in advance electrolyte solutions is also similar to that in spent electrolyte solutions. Variations of nominal Fe^{3+}/Fe^{2+} ratios and total Cu(II) amount do not exhibit apparent influence on chemistry of Fe(II), Fe(III) and Cu(II) in the two aqueous Fe(II, III)-Cu(II)-H_2SO_4 systems. Only temperature plays a crucial role on the distribution of each studied species. Since the concentrations of Fe^{2+} and Fe^{3+} have been quantified, the real Fe^{3+}/Fe^{2+} ratio thus can be calculated.

8.3 Summary

Speciation of Fe(II)-Fe(III)-Cu(II)-H_2SO_4-H_2O aqueous systems was studied here by thermodynamic modeling under conditions related to the current industrial copper electrowinning electrolyte from 25 to 60 °C. The thermodynamic model could quantify the species distribution and provide fundamental data for the understanding of Fe (ferric ion and ferrous ion) and cupric ion behavior during copper electrowinning process.

The calculated distribution of each Fe(II and III) and Cu(II) species in the Fe(II)-Fe(III)-H_2SO_4-H_2O and Fe(II)-Fe(III)-Cu(II)-H_2SO_4-H_2O systems reveals that Fe(II) is primarily distributed as free Fe^{2+}, $FeHSO_4^+$ and $FeSO_4°$; Fe(III) is mainly distributed as free Fe^{3+}, $FeSO_4^+$, $FeHSO_4^{2+}$, and $Fe(SO_4)_2^-$; Cu(II) is mainly dissolved as Cu^{2+}, $CuSO_4°$, and $CuHSO_4^+$. Especially, after the addition of a high amount of copper (45-55 g/L), the overall distribution trends of each Fe(II) and Fe(III) species do not have substantial changes.

Furthermore, this work provides an alternative method of estimating the pH by the validated modeling results under extreme acidic conditions. As expected, the pH values of iron sulfate/iron-copper sulfate solutions are generally less than 0 over the studied conditions and increase gradually with temperature. The pH values in iron sulfate solutions are overall lower than those in iron−copper sulfate solutions. It is also worth noting that the real ionic strength calculated by the concentrations of ionic species based on modeling results is significantly lower than the nominal ionic strength calculated by nominal species concentrations. Although the effective ionic strength is still relatively high, the excellent agreement of redox potentials between experimental measurements and model prediction justifies the reasonable use of the B-dot model for the calculation of activity coefficients of dissolved species.

It should be emphasized that this work provides a reliable set of thermodynamic data, and the model developed in this study is a feasible and promising method for the studies on the speciation of the Fe(II)−Fe(III)−Cu(II)$-_2SO_4$−H_2O system over a wide range of solution conditions, allowing a comprehensive description of Fe and Cu behavior such as the valence distribution, redox potential calculation, and pH estimation in the acidic iron sulfate solution with copper. The reliable prediction of the redox potential by the speciation model and the developed expression with high accuracy is particularly valuable and attractive. Therefore, it can be expected that the findings in the present work will facilitate our further investigation on the speciation of more complicated acidic iron sulfate solutions as well as solutions in other copper hydrometallurgical processes.

9. CONCLUSIONS, INDUSTRIAL APPLICATIONS AND RECOMMENDATIONS

A previously developed thermodynamic model is shown in this thesis to be capable of simulate the species distribution under conditions most related to the industrial processes of hydrometallurgical extraction of copper. The modelling result has confirmed its validity to predict the redox potential of the ferric/ferrous couple in complicated acidic sulfate solutions containing 1-55 g/L cupric ion. Furthermore, the modelling also is employed to investigate and better understand the iron chemistry of the solutions generated during heap leaching, SX, traditional Cu EW, and novel Cu EW processes.

9.1 Conclusions

In the pure quaternary H_2SO_4-$Fe_2(SO_4)_3$-$FeSO_4$-H_2O system, the applicability of Eq. (1) is proved. In our present study, the nominal sulfuric acid concentration is as high as 1.84 mol/L, corresponding to a nominal pH value of about -0.26 (the actual pH values of the solutions should be different based on the solution composition). Furthermore, it is shown that the co-existence of cupric ion up to 0.87 mol/L does not exert an obvious influence on the accurate prediction of redox potentials calculated by Eq. (1). Based on the above analysis, a conclusion can be drawn that Eq. (1) is applicable across a wide range of pH, copper concentration and temperature, even at the temperature as low as 5 °C.

The applicability of the equation developed previously in different solution compositions with various temperatures (especially lower than 25°C) and higher copper concentration for the pregnant leaching solutions, SX solutions and copper electrowinning solutions was confirmed in this thesis. The comparison of experimental and calculated results suggested that Eq. (1) is quantitatively validated with nominal ferric/ferrous ratios from 0.01 to 100, temperature ranging from 5 °C to 60 °C, various concentrations of cupric ion from 1 g/L to 55 g/L, iron from 1 to 45.3

g/L and sulfuric acid from 3 to 200 g/L. It could be concluded that the redox potentials depend significantly on the nominal ferric/ferrous ratio and temperature, but it is almost unaffected by the various concentrations of cupric ion and sulfuric acid. The equation can still be used under lower temperatures as well. It is expected that the findings in this work could facilitate the understanding of iron chemistry and the kinetics/mechanism analysis in the above-mentioned industrial processes, and potentially other processes for hydrometallurgical production of copper.

Results reveal that most of the Fe(III) is distributed as complexes and the free Fe^{3+} accounts for only a minor percentage, whereas a large amount of Fe(II) exists in the form of free Fe^{2+}. The Cu(II) species mainly distributes as Cu^{2+}, $CuSO_4^o$ and $CuHSO_4^+$, and a considerable proportion of Cu(II) exists as $CuHSO_4^+$.

The validity of the proposed model was confirmed by reliable and accurate prediction of the measured redox potential throughout all solution conditions. The excellent agreement between measured potentials and those calculated proves that this expression can also be employed to predict the redox potential in the studied solutions with a much higher acid and copper concentration. A detailed analysis of the model-calculated results in terms of the free ferric and ferrous ion concentration ratios and their accompanying activity coefficients, together with the fact that the experimental ORP values in the two solution systems are almost identical to each other, strongly supports that the redox potential of acidic iron sulfate solutions with a much higher acid concentration and a high amount of copper can still be solely determined by the Fe^{3+}/Fe^{2+} couple. The speciation model and developed expression explain the change of the redox potential with temperature for all nominal Fe^{3+}/Fe^{2+} ratios.

9.2 Industrial Applications

The validity of the proposed model was confirmed by reliable prediction of measured redox potential from 5 to 60 °C. The fact that there exists an excellent agreement between the redox potential calculated by previously developed equation and measured by this work, further extends its applicability and provides an alternative method of predicting redox potential. It is expected that the findings in this work will facilitate the development of combined SX/EW technology to achieve higher current efficiency.

This thesis provides a reliable set of thermodynamic data, and the model developed in this study is a feasible and promising method for the studies on the speciation of the Fe(II)−Fe(III)−Cu(II)−$_2$SO$_4$−H$_2$O system over a wide range of solution conditions, allowing a comprehensive description of Fe and Cu behavior such as the valence distribution, redox potential calculation, and pH estimation in the acidic iron sulfate solution with copper. The reliable prediction of the redox potential by the speciation model and the developed expression with high accuracy is particularly valuable and attractive. Therefore, it can be expected that the findings in the present work will facilitate our further investigation on the speciation of more complicated acidic iron sulfate solutions as well as solutions in other copper hydrometallurgical processes.

9.3 Recommendations

This work provides an accurate simple method of determining the ORP by the equation and forms a baseline to contribute to the understanding of the iron chemistry by validated modeling results for the electrolyte generated during hydrometallurgical extraction of copper. The following investigations are highly recommended in order to enable a better understanding of the iron chemistry:

(1) The developed and validated thermodynamic model was applied to a restricted range of conditions shown in this work because of the limited availability of experiment data. When the developed model is extended the application to a wider range of electrolyte composition and temperature, further work will be required to expand a deeper understanding of the quaternary system. The influence of other ions and additives on the distribution of the species and the accurate determination of the ORP also need further study in detail.

(2) The equation is highly useful for the understanding of the iron chemistry and could be applied to determine the ORP solely by the nominal ferric/ferrous ratio and experiment temperature. Further work requires to be done to extend the range of the applicability of the equation to more complicated acidic iron sulfate solutions.

(3) An excellent agreement between the redox potential calculated by previously developed equation and measured by this work, which further extends its applicability and provides an alternative method of determine the ORP. Additional investigation will be required to determine the optimum electrolyte composition and operation parameters for Cu EW process in order to lower the energy cost and be environment-friendly.

REFERENCES

1. Schlesinger, M.E., King, M.J., Sole, K.C., and Davenport, W.G., 2011. Extractive Metallurgy of Copper, Fifth edition. Amsterdam: Elsevier Ltd.,. DOI: 10.1016/C2010-0-64841-3.
2. Free, M., Moats, M.S., Robinson, T.G., Neelameggham, N., Houlachi, G., Ginatta, M., Creber, D., Holywell, G., 2012. Electrometallurgy-now and in the future. In Electrometallurgy 2012; Free, M., Moats, M., Houlachi, G., Asselin, E., Allanore, A., Yurko, J., Wang, S. Eds.; Wiley: NJ,; Vol 1, pp 1-27, DOI: 10.1002/9781118371350.ch1.
3. Robinson, T. G., Davenport, W. G., Moats, M., Karcas, C., and Demetrio, S., 2007. Copper Electrorefining and Electrowinning Copper Vol, V, Eds. G. E. Houlachi, J. D. Edwards and Robinson TG, 375 (2007)
4. Moats, M.S., and Khouraibchia, Y., 2009. Min. And Metall. Proceeding, 26, 179.
5. Bartlett, R.W., 1998. Solution Mining, Leaching and Fluid Recovery of Materials. 2nd edition. Gordon and Breach Science Publishers 90-5699-633-9.
6. Davenport, W.G., King, M., Schwarz, M., Biswas, A.K., 2002. Concentrating Copper ores. Extractive Metallurgy of Copper, 4th ed. Elsevier Science Ltd., The Boulevard,
7. Langford Lane Kidlington, Oxford OX5 IGB, UK, pp. 31–54.
8. Demergasso, C., Galleguillos, P., Escudero, L., Zepeda, V., Castillo, D., Casamayor, E., 2005. Molecular characterization of microbial populations in low-grade copper ore bioleaching test heap. Hydrometallurgy 80, 241–253.
9. Dew, D.W., Rautenbach, G.F., van Hille, R.P., Davis-Belmar, C.S., Harvey, I.J., Truelove, J.S.,2011. High temperature heap leaching of chalcopyrite: method of evaluation and process model validation. In International Conference: Percolation

Leaching: The Status Globally and in Southern Africa. Misty Hills, Muldersdrift, South Africa, 8–9 Nov; SAIMM Symposium Series S69. ISBN: 978-1-920410-24-7, pp. 201–220.

10. Dixon, D.G., 2000. Analysis of heat conservation during copper sulphide heap leaching. Hydrometallurgy 58, 27–41.
11. Dlamini, Z., 2015. Techno-Economical Comparison of Three Process Routes for the Treatment of Gamsberg Zinc ore MSc thesis University of Cape Town.
12. Filippou, D., 2004. Innovative hydrometallurgical processes for the primary processing of zinc. Miner. Process. Extr. Metall. Rev. 25 (3), 205–252.
13. Gálvez, E.D.,Moreno, L.,Mellado, M.E., Ordóñez, J.L., Cisternas, L.A., 2012. Heap leaching of caliche minerals: phenomenological and analytical models-some comparisons. Miner. Eng. 33, 46–53.
14. Garcia, C., Arias, H., Campos, J., Roco, J., San Martin, O., Whittaker, J., 1999. Bioleaching at Zaldivar. Biomine '99 and Water Management in Metallurgical Operations —Conference Proceedings. 1999 August 23–24; Perth, Australia. Australian Mineral Foundation Inc., Glenside, Australia, pp. 72–81.
15. Gericke, M., Seyedbagheri, A., Neale, J., van Staden, P.J., 2011. Advancements in the approach to research and design of heap bioleaching processes. The 19th International Biohydrometallurgy Symposium (IBS2011)., September 18–22, 2011, Changsha-China I, pp. 698–705.
16. Ghorbani, Y., Petersen, J., Becker, M., Mainza, A.N., Franzidis, J.-P., 2013. Investigation and modelling of the progression of zinc leaching from large sphalerite ore particles. Hydrometallurgy131–132, 8–23.

17. Ghorbani, Y., Petersen, J., Harrison, S.T.L., Tupikina, O.V., Becker, M., Mainza, A.N., Franzidis, J., 2012. An experimental study of the long-term bioleaching of large sphalerite ore particles in a circulating fluid fixed-bed reactor. Hydrometallurgy 129–130, 161–171.
18. Govender, E., Bryan, C.G., Harrison, S.T.L., 2013. Quantification of growth and colonisation of low-grade sulphidic ores by acidophilic chemoautotrophs using a novel experimental system. Miner. Eng. 48, 108–115.
19. Grosse, A.C., Dicinoski, G.W., Shaw,M.J., Haddad, P.R., 2003. Leaching and recovery of gold using ammoniacal thiosulphate leach liquors (a review). Hydrometallurgy
20. Ilyas, S., Lee, J.-C., Chi, R.-A., 2013. Bioleaching of metals from electronic scrap and its potential for commercial exploitation. Hydrometallurgy 131 – 132, 138 – 143.
21. John, L., 2011. The art of heap leaching — the fundamentals. In International Conference: Percolation Leaching: The Status Globally and in Southern Africa. Misty Hills, Muldersdrift, South Africa, 8 – 9 Nov; SAIMM Symposium Series S69. ISBN: 978-1-920410-24-7, pp. 17 – 42.
22. Kappes, D.W., 2002. Precious metal heap leach design and practice. In Proceedings— Mineral Processing Plant Design, Practice and cControl, SME, Colorado, USA. 2. ISBN: 0-87335-223-8, pp. 1606 – 1630.
23. Lahtinen,M., Svens, K., Haakana, T., Lehtinen, L., 2008. Zinc plant expansion by Outotec direct leaching process. 47th Annual Conference of Metallurgists of CIM, Winnipeg, Manitoba Canada, Zinc and Lead Metallurgy, p. 167.
24. Lizama, H.M., Harlamovs, J.R., Belanger, S., Brienne, S.H., 2003. The Teck Cominco Hydrozinc™ process. In: Young, C.A., et al. (Eds.), Hydrometallurgy 2003 – Fifth

International Conference in Honour of Professor Ian M. Ritchie – Volume 2: Electrometallurgy and Environmental Hydrometallurgy, volume 2 ed. TMS (The Minerals, Metals & Material Society), pp. 1503–1516.

25. Logan, T.C., Seal, T., Brierley, J.A., 2007. Whole-ore heap bio-oxidation of sulfidic gold-bearing ores. In: Rawlings, D.E., Johnson, D.B. (Eds.), Biomining. Springer Verlag, Berlin. ISBN: 978-3-540-34909-9, pp. 113–138.
26. Ojumu, T.V., Petersen, J., Hansford, G.S., 2008. The effect of dissolved cations on microbial ferrous-iron oxidation by Leptospirillum ferriphilum in continuous culture. Hydrometallurgy 94, 69–76.
27. Paul H., Johnson, P.H. "Thin Layer Leaching Method" U.S. Patent 05.562962. 28 March 1975.
28. Petersen, J., Dixon, D.G., 2007a. Modeling and optimisation of heap bioleach processes. In: Rawlings, D.E., Johnson, D.B. (Eds.), Biomining. Springer Verlag, Berlin. ISBN: 978-3-540-34909-9, pp. 153–176.
29. Petersen, J., Dixon, D.G., 2007b. Principles, mechanisms and dynamics of chalcocite heap bioleaching. In: Donati, E., Sand, W. (Eds.), Microbial Processing of Metal Sulfides. Springer Verlag, Berlin. ISBN: 978-1-4020-5588-1, pp. 193–218.
30. Petersen, J., Minnaar, S.H., du Plessis, C.A., 2010. Carbon dioxide and oxygen consumption during the bioleaching of a copper ore in a large isothermal column. Hydrometallurgy104, 356–362.
31. Readett, Fox, 2010. Commercialization of nickel heap leaching at Murrin Murrin operations. Proceedings of XXV International Mineral Processing Congress (IMPC),

Brisbane, Queensland, Australia, 6 – 10 September, pp. 3611 – 3616.

32. Saari, P., Riekkola-Vanhanen, M., 2011. Talvivaara bio-heap leaching process. Percolation Leaching: Southern African Institute of Mining and Metallurgy Percolation Leaching: The status globally and in Southern Africa 2011, pp. 53 – 66.
33. Sánchez-Chacón, A.E., Lapidus, G.T., 1997. Model for heap leaching of gold ores by cyanidation. Hydrometallurgy 44 (1 – 2), 1 – 20.
34. Sand,W., Gehrke, T., Josza, P.-G., Schippers, A., 2001. (Bio)chemistry of bacterial leaching — direct vs indirect bioleaching. Hydrometallurgy 51, 115 – 129.
35. Scheffel, R., 2002. Copper Heap Leach Design and Practice. In: Mular, A.L., Halbe, D.N., Barratt, D.J. (Eds.), Mineral Processing Plant Design, Practice, and Control: Proceedings 2, pp. 1571 – 1605 Chapter 12.
36. Watling, H.R., 2006. The bioleaching of sulphide minerals with emphasis on copper sulphides—a review. Hydrometallurgy 84, 81 – 102.
37. Welham, N.J., “Method for ammoniacal leaching” A.U. Patent 07.903815. 13 July 2007.
38. Alfantazi, A.M., and Valic D., 2003. A study of copper electrowinning parameters using a statistically designed methodology, Journal of Applied Electrochemistry 33:217-225.
39. Sandoval, S.P., Lei, K.V.P., 1993. Proceedings of Milton E. Wadsworth (IV) International Symposium on Hydrometallurgy, Eds. Hiskey JB, and Warren GW, 1091.
40. Khouraibchia, Y., 2010. Evaluation of the effect of copper electrowinning parameters on current efficiency and energy consumption using surface response methodology, ECS Transaction, 28(6) 295-306.
41. Sandoval, S., Cook, P., Morales, C., and Robinson, T., 2010. Demonstration of the

Ferrous/Ferric Anode Reaction for Copper Electrowinning, Proceeding of Cu.

42. Pablo, E., Aqueveque, Eduardo, P., Wiechmann, Javier Herrera, 2013. Measurable variables in copper electrowinning and their relevance to predict process performance, IEEE.
43. Wiechmann, E.P., Morales, A.S., Aqueveque, P., Mayne-Nicholls, R., 2011. Reducing Specific Energy to Shrink the Carbon Footprint in a Copper Electrowinning Facility, Industry Applications, IEEE Transactions on, Vol. 47, no.3, pp.1175-1179, May-June 2011.
44. Subbaiah, T., Singh, P., Hefter, G., Muir, D., Das, R.P., 2000. Sulphorous acid as anodic depolarizer in copper electrowinning Part II, Journal of Applied Electrochemistry 30:181-186.
45. Paschen, P., Langfellner, M., Mori, G., 1991. in W.C. Copper, D.J. Kemp, G.E. Lagos and K.G. Tan, Hydrometallurgy and Electrometallurgy of Copper, Copper 91, Vol.3(Pergamon, New York, 1991), page. 575.
46. Cifuentes, L., Simpson, J., 2005. Temperature dependence of the cathodic and anodic kinetics in a copper electrowinning cell based on reactive electrodialysis, Chemical Engineering Science, 60, 4915-4923.
47. Sandoval, S., Geol, N., Luzanga, A., and Tshifungat, O., 2016. Improvement in copper electrowinning at Tenke Fungurume Mining Company, Journal of The Southern-African Institute of Mining and Metallurgy, Vol 116, pp 497-501, June 2016.
48. Cifuentes, L., Grageda, M., Crisostomo, G., 2006. “Electrowinning of copper in two- and three-compartment reactive electrodialysis cells”, Chemical Engineering Science 61, 3623-3631.

49. Cifuentes, L., Mella, M., 2006. On the physical quality of copper electrodeposits obtained on mesh cathodes. Canadian Metallurgical Quarterly, vol 45, pp 9-15.

50. Cifuentes, L., Ortiz, R., Casas, J.M.,2005. “Electrowinning of Copper in a lab Scale Squirrel Cage Cell with Anion Membrane”, AIChE Journal, vol.51, pp. 2273-2284.

51. Panda, B., Das, S.C., 2001. “Electrowinning of copper from sulfate electrolyte in presence of sulfurous acid”, Hydrometallurgy 59, 55-67.

52. Moats, M., and Khouraibchia, Y., 2009. “Effective diffusivity of ferric ions and current efficiency in stagnant synthetic copper electrowinning solutions,” Miner. Metall. Process., vol. 26, no. 4, pp. 179–186.

53. Rudnik, E., and Dashbold, N., 2017. “Study on copper recovery from smelted low-grade e-scrap using hydrometallurgical methods,” *Miner. Metall. Process.*, vol. 34, no. 1, pp. 20–29.

54. Gendel, Y., and Lahav, O., 2008. “Accurate determination of Fe(II) concentrations in the presence of a very high soluble Fe(III) background,” *Appl. Geochemistry*, vol. 23, no. 8, pp. 2123–2129.

55. T. T. Chen and J. E. Dutrizac, “The mineralogy of copper electrorefining,” *Jom*, vol. 42, no. 8, pp. 39–44, 1990.

56. G. Yue, L. Zhao, O. G. Olvera, and E. Asselin, “Speciation of the H_2SO_4-$Fe_2(SO_4)_3$-$FeSO_4$-H_2O system and development of an expression to predict the redox potential of the Fe^{3+}/Fe^{2+} couple up to 150 °C,” *Hydrometallurgy*, vol. 147–148, pp. 196–209, 2014.

57. T. Kalliomäki, J. Aromaa, and M. Lundström, “Modeling the effect of composition and temperature on the conductivity of synthetic copper electrorefining electrolyte,” *Minerals*, vol. 6, no. 3, 2016.

58. T. Kalliomaki, “Effect of composition and temperature on physico-chemical properties of copper electrolyte,” Master Thesis, School of Chemical Technology, Aalto University, Finland, Nov 2015.

59. A. P. Brown, R. O. Loutfy, G. M. Cook, and N. P. Yao, “The Electrorefining of Copper from a Cuprous Ion Complexing Electrolyte,” *JOM J. Miner. Met. Mater. Soc.*, vol. 33, no. 7, pp. 49–57, 1981.

60. J. E. Dutrizac, “The kinetics of dissolution of chalcopyrite in ferric ion media,” *Metall. Trans. B*, vol. 9, no. 4, pp. 431–439, 1978.

61. A. J. Bard and L. R. Faulkner, *Fundamentals and Applications*, vol. 30. 1980.

62. E. Mostad, S. Rolseth, and J. Thonstad, “Electrowinning of iron from sulphate solutions,” *Hydrometallurgy*, vol. 90, no. 2–4, pp. 213–220, 2008.

63. J. M. Casas, G. Crisóstomo, and L. Cifuentes, “Speciation of the Fe(II)–Fe(III)–H_2SO_4–H_2O system at 25 and 50 °C,” *Hydrometallurgy*, vol. 80, no. 4, pp. 254–264, 2005.

64. C. G. Anderson, “Optimization of industrial copper electrowinning solutions,” *IMPC 2016 - 28th Int. Miner. Process. Congr.*, vol. 2016-Septe, no. 1, pp. 1–3, 2016.

65. Guikuan Yue, Edouard Asselin, “Kinetics of ferric ion reduction on chalcopyrite and its influence on leaching up to 150 ^{o}C,” Electrochemica Acta, 2014, Volume 146, Pages 307-321.

66. G. Yue, A. G. Guezennec, and E. Asselin, “Extended validation of an expression to predict ORP and iron chemistry: Application to complex solutions generated during the acidic leaching or bioleaching of printed circuit boards,” *Hydrometallurgy*, vol. 164, pp. 334–342, 2016.

67. R. Al Shakarji, Y. He, and S. Gregory, “Statistical analysis of the effect of operating

parameters on acid mist generation in copper electrowinning," *Hydrometallurgy*, vol. 106, no. 1–2, pp. 113–118, 2011.

68. Cifuentes, L., Glasner, R., Crisostomo, G., Casas, J.M., Simpson, J., "Aspects of the Development of a New Copper Electrowinning Cell based on Reactive Electrodialysis," vol. 147, no. 2, pp. 347–348, 2001.
69. E. L. Cussler, *Diffusion Mass Transfer in Fluid Systems*, 3rd ed. Cambridge University Press, 2009.
70. G. Cifuentes, J. Simpson, F. Lobos, L. Briones, and A. Morales, "An alternative copper electrowinning process based on reactive electrodialysis (RED)," *Chem. Eng. Trans.*, vol. 19, pp. 157–162, 2010.
71. J. M. Casas, G. Crisóstomo, and L. Cifuentes, "Dissolution of metallic copper in aqueous sulphuric acid - Ferric sulphate solutions," *Can. Metall. Q.*, vol. 45, no. 3, pp. 243–248, 2006.
72. M. J. Nicol and I. Lázaro, "The role of EH measurements in the interpretation of the kinetics and mechanisms of the oxidation and leaching of sulphide minerals," *Hydrometallurgy*, vol. 63, no. 1, pp. 15–22, 2002.
73. M. S. Moats, A. Luyima, and W. Cui, "Examination of copper electrowinning smoothing agents. Part I: A review," *Miner. Metall. Process.*, vol. 33, no. 1, pp. 7–13, 2016.
74. J. Zhu, X. Yang, F. Fan, and Y. Li, "Factors affecting the determination of iron species in the presence of ferric iron," *Appl. Water Sci.*, vol. 8, no. 8, pp. 1–4, 2018.
75. N. Hiroyoshi, H. Miki, T. Hirajima, and M. Tsunekawa, "Enhancement of chalcopyrite leaching by ferrous ions in acidic ferric sulfate solutions," *Hydrometallurgy*, vol. 60, no. 3, pp. 185–197, 2001.

76. N. Hiroyoshi, M. Arai, H. Miki, M. Tsunekawa, and T. Hirajima, “A new reaction model for the catalytic effect of silver ions on chalcopyrite leaching in sulfuric acid solutions,” *Hydrometallurgy*, vol. 63, no. 3, pp. 257–267, 2002.

77. N. Hiroyoshi, H. Kitagawa, and M. Tsunekawa, “Effect of solution composition on the optimum redox potential for chalcopyrite leaching in sulfuric acid solutions,” *Hydrometallurgy*, vol. 91, no. 1–4, pp. 144–149, 2008.

78. D. H. Angell and T. Dickinson, “The kinetics of the ferrous/ferric and ferro/ferricyanide reactions at platinum and gold electrodes. Part I. Kinetics at bare-metal surfaces,” *J. Electroanal. Chem.*, vol. 35, no. 1, pp. 55–72, 1972.

79. Bard, A.J., Parsons, R., &Jordon, J. (1985). *Standard potentials in aqueous solution*. New York: Marcel Dekker, Inc.

80. Bosch, R.W., Bogaerts, W.F., & Zheng, J.H. (2003). Simple and robust external reference electrodes for high-temperature electrochemical measurements. *Corrosion,* 59, 162–171.

81. Crundwell, F.K. (1987). Kinetics and mechanism of the oxidative dissolution of a zinc sulphide concentrate in ferric sulphate solution. *Hydrometallurgy,* 19, 227–242.

82. Dew, D.W., & Philips, C.V. (1985). The effect of Fe(II) and Fe(III) on the efficiency of copper electrowinning from dilute acid Cu (II) sulphate solutions with the chemelectro cell. *Hydrometallurgy*, 14, 331-367.

83. Dry, M.J., & Bryson, A.W. (1988). Prediction of redox potential in concentrated iron sulphate solutions. *Hydrometallurgy*, 21, 59–72.

84. Liu, W., & Granata, G. (2018), Temperature control in copper heap bioleaching, *Hydrometallurgy,* 176, 26-32.

85. Nicol, M.J., & Lázaro, I. (2002). The role of E_H measurements in the interpretation of the kinetics and mechanisms of the oxidation and leaching of sulphide minerals. *Hydrometallurgy,* 63, 15–22.

86. Sandoval, S., Cook, P., Morales, C., & Robinson, T. (2010). Demonstration of the ferrous/ferric anode reaction for copper electrowinning. *Proceedings of Cu of the 7th International Conference on Copper*, Hamburg, Germany, 1617-1634.

87. Sapieszko, R.S., Patel, R.C., & Matljevlc, E. (1977). Ferric hydrous oxide sols. 2. Thermodynamics of aqueous hydroxo and sulfato ferric complexes. *Journal of Physical Chemistry*, 81, 1061–1068.

88. Stipp, S.L. (1990). Speciation in the Fe(II)-Fe(III)-SO_4-H_2O system at 25 °C and low pH: sensitivity of an equilibrium model to uncertainties. *Environmental Science &Technology*, 24, 699–706.

89. Tanaka, N., & Tamamushi, R. (1964). Kinetic parameters of electrode reactions. *Electrochim Acta*, 9, 963–989.

90. Peters, E. (1986). Leaching of sulfides (Chapter 26). In: Somasundaran P. (Ed.), *Advances in Mineral Processing*. SME/AIME, Littleton, CO (pp. 445-462).

91. Winand, R. (1975). Electrocrystallization of copper. *Trans. Inst. Min. Metall. (Sect. C)*, 84, 67-75.

92. Yue, G. (2015). Speciation of the sulfuric acid-ferric sulfate-ferrous sulfate-water system and its application to chalcopyrite leaching kinetics up to 150 °C. Ph.D. Thesis. University of British Columbia, Vancouver, Canada.

93. Zoski, C.G. (2007). *Handbook of Electrochemistry* (1st ed.). Amsterdam: Elsevier.

94. Robinson T et al. (2008) Copper solvent extraction 2007 world operating data. Paper presented at International solvent extraction conference ISEC 2008, Tucson, Arizona, USA, 15-19 Sept 2008.

95. Casas, J.M., Alvarez, F., Cifuentes, L. 2000. Aqueous speciation of sulfuric acid-cupric sulfate solutions. Chem Eng Sci 55:6223–6234

96. Casas, J.M., Etchart, J.P., Cifuentes, L. 2003. Aqueous speciation of arsenic in sulfuric acid and cupric sulfate solutions. AIChE J 49(8):2199–2210

97. Cifuentes, L., Casas, J.M., Simpson, J. 2006. Temperature dependence of the speciation of copper and iron in acidic electrolytes. Chem Eng Res Des 84(A10):965–969

98. Powell, K.J., Brown, P.L., Byrne, R.H., Gajda, T., Hefter, G. 2007. Chemical speciation of environmentally significant metals with inorganic ligands part 2: the Cu^{2+}–OH^{-}, Cl^{-}, CO_3^{2-}, SO_4^{2-}, and PO_4^{3-} systems. Pure Appl Chem 79(5):895–950

99. Akilan, C. 2008. Thermodynamic and related studies of aqueous copper(II) sulfate solutions. Ph.D. thesis. Murdoch University, West Australia

100. Dong Y et al (2019) Speciation of iron-arsenic-copper-sulfuric acid solution during copper electrorefining from 25 to 70 ℃. Paper presented at the COM 2019, Vancouver, BC, Canada, 21–23 Aug 2019

101. Xu J et al. (2019) Extended validation of an expression to predict ORP: application to pregnant leaching solution generated during heap leaching and copper electrowinning solution. Paper presented at the COM 2019, Vancouver, BC, Canada, 21–23 Aug 2019

102. Dong, Y., Xu, J., Wesstrom, B., Olave, B. R., Quinn, J. P., Yue, G. 2021. Thermodynamic Modeling of the Fe(II)-Fe(III)-Cu(II)-H2SO4-H2O Solution and its Application to Determination of Redox Potential during Copper Electrorefining up to 70°C.

Ind. Eng. Chem. Res. 60(44) 15921-15935. Solution and Its Application to Determination of Redox Potentialduring Copper Electrorefining up to 70 °C

103. Hossein Aminian, Claude Bazin, Daniel Hodouin, Claude Jacob, “Simulation of a SX-EW pilot plant”, Hydrometallurgy, Volume 56, Issue 1, May 2000, Pages 13-31.

104. Das, S.C., and Krishna, P.G., 1996. Effect of Fe(III) during copper electrowinning at higher current density International Journal of Mineral Processing, Volume 46, pages 91-105.

105. ICSG (2010) Directory of copper mines and plants 2008–2013. Lisbon, Portugal: International Copper Study Group. https://www.icsg.rog

106. Robinson T et al. (2008) Copper solvent extraction 2007 world operating data. Paper presented at International solvent extraction conference ISEC 2008, Tucson, Arizona, USA, 15–19 Sept 2008 Helgeson, H.C., Kirkham, D.H., Flowers, G.C., 1981. Theoretical prediction of the thermodynamic behavior of aqueous electrolytes at high pressures and temperatures: IV. Calculation of activity coefficients, osmotic coefficients, and apparent molal and standard and relative partial molal properties to 600°C and 5 kb. Am. J. Sci. 281, 1249-1516.

107. Stumm, W., Morgan, J. J. 1996. Aquatic Chemistry, third edition. John Wiley & Sons, New York.

108. Langmuir, D. 1997. Aqueous Environmental Geochemistry. Prentice Hall, New Jersey.

109. Liu, H., Papangelakis, V. G. 2005. Chemical modeling of high temperature aqueous processes. Hydrometallurgy 79, 48-61.

110. Werner, J. M. Modeling and validation for optimization of electrowinning performance. PhD thesis; The University of Utah, 2017.

111. Pourbaix, M. 1966. Atlas of Electrochemical Equilibria in Aqueous Solutions, first edition, Pergamon Press, Oxford.

112. Latimer, W. M. 1938. The Oxidation States of the Elements and Their Potentials in Aqueous Solutions. Englewood Cliffs, NJ, Prentice-Hall, Inc, 359-369.

113. Wiberg, N., Holleman, A. F., Wiberg, E. 2001. Holleman-Wiberg's Inorganic chemistry. Elsevier Science, San Diego.

114. Baes Jr., C. F., Mesmer, R. E. 1976. The Hydrolysis of Cations. Wiley-Interscience, New York.

115. Smith, R. M., Martell, A. M. 1976. Critical Stability Constants, Volume 4: Inorganic Complexes. Plenum Press, New York.

116. Perrin, D. D. 1982. Ionisation Constants of Inorganic Acids and Bases in Aqueous Solution, second edition. Pergamon Press, New York.

117. Antti, R. HSC Chemistry 7, Chemical Reaction and Equilibrium Modules. Outotec Research, 2009.

VITA

In 2014 Jiahao Xu obtained his bachelor degree in Chemical Engineering from Yangzhou University, Yangzhou, Jiangsu Province, China. He studied in National Kyushu Institute of Technology, Kitakyushu, Fukuoka Prefecture, Japan, as an exchange student from 2013 to 2014. Before he was enrolled into Department of Metallurgical, Materials and Biomedical Engineering of The University of Texas at El Paso in August 2017, he studied in Department of Chemistry in University of Siegen, Siegen, NRW, Germany, as a master student for 3 years. He received his Ph.D. degree in Materials Science and Engineering under supervision of Dr. Guikuan Yue from The University of Texas at El Paso, 2022. His doctoral research work was found by Freeport-McMoRan, Inc with a focus on hydrometallurgical production of high-purity copper. Please contact Jiahao Xu at jxu3@miners.utep.edu